Development of graphene oxide/Nafion polymeric membranes toward the improvement of Direct Methanol Fuel Cell membranes

Ph.D Thesis
Energy and Environment

Gabriele Guglielmo Gagliardi

Tutor: Franco Rispoli
Supervisor: Domenico Borello

Index

Figures Index

Tables Index

Nomenclature

Acronyms

ACL	Anode catalys layer
AFR	Anode flow rate
AGDL	Anode gas diffusion layer
ANA	Analcime
BP	Bipolar plate
CCL	Cathode catalyst layer
CGDL	Cathode gas diffusion layer
CL	Catalyst layer
DI	Deionized
DMFC	Direct methanol fuel cell
EL	Electrolyte
FCs	Fuel cells
GDE	Gas diffusion electrode
GDL	Gas diffusion layer
GO	Graphene oxide
ICE	Internal combustion energy
IEC	Ion exchange capacity
MEA	Membrane electrode assembly
MMT	Montmorillite
MOR	Mordenite
OCV	Open circuit voltage
PANI	Polyaniline
PBI	Polybenzimidazole
PEEK	Poly ether ether ketone
PEM	Proton exchange membrane
PFSA	Perfluorosulfonic acid

PPy Polypyrrole

PPSU Polyphenylsulfone

PSS Polystyrene sulfonate

PTFE Polytetrafluorofluoroethylene

PVA Polyvynil alcohol

PVDF Polyvinylidene fluoride

RH Relative humidity

RIU Refractive index unit

SEM Scanning electrode microscope

SGO Sulphonated graphene oxide

SPAEK Sulphonated polyarylene ether ketone

SPAES Sulphonated polyarylene ether sulfone

SPEEK Sulphonated poly ether ether ketone

TEOS Tetraethylorthosilicate

TGA Thermogravimetric analysis

WU Water uptake

Latin

A Area, m^2

C Molar concentration, mol/dm^3

E Electric potential, V

F Faraday constant, 96845 C/mol

G, ΔG Gibbs free energy kJ/mol

H, ΔH Enthalpy kJ/mol

I Current, A

K Boltzmann constant, $1.38*10^{-23}$ J/K

M Molarity

P Power, W

T Temperature, K

V Voltage, V

VOL Volume

W Energy, kJ

WE Weight, g

I Current density, A/m^2

t Thickness, m

x Molar fraction

z Number of electrons moles

Greeks

α Angle of diffraction

β Symmetry coefficient

δ Drag coefficient

η Efficiency

μ Dynamic viscosity, Pa s

Superscripts

0 Standard, equilibrium conditions

Subscripts

a anode

act Activation

c Cathode

d Dry

eq equivalent

m membrane

met methanol

ohm Ohmic

ox Oxygen

r Reaction

re Real

w Wet

Introduction

Fuel Cells (FCs) are energy conversion systems that electrochemically convert chemical energy (stored in a fuel) to electricity without any intermediate combustion process. This technology offers superior efficiency and performance compared to the incumbent combustion-based energy generation technologies [**1-3**]. Fuel cells are eco-friendly devices with potential zero emission at the point of use. Moreover, if the energy vectors used in fuel cells were generated from renewable sources (i.e. from biomass or from electrochemical processes utilising renewable electric energy), the resulting carbon dioxide cycle is null. So, they may be the energy conversion devices of the future. In addition, they are a silent technology, without noise or vibration, and their design flexibility allows for simple construction and a diverse range of applications, including portable, stationary and for mobility.

Among FCs technologies, Proton Exchange Membrane (PEM) FCs represent the more developed solution. They are usually fed by hydrogen, but recently innovative solution using methanol as fuel were proposed [**4**]. For these devices, the structure remains the same while the catalyst load changes. Methanol has a noticeable quantity of hydrogen, in fact, the content of hydrogen is higher in a litre of methanol (98g), at standard temperature and pressure, than in a litre of pure hydrogen (35g), at 350 bar and standard temperature. Furthermore, methanol is in a liquid phase at standard condition and then its storage and use are easier than hydrogen (see Table 1).

Table 1- Methanol vs Hydrogen

	Energy density per mass unit (kWh/kg)	Volumetric energy density (kWh/L)	Specific weight of storage ($kg_{storage}$/kWh)	Storage efficiency %	Net energy density per mass unit (kWh/kg)
Hydrogen	33	$3 \cdot 10^{-3}$	2	1.5	0.5
Methanol	6	4	0.2	83	5

Direct Methanol Fuel Cells (DMFCs) have significant advantages over the other FCs such as high start-up velocity, compactness, easy storage and transportation of methanol [**5**]. Nevertheless, they are affected by some drawbacks when compared with hydrogen PEMFC such as low energy density power (per mass unit), and reduced performance.

However, several issues hinder the spreading of this technology. Firstly, the fuel cell membrane is prone to allow the passage of methanol (the so-called cross-over) that reacts directly at the cathode strongly reducing

DMFC performance. Furthermore, high cost and limited operating temperature range represent a strong limit to the commercialization of that technology. Research activities are focused on developing new polymer electrolyte membrane (PEM) materials aiming at contrasting the crossover. Among several types of material, graphene oxide (GO) has been considered as an appropriate element offering excellent results in terms of water uptake and mechanical stability, especially at high temperature. Several authors have reported that GO contributes to reduce methanol permeability because it acts as a barrier, due to its higher tortuosity. In addition, it is well known that temperature, methanol concentration, as well as flow rate, affect proton conductivity and methanol crossover and, ultimately, DMFC performance. Up to now, a lot of novel membranes were developed but thus there is still a lack of optimized membranes for use in the DMFC. It is therefore necessary to investigate what are the best conditions to make better use of this innovative material.

The aim of this work is to develop and characterize a composite membrane to be used as a PEM in DMFC and to make best use of it. The membrane consists of a solution of Nafion and different GO loading.

The following objectives are set in order to fulfil this aim:

- Evaluate the influence of the graphene oxide on the properties of the composite membrane.
- Estimate the optimum loading.
- Study how the operating conditions change the best power output.
- Estimate the optimal operating conditions to better exploit that membrane.

All the results obtained were compared with the baseline Nafion membrane.

The thesis is structured into seven chapters. Below is a short summary of each one:

Chapter I: Introduction

Chapter II: Literature Review – This chapter focuses on the membranes reported in the literature for DMFC paying special attention to graphene oxide.

Chapter III: Membranes Preparation – It summarizes the protocol to prepare the composite membranes.

Chapter IV: Test bench – This chapter describes all the components of the test bench.

Chapter V: Influence of GO on the Membrane properties– It focuses on the properties of the homemade graphene oxide membranes.

Chapter VI – Single cell tests: It analyses the performance of the membranes made of GO. The performance is compared with that of bare Nafion.

Chapter VII – Summary and Conclusions This last chapter presents the mains conclusions of this work and the future studies based on the present one.

1.Introductory remarks

Direct Methanol Fuel Cells (DMFCs) (Figure 1) directly convert the chemical energy of a mixture of methanol and water in electrical energy without introducing an intermediate thermodynamic cycle as, for example, in gas turbine or internal combustion engine (ICE). The main advantage of this conversion process is related to its high efficiency because it is not dependent on the two characteristic extremes temperatures involved in classic thermodynamic cycles (i.e. Carnot cycle).

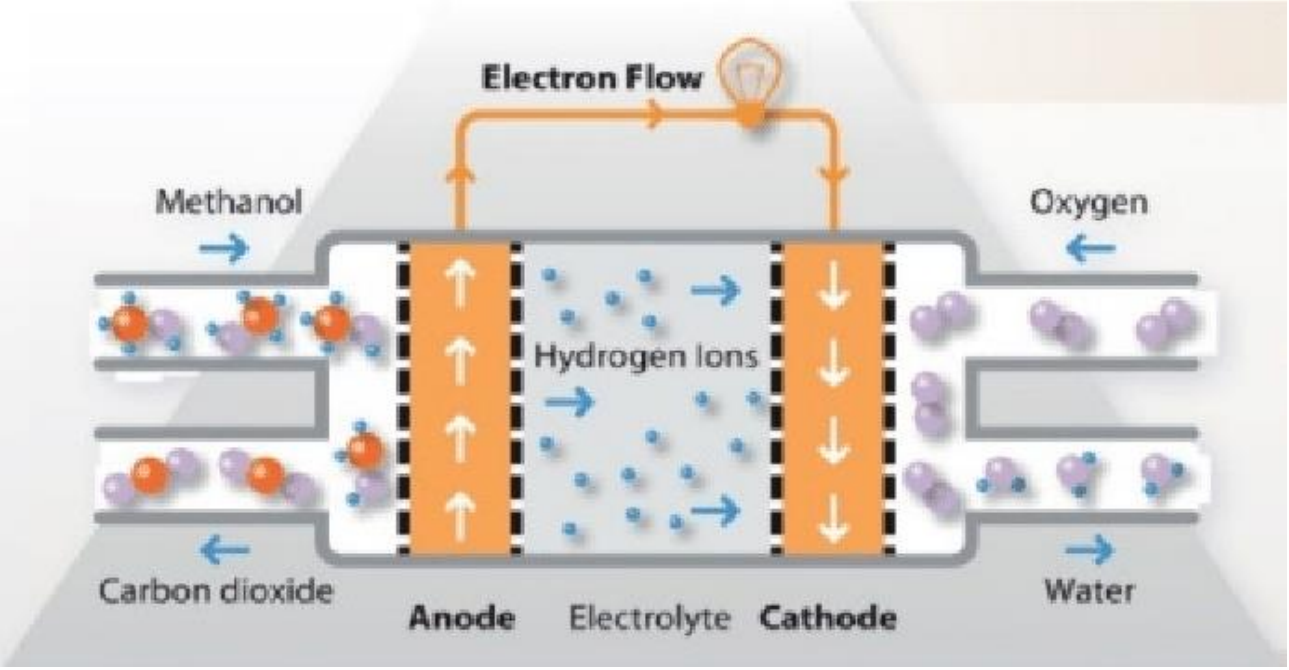

*Figure 1- DMFC scheme [**6**]*

In DMFCs, reactions occur at the two cell electrodes on the catalyst active area: at the anode methanol oxidation occurs, whereas at the cathode oxygen reduction takes place as following **[7]**:

$$CH_3OH + H_2O + 131.5\frac{kJ}{mol} \rightarrow CO_2 + 6H^+ + 6e^- \qquad (1)$$

$$\frac{3}{2}O_2 + 6H^+ + 6e^- \rightarrow 3H_2O + 857.4\frac{kJ}{mol} \qquad (2)$$

$$CH_3OH + \frac{3}{2}O_2 \rightarrow 2H_2O + CO_2 + 726.4\frac{kJ}{mol} \qquad (3)$$

The reaction of one mole of methanol yields six electrons and six cations, the electrolyte allows only one active specie to pass, leading the ions to move from anode to cathode or vice-versa, while the electrons flow through an external electric circuit.

The efficiency of the process is calculated as the maximum amount of available energy contained on the reactants, given by the change in Gibbs free energy, divided by the enthalpy difference related to the reaction (3) at standard condition [**8**]:

$$\eta_{id} = \Delta G_r^0 / \Delta H_r^0 \qquad (4)$$

Where ΔG_r^0=702.4$\frac{kJ}{mol}$ and ΔH_r^0=726.4$\frac{kJ}{mol}$. So, the ideal efficiency of the cell is η=0.97. However, the real efficiency also depends on the real energy generated by the reaction, W_{re}, and the chemical energy owned by the reactants (W_{useful}) which corresponds to the differential enthalpy of the reactants (Eq.5).

$$\eta_{re} = \frac{W_{re}}{W_{useful}} = \frac{W_{re}/\Delta t}{W_{useful}/\Delta t} = \frac{P_{re}}{\Delta H_r^0/\Delta t} = \frac{P_{re}}{\Delta G_r^0/0.97\Delta t} = \frac{P_{re}}{zFE/0.97\Delta t} = 0.97\,\frac{V_{re}I}{EI} = 0.97\,\frac{V_{re}}{E} = 0.80\,V_{re} \qquad (5)$$

where

$$I = \frac{zF}{\Delta t} \qquad (6)$$

is the current generated by the reactions of a mole of methanol (which corresponds to z electrons moles) in the interval Δt.

The ideal voltage of the cell, ΔE, is calculated at standard conditions as the difference between the two half-cells standard potential [**9**]

$$\Delta E = E_{ox}^0 - E_{met}^0 = 1.23 - 0.02 = 1.21\ V \qquad (7)$$

The operation made from equation 4 to 7, can be extended for the cell fed by hydrogen obtaining an ideal voltage of 1.23 V [**10**]. Voltage comparison between hydrogen and methanol fuel cell shows that they are similar and they seem to be able to generate a comparable power, but, aside from several effects: activation, ohmic and concentration losses, which are common to all fuel cells type, for DMFCs, fuel cross-over and losses due to two phase flow contribute to decrease even more the efficiency [**11**]. The fuel cell cross-over significantly reduces the cell voltage, at open circuit voltage condition, from 1.21 V to about 0.6 V, while for hydrogen fuel cell, the cell voltage is roughly 1V. Therefore, if the crossover could be mitigated, the potential would be significant. Furthermore, unlike hydrogen fuel cell, CO_2 (gaseous) is generated at the anode of a DMFC, as showed by equation (1), denying the fuel access to the active area of the anode so partially repressing methanol oxidation and lowering cell performance. In the following section, all the losses related to the DMFC technology are discussed at length.

1.1 Polarization curve

As stated previously, the losses that affect the performance of the DMFC are:

- Activation losses;
- Ohmic losses;
- Concentration polarization;
- Fuel cross-over;
- Anode channels CO_2 bubbles clogging.

In Figure 2, a typical polarization curve for a PEMFC is shown. The effective OCV, as can be seen, is lower than the ideal voltage.

Starting from the OCV, at lowest values of current density, a sharp decrease in voltage initially occurs (Activation losses) followed by a region of constant slope (Ohmic Losses). Finally, in the region where concentration losses are dominant, the voltage reduction increases for higher current density and the cell voltage goes rapidly to zero.

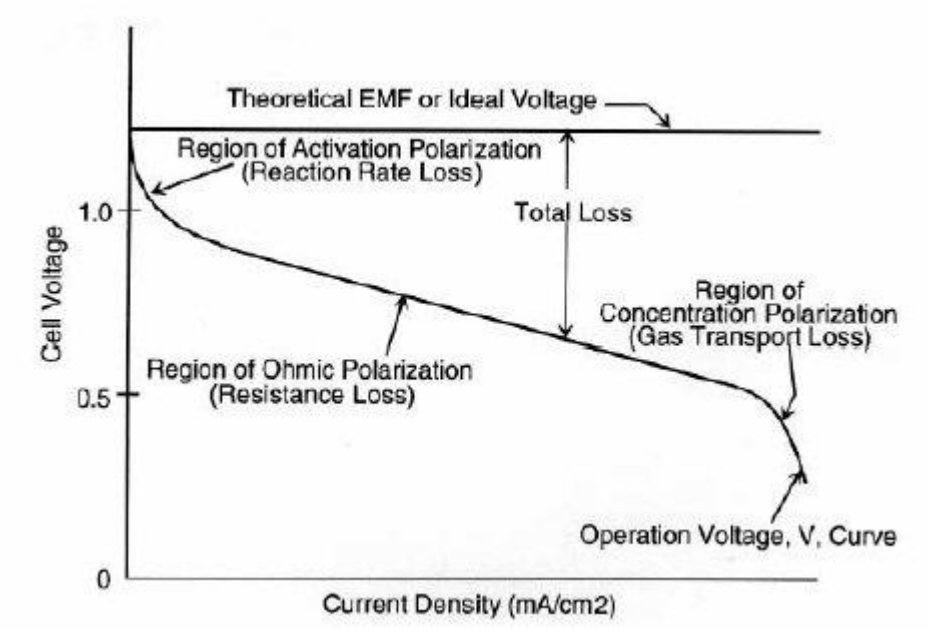

*Figure 2- Typical fuel cell polarization curve [**12**]*

In the following sections, all the losses will be described deeply.

1.1.1 Activation losses

The activation polarization is the loss in voltage related to the activation energy used for the activation of the reaction [**13**]. The Tafel equation [**14**] (8) describes the electrode overvoltage:

$$\Delta V_{act} = A\ ln(\frac{i}{i_0}) \qquad (8)$$

The parameter A increases as the electrochemical reactions velocity decreases and it is given by:

$$A = \frac{RT}{z\beta F} \qquad (9)$$

Where β is the charge transfer coefficient, a number between 0 and 1 (for the DMFC is roughly 0.5), which depends on the electrochemical reaction type and the electrode material; z is the number of moles of electrons involved in the reaction. Although an increase in temperature leads to an increase in activation voltage drop, from equation (8) and (9), it also improves reaction kinetics resulting in higher cell performance.

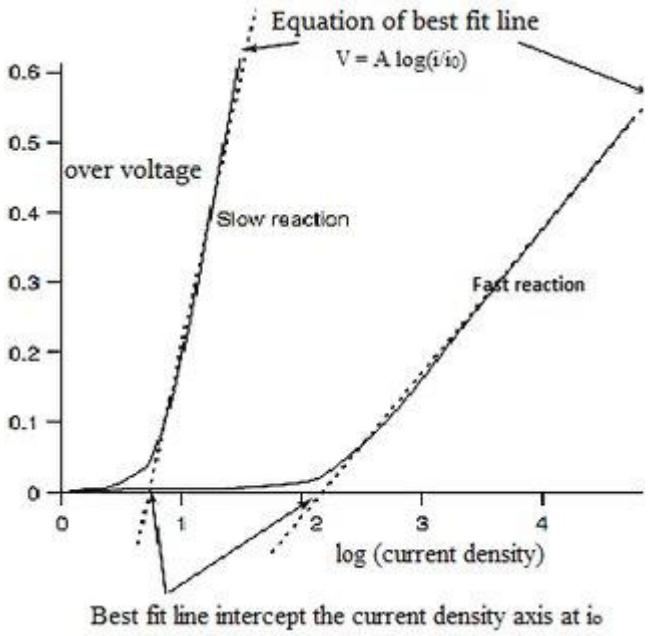

*Figure 3-Tafel slope **[8]***

The Tafel slope is shown in Fig.3, where on the *x*-axis is represented the logarithm of the ratio between the current density and the equilibrium current of the reaction. The i_0, included in the equation (8), is known as exchange current density, figuring the electrons flow rate between the electrode and the analyte when the reaction is in equilibrium at zero overpotential. Considering figure 3, i_0 is found at the intersection between the *x*-axis and the tangent at the curve of Tafel. The value of *i* can be expressed in function of i_0 by using equation (8) and (9), resulting in the Butler-Volmer expression [**15**] as following:

$$i = i_0 \cdot e^{\frac{z\beta F\Delta V_{act}}{RT}} \qquad (10)$$

If all the other losses are considered negligible (ohmic, concentration, etc.) the following expression can be written:

$$V_{cell} = E_0 - A\, ln(\frac{i}{i_0}) \qquad (11)$$

In Figure 4 the cell voltage in dependence on current density is shown considering the polarization losses only.

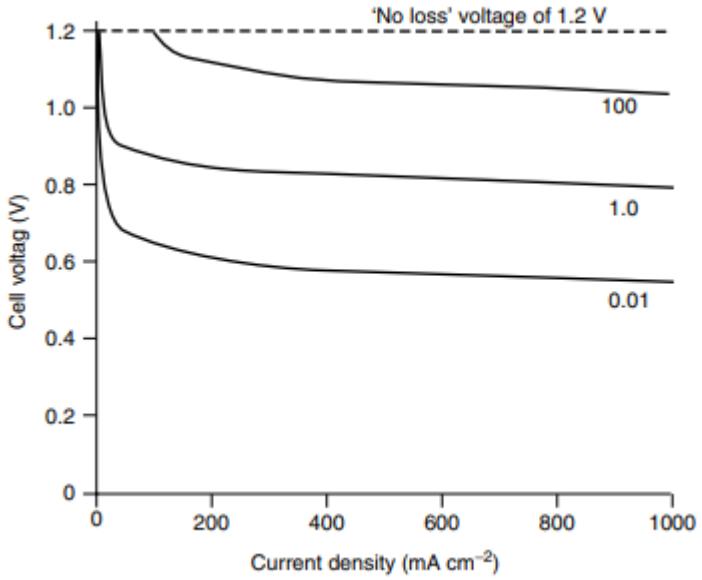

*Figure 4-Polarization curve at different exchange current densities i_0 [**8**]*

Three curves (Figure 4) have been plotted for three different values of i_0 (0.01, 0.1, and 100 mA cm^{-2}). It can be noticed that for high values of i_0 and low values of *i,* the activation losses are zero.

Several techniques can be adopted to reduce the effects of activation overvoltage, which is the more significant irreversibility:

- Raising of operative temperature.
- Using pure oxygen.
- Using precious catalysts (such as Pt and Ru).
- Increasing the roughness of the porous electrodes, in order to increase the available catalysts area and then the reaction rate [**16**].

1.1.2 Ohmic losses

Ohmic polarization represents the overvoltage due to:

1. Electric resistance due to the electrons flow.
2. Contact resistance between two adjacent layers of different materials.
3. Resistance of the electrolyte to the ions flow.

All the components of the fuel cell can be schematically considered as a series of electric resistance [**17**], except for the membrane. The membrane acts an insulator for the two electrodes: if it was a conductor with a small electric resistance, the two electrodes would be in short circuit. Thus, considering the cell as a series of resistances, the voltage drop due to this polarization loss can be written as:

$$\Delta V_{ohm} = R_{eq} i = (R_{BP} + R_{GDL} + R_{CL} + R_{EL}) i \qquad (12)$$

where EL is the electrolyte, CL is catalyst layer, GDL is the gas diffusion layer, and BP is the bipolar plate.

1.1.3 Concentration losses

The cell is usually fuelled with low methanol concentration from 0.5 M up to 2 M (i.e., respectively 1.5 and 6% in weight percentage of the solution). When the concentration of methanol in the surrounding area of the catalyst is too low, the electrical potential drops. It usually happens at the outlet of the channels when methanol concentration in the flow can be low and the resulting current is not homogeneously distributed upon the catalyst surface.

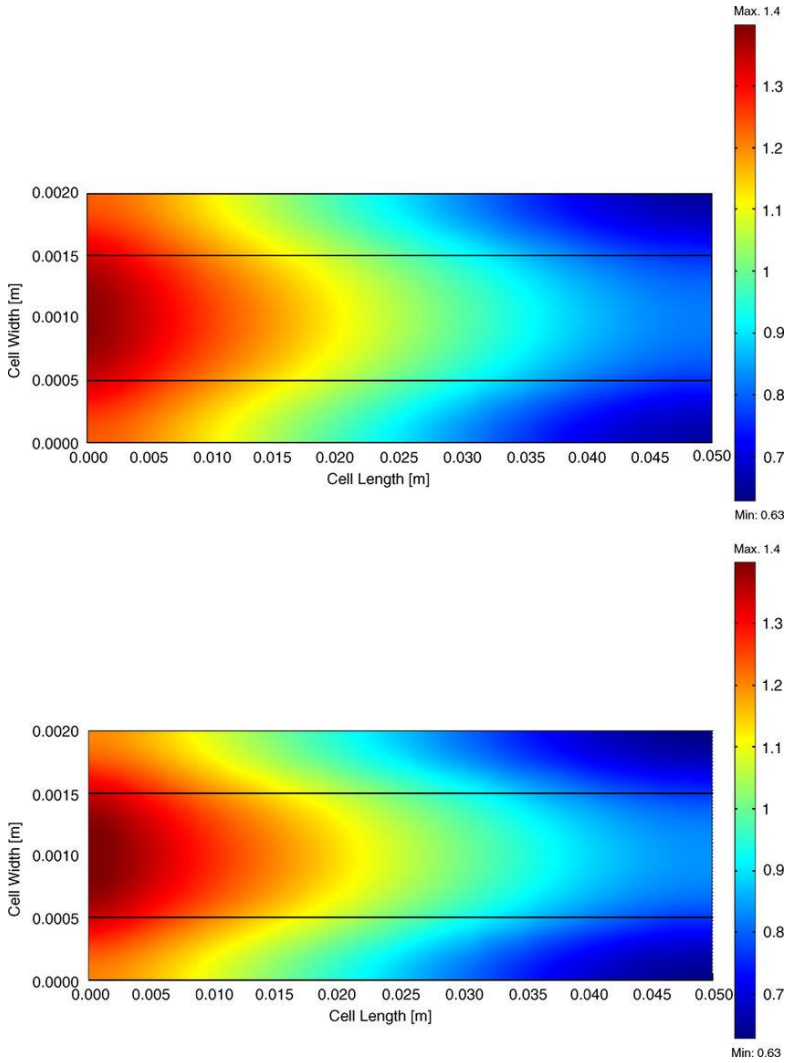

*Figure 5-Current density distribution over the catalyst layer [**18**]*

In Figure 5, a simulation of the current distribution over the catalyst area, carried out performing a simulation using COMSOL, is shown. A sharp decreasing in current density from the element of the anode channel inlet up to the outlet of the channel can be seen. The decrease in reactant concentration along the channels leads to a decreasing of reactants upon the CL thus lowering the global potential of the electrode.

The concentration losses can be described by the equation [**19**]:

$$\Delta V_{conc} = m \cdot e^{ni} \qquad (13)$$

Where m and n are two empirical parameters. Furthermore, this distribution can cause further ohmic voltage drop on the ACLs due to the electron flow from higher potential area towards zero potential areas as shown in Figure 5.

1.1.4 Losses due to fuel cross-over

Cross-over losses are due to methanol molecules that, instead of reacting at the anode catalyst layer, cross the membrane and eventually react with oxygen once they reached the cathode electrode. This phenomenon strongly reduces the cell voltage resulting in a mixed potential [**20**]. It leads to a decreasing in OCV up to 0.6 V from an ideal value equal to 1.21 V [**21**]. The driving forces that support the methanol mass transport into the membrane have a different nature:

- Diffusive
- Osmotic
- Drag forces

As can be seen from (14) [**22**],

$$J_{met} = D_{met}\frac{(C_{met,a}-C_{met,c})}{t_m} + \frac{C_{met,a}k\Delta p}{t_m\mu} + x_{met,a}\delta\frac{i}{F} \qquad (14)$$

The diffusive component depends on the different methanol concentration between anode and cathode side of the membrane and it is the most relevant component, especially close to zero current condition, where the electric circuit is turned off and the drag component is zero. The osmotic component depends on the different pressure between anode and cathode side of the membrane and it is often neglected [**23**]. Mixed potential due to the methanol cross-over is another over potential component [**24**]. The effect of the methanol crossover on the voltage is shown in Figure 6.

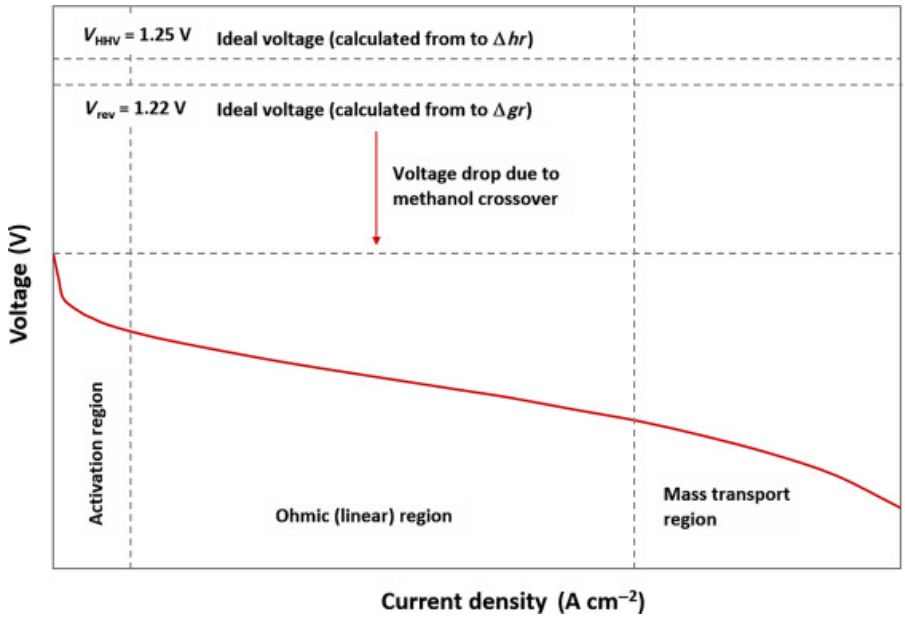

*Figure 6-Cell voltage drop due to methanol cross-over [**25**]*

1.1.5 Anode channels blocking

Carbon dioxide generated from methanol oxidation reaction (1) can further increase the effect of concentration losses, in fact the CO_2 bubbles nucleate into the GDL, blocking some pores so reducing the available volume for methanol transport towards the anode catalysts. The higher is the bubbles density over the GDL, the lower is the residence time of the fuel [**26-27**] in the channels, so reducing the mass transport in the GDL.

1.2 Stack structure

BASIC CONFIGURATION

A single cell is made of 7 components (Figure 7):

1) Anode Current Collector
2) Anode Gas Diffusion Layer (AGDL)
3) Anode Catalyst Layer (ACL)
4) Electrolytic membrane
5) Cathode Catalyst Layer (CCL)
6) Cathode Gas Diffusion Layer (CGDL)
7) Cathode Current Collector

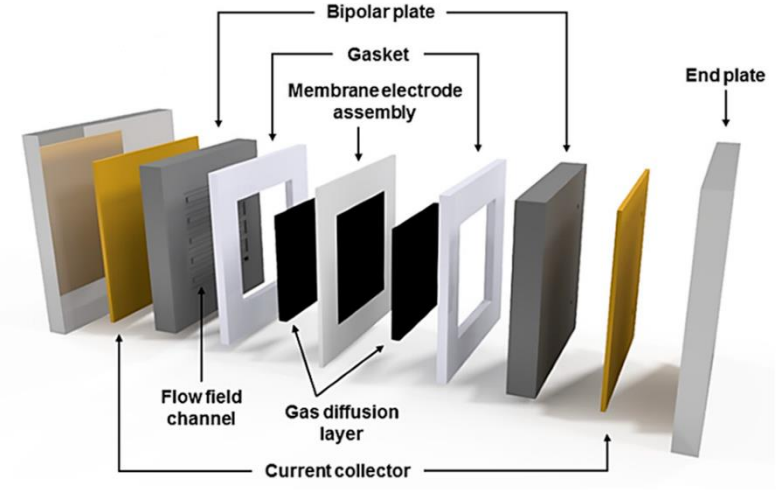

*Figure 7-Direct Methanol Single fuel Cell [**28**]*

The core of a cell is the Membrane Electrode Assembly (MEA). A MEA is composed of a polymer electrolyte membrane, two catalyst layers (ACL and CCL, each on one side) and two gas diffusion layers (AGDL and CGDL, each on one side). The reactants diffuse through the GDL towards the CL. At the ACL, the oxidation reaction occurs with the generation of electrons and cations. Cations cross the membrane, moving from anode towards the cathode, while electrons move through the GDL reaching the current collector connected to the external electrical circuit. At the cathode side, electrons, cations, and the reactant (air or pure oxygen) react at the CCL creating heat and water.

A fuel cell stack (figure 8) consists in a sequence of single MEA connected between them through graphite bipolar plates. The sequence is closed by the end plates, two metal conductive terminals coated with gold (Golden end plates). The whole assembly is kept together with a series of screw joints, useful to pack and avoid reactants leakage from bipolar plates.

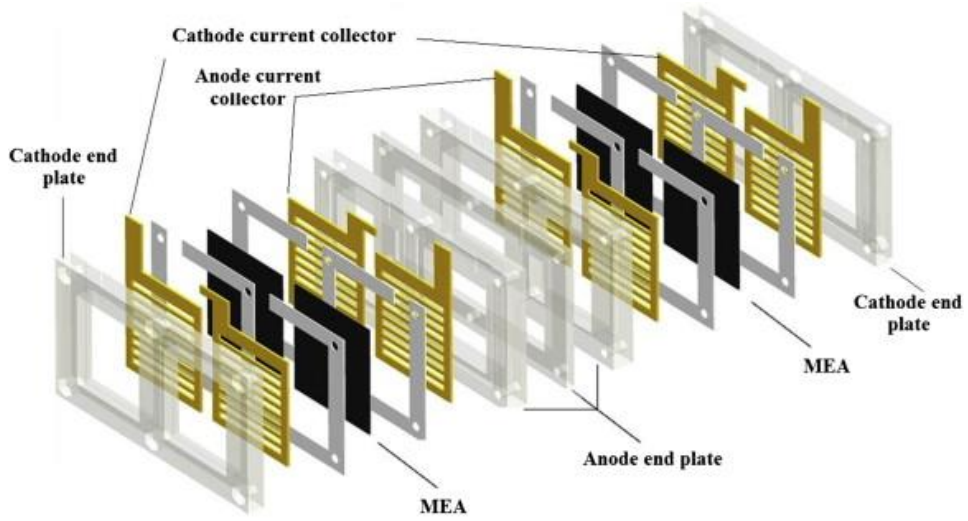

Figure 8-Direct Methanol Fuel Cell Stack ***[29]***

END PLATES AND CURRENT COLLECTORS

The stack is supported by two steel plates at the two ends. They are electrically insulated from the golden end plates and they have the task to homogeneously distribute the pressure over the cells surface. The two golden plates collect the current generated by the stack and allow the connection to an external load through two terminals.

BIPOLAR PLATE

The bipolar plate (Figure 9) allows the delivery of the reactants and the conduction of electrons generated over the catalyst layers. Their material should be easily machined, chemical resistant to reactant corrosion and should have a high electrical conductivity (usually, bipolar plates are made with graphite or sometimes with metals, aluminium or steel). They have a thickness of 2-3 mm and the channels have a size of about 1 mm.

Figure 9-Example of graphite bipolar plates **[30]**

The two most important flow field pattern are shown in Fig.10

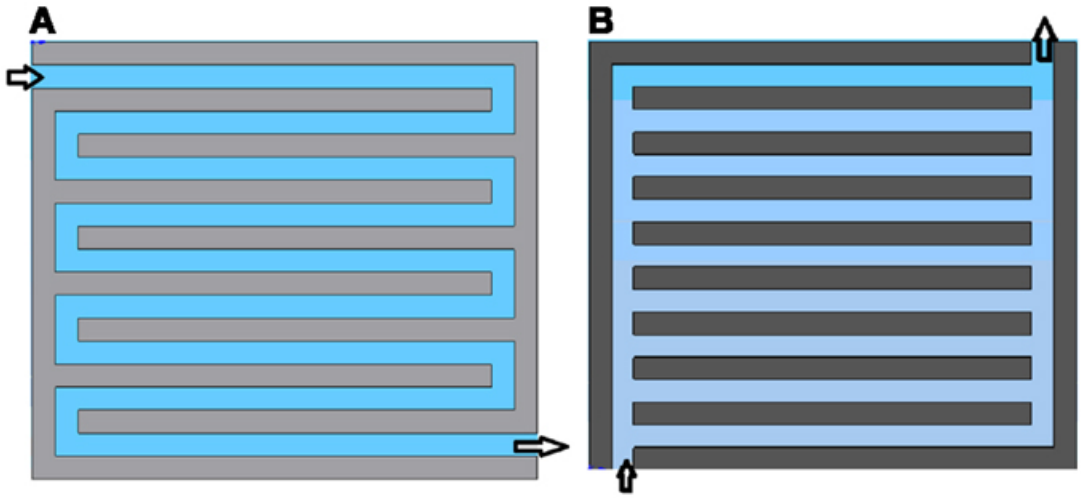

Figure 10- Flow field pattern. A serpentine, B parallel [**31**]

Geometry *a)* has the advantage of easy removal of reaction products (such as carbon dioxide or water). Geometry *b)* with parallel channels allows lower pressure losses while the geometry with serpentine cause higher pressure losses.

CATALYST LAYERS

The catalyst layers are the key part of the cell because they are responsible for the electrochemical reactions. They should be both high porous and conductive to allow reactants diffusion and the passage of electrons [**32**]. The thickness of this layer is usually in a range between 10 and 50 µm.

In the anode, a high quantity of catalyst is required due to the low kinetics of methanol oxidation: DMFCs have a catalyst load of around 3-4 mg cm^{-2}. As it can be seen from Fig. 11, methanol oxidation reaction occurs in four steps through a chain of intermediated reactions.

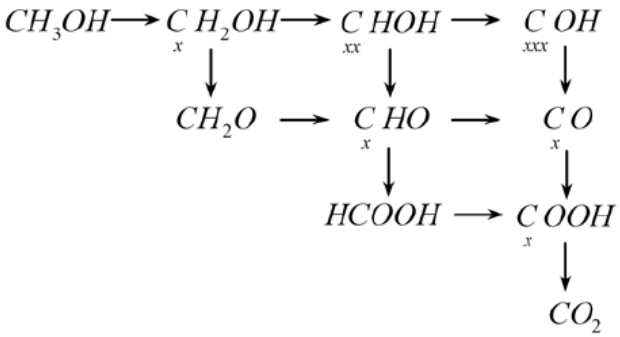

Figure 11-Intermediated reactions chain for methanol oxidation reaction [**33**]

The catalyst at the anode consists of a bimetallic system with Platinum and Ruthenium to improve the reaction kinetics. The most common alloy is Pt/Ru with a ratio 1:1. At the cathode, the catalyst is made of Platinum.

GAS DIFFUSION LAYERS

Gas Diffusion Layers are the thickest components of MEA, with thickness ranging between 100 and 400 µm, they are coupled to the Catalyst Layers and packed on both sides of the membrane with a thermal process.

They have a double role:

- Allowing the homogeneous diffusion of reactants towards the electrodes and the transport of reaction products from the catalyst towards the current collector channels.
- Promoting the conduction of the electrons from the catalyst towards the current collector at the anode (and vice versa at the cathode).

GDLs are made with porous carbon (Carbon Cloth or Carbon Paper) and sometimes with porous graphite. Carbon Paper is a material with a needle structure, obtained through sintering at high temperatures and produced with thin layers: it is a highly conductive, tough and with a low resiliency, it is useful for high compact cell design. Carbon Cloth is made as a carbon fiber texture, very flexible and thicker than Carbon Paper. The main advantage of Carbon Cloth is the tolerance to the compression, it makes the assembly operation of the MEA easier and it has a higher hydrophilicity than carbon paper.

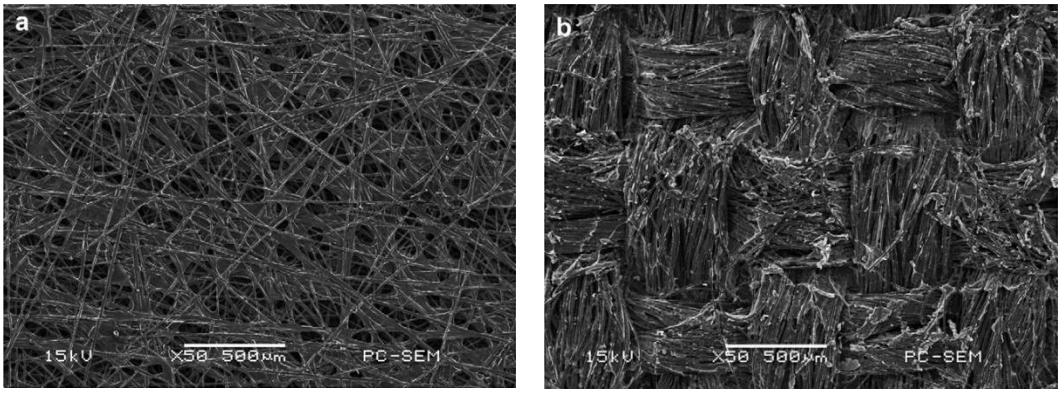

Figure 12-Microscopic structures of di a) Carbon Paper e b) Carbon *Cloth [**34**]*

A usual phenomenon occurring into the GDLs is the pores *"clogging"*, due to the low efficiency of the transport of the reaction products towards the external channels. It decreases the reactant flow towards the catalyst decreasing the global FC efficiency. In DMFCs, the porous media *"clogging"* is mainly due to the produced carbon dioxide, which hinders the transport of methanol and water through the GDL up to the catalyst layer. To reduce such issues, a hydrophobic material is usually added at the cathode while a hydrophilic material is added at the anode.

ELECTROLYTE MEMBRANE

In the PEMFCs, the electrolyte is a polymeric membrane that allows the selective transport of hydrogen ions moving from the anode to the cathode hindering the electron conduction. Ion transport from the anode to the cathode through the membrane is ruled by three mechanism:

1. Vehicular diffusion: due to the presence of a 'vehicle', which transports ions from one side to the other side. This action of transport is made by the water permeating the membrane.

2. Grotthuss diffusion: due to the continuous formation and breaking of covalent bonds between a water molecule and H^+ ions; water molecules close to the membrane, on the anode side, release a proton accepting a new one from oxidation anode reaction; the released proton bonds to an adjacent water molecule. This process continues until the proton reaches the cathode where it reacts with oxygen, producing the water.

3. Superficial diffusion: it is due to the continue formation and breaking of bonds between water and sulfonate groups which favour the ionic transport.

Grotthuss and vehicular diffusion are the most relevant mechanisms (Fig.13).

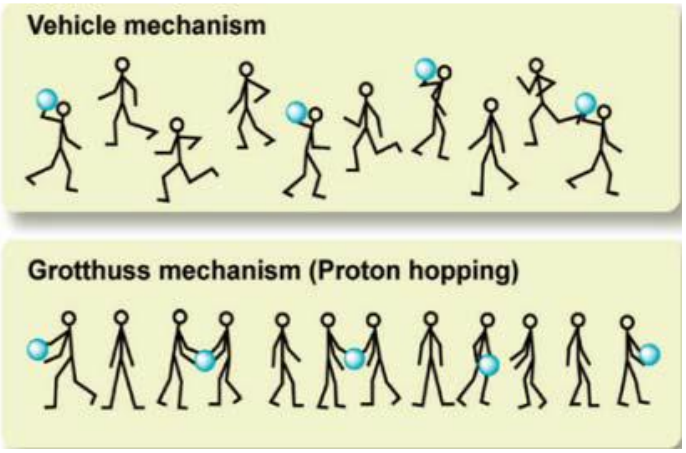

Figure 13--Grotthuss and vehicular mechanism comparison [**35**]

The most popular membranes are made of perflourosulfonic acid (PFSA) ionomers. The main characteristics and drawbacks of this material are described in the next section.

1.3 A Short Review on PFSA polymers (Nafion Polymers)

Nafion is a fluoropolymer made by sulfonated polytetrafluorethylene introduced by DuPont in the mid-1960s. It is commercially available with a thickness between 25 and 250 µm. As for Teflon, its structure (Figure 14) consists of CF_2 (difluorocarbene) radicals, alternated to $CFOCF_2$ and with end chains of sulfonic acid SO_2OH.

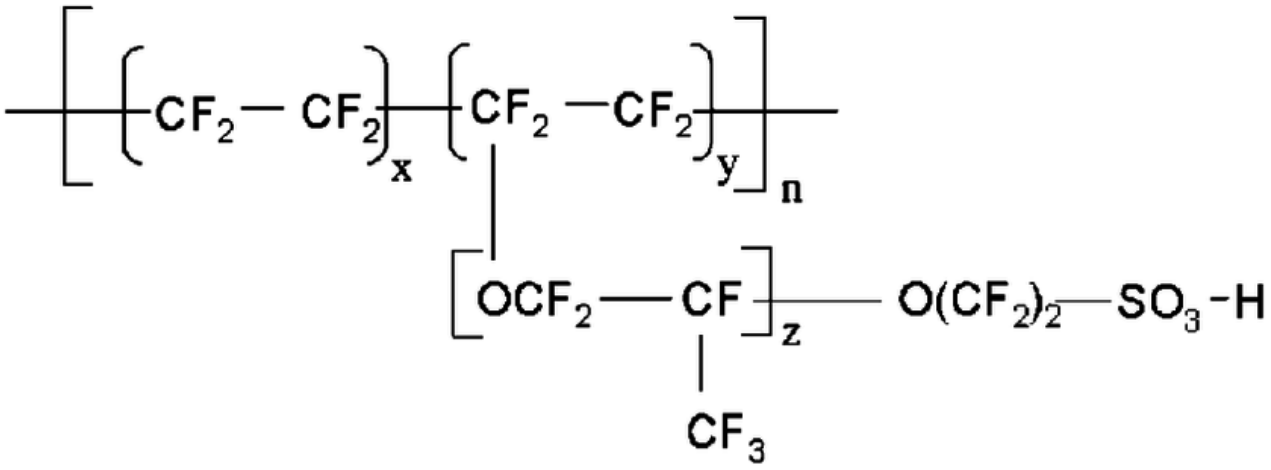

*Figure 14- Nafion polymer structure [**36**]*

Main Nafion characteristics are the following:

- High proton conductivity: when the pendant sulfonyl fluoride groups (SO_2F) are chemically converted to sulfonic acid (SO_3H), the ionic functionality is introduced [**37**].
- Water permeability.
- High chemical resistance: only alkaline metals as sodium can damage the Nafion at STP (standard temperature and pressure).
- High electronic resistance: forcing electrons to flow through the external circuit to generate electrical power.

In addition, regarding the use in DMFC, Nafion has high methanol permeability due to:

1. Active transport of protons and water.
2. Diffusion through the water-filled pores within the Nafion-structure.
3. Diffusion through the Nafion itself.

Various approaches to minimize or eliminate methanol crossover have been carried out: increasing membrane thickness [**38**], increasing the cathode reactant pressure [**39**], decreasing both cell temperature [**40**] and methanol concentration [**41**]. Another innovative way is to modify the membrane using materials that allow obtaining the same chemical and thermal characteristics of Nafion but with lower crossover and cost.

To overcome the drawbacks of Nafion membranes, composite membranes have been developed. A composite (or hybrid) material is defined as a material that includes two or more compounds blended at the

molecular scale [**42**]. The use of filler material (i.e. another polymer, ceramic, metal...) mixed into the Nafion matrix (or an alternative ionomer) provides additional properties such as mechanical reinforcement, chemical resistance, and proton conductivity. For instance, hydrophilic fillers help to increase membrane water uptake, optimal at low relative humidity (RH) operating conditions. These filler materials can also be functionalised to provide secondary functionalities (e.g., sulphonating a hydrophilic filler) or boost the functionality it already has. Another example is the use of cerium oxide that is used to slow down membrane degradation [**43**].

The following section describes and analyses studies found in literature focusing on the development of composite membranes to improve the performance of the DMFC.

2. Literature review

In this part, the range of composite membranes, that have been developed to improve the performance of the DMFC at low temperature with reduced methanol crossover and low cost, is reviewed.

Two categories of composite membrane materials are considered in the literature: modified Nafion and non-perfluorinated polymers.

2.1 Nafion-Based Membrane

Composite Nafion membranes can be loaded with organic and inorganic fillers that have been used predominantly to increase proton conductivity and to act as a barrier to methanol crossover [**44,45**]. The following sub-sections discuss the latest developments in the organic, inorganic and carbon nano-material filler-based membrane, paying particular attention to graphene oxide.

2.1.1 Organic Fillers

Organic materials are commonly used as fillers in the polymeric composite membrane for fuel cells. They supply reinforcement and allow higher stability of the polymer matrix while making it more cost-effective. One of the most applied organic filler is polytetrafluoroethylene (PTFE). PTFE is highly hydrophobic and although it is not suitable alone for membrane application for fuel cells [**46**], it can be used as a reinforcement of Nafion membrane due to its chemical stability, corrosion resistance and mechanical strength [**47**]. Few papers focused on testing DMFC performance using Nafion/PTFE membranes. Lin et al. [**48**] conducted a study on the application of this composite membrane; the authors investigated the effect of this polymer on conductivity, methanol crossover, and cell performance, and compared them with that of commercial Nafion membrane. Experimental data indicated that introducing PTFE into the Nafion polymer reduced both methanol diffusion and methanol electro-osmosis crossover in the membrane. The comparison between Nafion 117 and Nafion/PTFE was performed in a DMFC at 70°C: Nafion/PTFE membrane was able to operate in a wider current density range achieving a maximum power output of 87.5 mW cm^{-2}, 1.3 times higher than Nafion 117. This positive effect of the Nafion/PTFE membrane was also obtained by Nouel et al. [**49**] and Yu et al. [**50**] who tested a fuel cell MEA made of Nafion/PTFE comparing results with Nafion 117, 115 and 112. The performance was higher than Nafion 117 and 115 but similar to 112.

To further enhance the performance of Nafion/PTFE membrane, Chen et al. [**51**] included zirconium phosphate (ZrP) into the membrane structure and so the Nafion matrix was modified with both PTFE and ZrP/PTFE for comparison. The composite membranes were prepared via two processes:

1. By impregnating PTFE directly in a Nafion/$ZROCL_2$ solution and then annealing it at high temperature.

2. By impregnating the PTFE membrane in a Nafion solution, annealing at high temperature to prepare Nafion/PTFE membrane, then impregnating again in a $ZrOCL_2$ solution.

Experimental results indicated that the introduction of ZrP led to reduced methanol crossover and proton conductivity. The impact of proton conductivity is stronger than methanol crossover on DMFC performance, thus, as confirmed by tests conducted on the cell, the performance of ZrP/PTFE was lower than Nafion/PTFE.

Most research is focused on the preparation and modification of various proton conductive membranes that are inexpensive and provide better performance and properties than Nafion membranes. To this end, innovative organic materials, which have good thermal and chemical stability and can be easily modified to be used as ionic conductive membranes such as polybenzimidazole (PBI) and polyvinyl alcohols (PVA), were studied [**52,53**].

Shao et al. [**54**] and Mollà et al. [**55**] fabricated Nafion/PVA membranes using casting [**56**] and impregnation method [**57,58**] respectively. PVA has higher affinity for water than to methanol (i.e., 55 wt. % and 10 wt. %, respectively), so it can be potentially used for DMFC applications. Both works demonstrated that comparable DMFC performance can be obtained using these membranes. Specifically, Mollà et al. focused on the characterization of Nafion/PVA membranes with varying operating temperature (45, 70°C), thickness of the membrane (19-47μm) and concentration of methanol (1-2M). The performance of pristine Nafion membrane and Nafion/PVA were roughly equivalent at very low thickness while Nafion/PVA exceeded the pristine Nafion performance only at higher thickness and higher temperature. At any fixed condition, thickness, temperature and methanol concentration, the OCV of Nafion/PVA was higher than pristine Nafion indicating reduced methanol crossover.

Hobson et al. [**59**] presented Nafion-PBI dipped and screen-printed films to investigate the effect on membrane performance. They concluded that the modification of Nafion with PBI by both spin coating and dipping reduced the methanol permeability; however, the benefit of low methanol crossover was counterbalanced by the negative effect of the too high impedance. Since neither of the techniques produced a suitable membrane for DMFC, screen printing was investigated and here methanol permeability was

reduced without an increase in impedance. The membranes were then tested in a single cell at 60°C. Using methanol solution of 3.2 M, the cell performance was greatly improved with the current density increased by 42% combined with an increase in maximum power output by 46% as compared with the pristine Nafion membrane. Ainla et al. [**60**] work on Nafion-PBI membrane was in agreement with the above results. In fact, they demonstrated that the Nafion-PBI membrane has lower methanol permeability and higher conductivity than a commercial membrane. It is important to note that the utilization of these composite membranes led to lower methanol permeability and enhanced the performance only at high methanol concentration.

Conductive Polymers such as polyaniline (PANI) and polypyrrole (PPy) have recently been incorporated into Nafion membranes to reduce its methanol permeability [**61,62**]. Composite Nafion polypyrrole membranes were prepared by two methods: electrodeposition of polypyrrole on Nafion-coated electrodes [**63**] or by in situ polymerization with a chemical oxidant [**64**]. Zhu et al. [**65**] made a membrane by in situ polymerization using Fe(III) and H_2O_2 as oxidising agents. The electrostatic interaction between the sulphonate groups of Nafion and polypyrrole decreased the pore volume of Nafion membrane which led to low methanol permeability. However, the electrostatic interaction between the polypyrrole chains and sulphonate groups of Nafion also decreased the proton conductivity and therefore increased membrane and cell resistances. So, the benefit of the reduced methanol crossover was neutralized particularly when DMFC worked at high current densities.

Polyaniline is a good conductive polymer that can improve both methanol oxidation and the stability of the catalyst; it can also be included in the Nafion structure through both electrochemical and chemical modification to improve its properties. Wang et al. [**66**] and Escudero-Cid et al. [**67**] assembled a composite membrane of Nafion/polyanilina and carried out DMFC performance tests including polarization curve and durability tests showing that both the ionic conductivity and methanol permeability of the Nafion membrane containing PANI decreased when compared with Nafion membrane. In particular, Wang et al. indicated that the performance of the fuel cell increased using the modified membrane especially at high methanol concentration (maximum power output at 6 M) while the power output using Nafion pristine membrane was reduced with increasing methanol concentration. Moreover, it was noted that the PANI composite membrane performed better than that with polypyrrole [**68**]. It is important to highlight here that the reviewed papers investigating the use of conductive polymers do not consider the change in the electronic conductivity of the membrane (short circuit current) in the composite membrane. This should be considered in any future work on these materials.

In recent years, two types of sulphonate fillers, sulphonate poly arylene ether ketone (SPAEK), and sulphonate poly ether ether ketone (SPEEK) have been developed and used to modify the Nafion membrane in DMFCs. Both SPAEK and SPEEK have good attributes: high proton conductivity and methanol resistance for SPAEK [**69,70**], good mechanical properties, proton conductivity, and good processing capacity of SPEEK polymers [**71,72**]. Regarding the behaviour in a methanol fuel cell [**73,74**], an increase by at least 30% in OCV and by 10% in highest power density were observed. The positive results suggest that these membranes could be taken into account for use in future DMFC application once durability is deeply investigated.

2.1.2 Inorganic Fillers

The implementation of inorganic particles into Nafion helps enhance the thermal stability and proton conductivity of composite membranes making them more attractive and appropriate than bare Nafion membranes [**75**]. This section focuses on silica, metal oxides, montmorillonite and zeolite fluorinated composite membranes; materials that have received considerable attention due to their chemical and thermal properties.

Silica materials have attracted a considerable attention because they possess high surface area and high chemical stability [**76**]. Generally, they are prepared using different precursors such as alkoxy silanes (like tetraethyl orthosilicate (TEOS)), sodium metasilicate and fumed silica [**77**]. The addition of silica compounds into polymer membrane is believed to lower methanol crossover [**78,79**]. In this context, Ren et al. [**80**] prepared a composite membrane modifying Nafion polymer with tetraethyl orthosilicate (TEOS) and sulfonic TEOS using the casting method. They investigated the influence of silica into Nafion matrix and the changes in proton conductivity, methanol permeability, and performance. The results showed that the proton conductivity of these composite membranes was lower than that of commercial Nafion membranes due to the hydrophobic side chain of the TEOS that reduced the water content of the membrane. However, the methanol permeability was also reduced. DMFC single cell tests were carried out at both 1 M and 5 M and at 75°C. The polarization curves depicted how the silica composite membrane could achieve better performance than the Nafion when using high methanol concentration because, although the proton conductivity of the composite membrane decreased, the methanol permeability also reduced. Works are necessary to increase proton conductivity of those composite membranes.

Some studies have been carried out to investigate experimentally the effect of Nafion membranes with metal oxides, such as SiO_2, TiO_2, WO_3, as fillers on the performance of DMFCs [**81**]. As a result of these experiments,

the Nafion-modified composite membranes provided higher power density in comparison to the commercial Nafion 115 membrane. Regarding the application in a DMFC, Nafion/TiO_2 improved water uptake and reduced methanol absorbance [**82**] while Nafion/SiO2 showed lower methanol permeability than commercial membrane [**83**]. Moreover, Nafion membrane modified with both SiO_2 and TiO_2 were prepared by solvent casting method and studied by Ercelik et al. [**84**], that investigated the effect of these particles on proton conductivity, water uptake, and performance varying temperature. The authors claimed that:

- proton conductivity of Nafion-TiO_2/SiO_2 increased with temperature. The maximum value obtained was 0.255 S cm^{-1} which is 25% higher than Nafion 117 at 75°C.
- water uptake values are similar with those of bare Nafion.
- power densities of MEAs with composite membranes are higher than the MEAs using Nafion 115: at 80°C and 1M of methanol concentration. The maximum power densities obtained by Nafion/TiO_2, Nafion/SiO_2 and by the MEA with bare Nafion are 641.16 W/m^2, 628.68 W/m^2 and 612.96 W/m^2, respectively.

The abovementioned studies demonstrated that the incorporation of inorganic particles like SiO_2 and TiO_2 provided better performance if compared with the Nafion membrane. Although, the use of metal oxides as filler has enabled many advantages, they too have some problems associated with them. The metal particles are often very difficult to disperse homogenously in the polymer membrane and it would mean that the performance of the composite will not be uniform throughout the bulk of the membrane. Moreover, metal oxides accelerate the degradation of membranes, and so durability studies are required to understand the actual benefits and drawbacks of these fillers.

Montmorillite (MMT) is a filler that has attracted much attention recently as Nafion/MMT membranes have been reported to have improved mechanical and thermal properties compared to pristine Nafion membranes [**85**]. But the incorporation of this filler into the Nafion matrix does not improve the proton conductivity. Wu et al. [**86**] prepared the composite membrane via casting solution and reported a slight decrease (about 9%) in proton conductivity compared with pristine Nafion but the methanol crossover decreased more than 90% by loading MMT of only 1% wt [**87**]. As described above, the utilization of this filler does not contribute to improve the proton conductivity, thus, to minimize the loss in performance Rhee et al. [**88**] and Lin et al. [**89**] modified the montmorillonite with an organic sulfonic acid group (MMT-SO_3H) varying the content of the filler. Their studies showed that the proton conductivity of the composite membranes generally declined from that of pristine Nafion membrane with the increase in the inorganic filler

content, but the methanol permeability was reduced by up to 90%. The combination of these effects led to an improvement in the performance of a DMFC. In fact, the polarization curve of the MEA with Nafion 115 and composite membrane, realized at 40°C and 2M of methanol concentration, showed that the performance of the DMFC improves initially with increasing the inorganic content, with a maximum power density at 5 wt. % loading. Curves revealed that all composite membranes achieved better performance than Nafion membrane at high current density region. However, the thermal stability of the membrane is not yet adequate and performance at higher temperature and methanol concentration deserves to be investigated.

To hinder permeation of methanol, another approach is to develop composite membranes using zeolites. Zeolites are micro porous crystalline materials containing silicon, aluminium and oxygen in their framework. They are based on an infinitely extending three-dimensional network of AlO_4 and SiO_4 tetrahedra linked by sharing oxygen atoms [**90,91**]. The chemical structural formula of a zeolite may be expressed by the following [**92**]:

$$Mx/n[(AlO2)_x(SiO2)_y]m\ H_2O$$

where M is a cation of valence n, m is the number of water molecules and the sum of x and y is the total number of tetrahedra in the unit cell.

Several authors [**93,94**] have claimed that zeolite membranes can be adopted for DMFC application. The approach of these studies was to take advantage of the molecular sieving property of zeolite to prevent methanol from passing through the membrane. However, a pure zeolite exhibits poor mechanical properties, such as brittleness and fragility, and hence is unsuitable for use as a membrane. Moreover, the performance of the zeolite composite membranes depends on the zeolite properties in terms of pore size and surface tension (hydrophobility or hydropholicity). It was reported that hydrophobic zeolites ensure low affinity to water so high permeability to methanol, however, hydrophilic zeolites lead to an opposite trend and therefore reduce methanol crossover [**95**]. When zeolites are combined with a polymer support (e.g., Nafion), the advantages of both polymer and zeolite are combined. Among the various type of zeolites, mordenite (MOR) and analcime (ANA) have attracted a lot of interest because they are hydrophilic substances that promote the adsorption of water, excluding alcohol, and provide a good proton pathway through the membrane. Prapainainara et al. [**96**] fabricated composite membranes with those two fillers studying and compared their properties and performance. The authors claimed that the presence of the filler benefited the proton migration through the membrane whilst the homogeneous distribution of the filler contributed to block the flow of methanol through the membrane, leading to lower methanol permeability.

The composite membrane with MOR filler gave better membrane properties, higher proton conductivity and lower methanol permeability, than those using ANA filler. The best DMFC performance was achieved by MOR composite membrane with a maximum power density of 10.75 mW/cm^2, 1.5 times higher than ANA membrane and 2 times higher than a commercial Nafion 117 membrane.

To enhance the performance of MOR/Nafion, Prapainainara et al. [**97**] incorporated graphene oxide (GO) to the matrix. The authors used GO to modify the surface of MOR by increasing the surface hydrophilic functional groups resulting in better incorporation of MOR to Nafion and comparable chemical properties with those of pristine Nafion and MOR/Nafion. The use of GO led to better proton conductivity, 1.5 times higher than that of Nafion/MOR and Nafion 117 at 70°C and it had the lowest methanol permeability too. The authors also tested the membrane in a single cell, obtaining a power density of 27.5 mW/cm^2; almost 5 times than that of Nafion 117 at the same operating condition (1 M methanol, 70°C). However, the operation lifetime was still not good enough for commercial applications.

2.1.3. Carbon Nanomaterial Fillers-Graphene oxide

Graphene oxide (GO) is a novel material, particularly attractive to be used as a filler because it can allow easy proton transport and a good water uptake due to its high surface area. It is a single graphene sheet with a carbon to oxygen ratio of approximately 2:1 [**98**]. Graphene sheets are separated from graphite stack when oxidation breaks π-π bond to form sp^2 graphitic domains, which is normally surrounded by sp^3 domains that involves oxygen groups. The different oxygen groups such as epoxide, hydroxide, carbonyls and carboxyls convert GO into insulating and hydrophilic material [**99**] while retain other properties like mechanical strength, surface area and gas impermeability. Moreover, graphene oxide has an excellent compatibility with Nafion, so it can be adopted as a modifier to improve the selectivity (to allow the passage of specific species), particularly meaningful for direct methanol fuel cell, and performance of such membranes. There are many methods to prepare those composite membrane, each of which has its pros and cons. Some of these, will be discussed briefly in the next section, before looking out at the application of graphene oxide in PEM fuel cell (both methanol and hydrogen).

<u>Preparation of GO membranes</u>

Different preparation method will be described briefly as follows:

- Vacuum filtration method is one of the simplest methods to prepare GO membrane and to control the thickness of the membrane. It consists on the uniform dispersion of the material in solvent and

then deposited on the substrate under vacuum filtration condition. Although the vacuum filtration method has the advantage of easy operation, it is difficult to prepare a large-area membrane by this method [**100**].

- Layer-by-layer self-assembly method (LBL) is carried out in aqueous solution without any organic solvents as vacuum filtration; it is based on the electrostatic interaction between ions that acts as the driving force of membrane formation. This method is suitable for preparing a very thin membrane, and the thickness is very uniform [**101**].

- Spin coating is a technique used to deposit uniform thin films to flat substrates. Usually, a small amount of coating material is applied on the centre of the substrate, which is either spinning at low speed or not spinning at all. The substrate is then rotated at high speed in order to spread the coating material by centrifugal force. This method allows to prepare large area and ultra-thin GO membrane with excellent mechanical properties [**102**].

- Dip coating: the substrate is soaked in a solution of graphene-based material, and then the substrate is taken out by a lifting machine after immersion is finished, and the graphene-based membrane is formed on the surface of the substrate after drying. Poor control over the membrane thickness is one of the issues of this method [**103**].

- Spraying is the process of using an airbrush to spray a graphene-based solution to a preheated substrate and the graphene-based membranes are obtained after solvent evaporation. This method can be used to prepare large-area membranes, but the uniformity of the membrane is not very good [**104**].

- Casting is a simple method that is characterized by pouring polymer and solvent solution into a flat surface. The solvent evaporation is obtained by utilising time and/or temperature. After the

evaporation, the polymer remains on the flat surface, forming a membrane or film. The method is highly scalable and produces highly continuous GO membranes but GO sheets can be deposited non uniformly and the membrane thickness is poor controlled [**105**].

Application in DMFC

As mentioned above, the most important benefit when using the graphene oxide in direct methanol fuel cell, is the reduction of methanol crossover. However, the addition of GO lowers the proton conductivity. A lot of researchers focused on how the properties of the membrane change with different GO loading and how a good balance between reduction of methanol crossover and proton conductivity should be chosen. Choi, et al. [**106**] developed a composite GO/ Nafion membrane. The authors claimed that the compatibility between both components was guaranteed by their strong interfacial attraction. GO enhanced thermal backbone and side chains stabilities due to the interaction between GO sheets and Nafion: the non-polar backbone of Nafion interacted with the hydrophobic structure of GO while the polar ionic clusters of Nafion with the hydrophilic groups of GO. Their study revealed that the permeability for methanol with just 0.5 wt.% of GO was reduced to 60.2% of Nafion 112 at 25 °C. However, the proton conductivity tests revealed an opposite trend showing a decrease with increasing the GO filler content and a loss of 55.3% in proton conductivity is reported with 2 wt. % GO loading. This was not completely unexpected as GO alone is not known to be an excellent proton conductor. The authors obtained the maximum power density of 62 mW cm^{-2} at 30 °C and 141 mW cm^{-2} at 70 °C after optimising the GO loading in the membrane (0.5% wt.) as depicted in Figure 15.

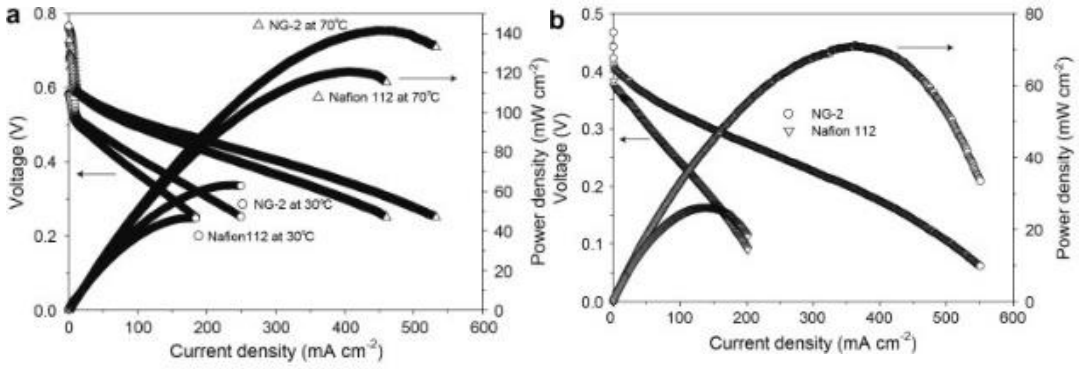

*Figure 15-Polarization curves of DMFC obtained for Nafion 112 and GO composite membranes at (a) 1M methanol at 30°C and 70°C and (b) 5M methanol at 30°C [**106**].*

Moreover, at high methanol concentration, where methanol crossover becomes critical, benefits provided from the incorporation of graphene oxide were more evident: the composite membrane showed much higher power density, 3 times higher than Nafion (71 mW cm^{-2} vs 26 mW cm^{-2}).

Chien, et al. [**107**] prepared a composite membrane with sulphonated graphene oxide (SGO)/Nafion for DMFC to avoid the aggregation of GO in the polymer matrix. It was reported that proton conductivity increases with increasing amounts of SGO, as the SGO was distributed throughout the matrix and created more interconnected transfer channels. However, with further SGO amounts, aggregation began to predominate, thus reducing the conductivity of the composite membrane. Methanol permeability was shown to decrease in the presence of SGO as they block the methanol migration through the membrane. In DMFC test, the SGO/Nafion composite membrane exhibited higher current and power densities than commercial Nafion 115, for example:

- in 1 M methanol solution, the current density and power density for the composite membrane at 0.4 V were 102.7 mA cm^{-2} and 42.9 mW cm^{-2}, whereas the commercial Nafion 115 revealed only 78.6 mA cm^{-2} and 32.6 mW cm^{-2}.

- in 5 M methanol solution, the composite membrane showed values of 83.2 mA cm^{-2} (at 0.4 V) and 34.6 mW cm^{-2}, which were better than the commercial membrane (54.1 mA cm^{-2} at 0.4 V and 22.1 mW cm^{-2}).

Additionally, the SGO/Nafion composite membrane had a lower catalyst activation loss than Nafion 115, which indicated that the composite membrane had lower methanol crossover and faster reaction kinetics.

Yan et al. [**108**] proposed an innovative way to modify Nafion membrane by sandwiching a graphene oxide layer between two Nafion membranes. With the addition of a monolayer graphene film, methanol permeability decreased by 68.6% while observing only a marginal decrease in proton conductivity of 7% at 80°C in comparison to pristine Nafion membrane. The authors tested the membrane in a DMFC varying methanol solution from 5 M to 15 M. Tests depicted that the graphene film allowed for a substantial performance improvement particularly when the passive DMFC was fed with high concentration methanol solutions enabling the passive DMFC to be operated at high concentrations.

Beside the Direct Methanol Fuel Cells, GO can be used also for hydrogen fuel cells. As mentioned above, the incorporation of GO increases the mechanical properties of the membrane as well as the gas impermeability allowing to work at high temperature using low membrane thickness. In the following section, a brief description about the use of the GO in the hydrogen fuel cell technology.

Application in PEMFC

Kumar et al. [**109**] prepared a GO/Nafion membrane for PEMFCs operation. Addition of GO in 2, 4, and 6% loading in the Nafion matrix led to an increase in water uptake from 21.1 to 27.9, 37.2 and 36.1% respectively. In addition, ion exchange capacity (IEC) changed from 0.891 to 1.21, 1.38 and 1.26 meq g^{-1} respectively. The authors argued that there is an optimum quantity of filler and any addition would result in increased membrane stiffness and subsequently reduced water uptake. Fuel cell tests at 100°C and 25% RH showed that the 4% GO composite membrane outperformed the reference recast Nafion by nearly 4 times (212 mW cm^{-2} to 56 mW cm^{-2}). Sahu et al. [**110**] functionalised graphene with sulfonic acid groups inside a Nafion matrix for low relative humidity operation. This is attractive use of graphene oxide as the sulfonation procedure would have reduced the hydrophobicity of the graphene filler making it more hydrophilic. This is shown in the water uptake and IEC tests: the addition of graphene slightly increases the water uptake up to 21.4%. while the recast Nafion had a water uptake of 20.1%. However, the introduction of sulphonated graphene, in 0.5, 1 and 1.5% loading results in improved water uptakes of 24.5, 27.3 and 29.2% respectively. The IEC values are: 0.88, 0.89, 0.92, 0.96 and 0.95 meq g−1 respectively. A similar trend was also observed with the proton conductivity, with the 1% sulphonated graphene having the best performance. Fuel cell testing at 70°C and 20% RH revealed that the composite membrane with sulphonated graphene (1%) produced a maximum power density of 300 mW cm^{-2} , whereas recast Nafion and Nafion-graphene (1%) produced peak power densities of 220 mW and 246 mW cm^{-2} respectively. Lee et al. [**111**] prepared Nafion/GO and a novel Pt on graphene/Nafion composite membranes for low humidity PEMFCs. The idea behind using platinum on graphene as a filler is to use platinum as a reaction site to produce water and "self-humidify" the membrane. Water uptake experiments showed that the GO composite membrane outperformed the pristine Nafion sample. In comparison, the Pt/Graphene filler led to a drop in water uptake. This is because of the less hydrophilic nature of platinum as well as the GO being reduced to graphene in the synthesis step. However, the Pt/Graphene membrane had a greater proton conductivity compared to the other two membranes, which was explained via the electronic tunnel effect. The GO composite had a lower proton conductivity due to the filler impeding the ionic pathways, but this issue was resolved when the loading was greater than 3%, resulting in an increase in proton conductivity. The GO/Nafion membrane was tested at 80 ◦C and under a range of RH. At 40% RH, the peak power densities of the membranes with different GO loadings were all around 0.5-0.6 W cm^{-2}. On the other hand, the Pt/Graphene membrane gave disappointing current output under anhydrous conditions, with peak current densities of 0.27, 0.36 and 0.14 A cm^{-2} for 0.5, 3 and 4% loading respectively. The authors followed up this work with designing a composite

membrane with platinum on graphene in addition to silicon dioxide to improve the "self-humidifying" capabilities of the membrane by using the silica to retain the water produced by the platinum-graphene [**112**]. The water uptake and proton conductivity of these novel membranes increased with increasing silica content. Maximum water uptake of 30% was achieved with 3% Pt-G and 3% silica content. Fuel cell experiments showed that the addition of silica improved the polarisation curve. However, performance dropped with too much silica at low RH, which the authors explain is possibly due to the filler blocking the ionic pathways. Filler optimisation was concluded by the authors, as increases in Pt-G loading also resulted in a drop in performance. Yang et al. [**113**] fabricated a composite membrane with platinum deposited on titania, which is then incorporated with graphene oxide into a Nafion polymer matrix. The composite membranes displayed a better IEC than recast Nafion, with increased until 20% GO is reached, where the IEC began to decrease beyond that. The proton conductivity followed a similar trend to the IEC, which also decrease past 20% GO loading. Fuel cell testing with varying levels of RH showed that the Pt-TiO2 improved the fuel cell performance, however the authors noted that this was still not enough at zero RH. Adding the GO led to an even greater improvement in cell polarisation. Nafion/0.8Pt–TiO2/0.2GO generated a current density of 0.54 A cm^{-2} at 0.6 V at 0% RH, which compared to Nafion/Pt–TiO_2 that produced a current density of 0.01 A cm^{-2} at the same RH. Furthermore, the introduction of GO not only improved the current density generation, but also helped alleviate significant OCV loss when the humidity was lowered. Kim et al. [**114**] fabricated a GO/Nafion composite where the GO is modified with phosphotungstic acid (H3[PW12O40] ·29H2O) to aid water uptake and proton conduction at low relative humidity PEMFC operation [**115**]. Fuel cell testing at 80 ◦C and 20% RH showed that the composite membrane with modified GO produced a maximum power density of 841 mW cm^{-2} , which is a great improvement in comparison to non-acid doped Nafion/GO which generated 488 mW cm^{-2} , and 208 mW cm^{-2} for recast Nafion.

Maiti et al. [**116**] synthesised a composite Nafion membrane comprising of graphene oxide and an ionic liquid (dihydrogen phosphate functionalised imidazolium) for high temperature PEMFCs. Thermogravimetric analysis (TGA) shows that the ionic liquid is stable up to 230 °C, which is more than enough for high temperature operation. The composite membranes displayed greater proton conductivity compared to Nafion 117 throughout the entire temperature range tested (70-110 °C). This improved performance was carried through to the single cell test where the composite membrane generated higher current densities in comparison to the Nafion 117 MEA (at 110 ◦C and dry conditions). Branco et al. [**117**] investigated the performance of multilayer membranes for intermediate temperature-PEFC applications. Multilayer membranes with two external Nafion outer layers and an inner layer of graphene oxide and another with

sulphonated polyindene were fabricated with solution casting and hot-pressing methods. The solution casting protocol involves heating the first Nafion layer at 100 ◦C for two hours to remove the solvents in the Nafion dispersion, followed by the addition of the graphene oxide solution/sulphonated polyindene (in deionized water) and another two hours at the same temperature. Lastly, the final Nafion layer was added and the multilayer membrane was heat treated for one hour at 120 ◦C. The increased temperature is to anneal the polymer. Multilayer membranes that were casted displayed better performance and proton conductivity than the hot-pressed multilayer membranes. This was explained by the casted membranes having better interface interaction compared to the hot-pressed membranes, which suffered delamination. Multilayer membranes with sulphonated polyindene showed higher performance than Nafion at 120 ◦C.

Ibrahim et al. [**118**] studied the behaviour of GO composite membranes fabricated via solution casting with different thicknesses at intermediate operating temperatures. The composite membranes had improved mechanical strength and a higher water uptake in comparison to pristine Nafion. In-situ fuel cell testing of the membranes as MEAs revealed that the 30 µm composite membrane at 100 and 120 ◦C outperformed the 50 µm Nafion membrane at 80 ◦C. This is most likely due to the reduction in thickness and the GO filler retaining more water, hence reducing the drop in proton conductivity.

2.2. Non-Perfluorinated Polymers Composite Membranes

Non-fluorinated membranes seem to have a promising future for DMFCs as a replacement for the expensive fluorinated membranes that have high methanol and ruthenium crossover [**119**]. Aromatic polymers are one of the most promising routes to obtain high performance polymer electrolytes because of their availability, variety of chemical composition and stability in the cell environments. Specifically, poly ether ether ketone, polyvinyl alcohol, and poly arylene ether and their derivatives are currently under investigation.

Poly (ether ether ketone)s (PEEKs) [**120**] are semicrystalline polymers that present high thermal and chemical stability. The sulfonation of PEEK produces copolymers with sulfonic acids into the aromatic backbone; membranes made of these sulfonated polymers show useful properties for DMFCs, such as: low methanol cross-over, good ion conductivity, thermal stability, and high mechanical strength [**121**]. The proton conductivity of SPEEK depends on the sulfonation degree [**122**], it generally increases with the sulfonation degree but high sulfonation results in high methanol permeability so that its application is limited [**123**]. The development of SPEEK composite membranes is currently being investigated by using SPEEK for the polymer

matrix and modifying it in order to reduce methanol permeability at high sulfonation degree. Many researches have focused on SPEEK-based membrane with phenoxy resin [**124**], polyphenylsulfone (PPSU) [**125**], solid heteropolyacids [**126**], polyaniline [**127**], SiO2 and zirconium phosphate (ZrP) [**128**], zeolite [**129**], polypyrrole [**130**]. As discussed above, the utilization of montmorillonite and polybenzimidazole into Nafion matrix improved the DMFC performance; in the same way, they can be used to modify the matrix of SPEEK polymer. In fact, Gosalawit et al. [**131**] used a SPEEK/MMT membrane in their work and compared its performance in a DMFC single cell with pristine SPEEK membrane and Nafion bare membrane. The study confirmed that the performance was higher: current density generated from the MEAs of Nafion 117, SPEEK, SPEEK/MMT 1wt.%, SPEEK/MMT 3wt.% and SPEEK/MMT 5 wt.% membranes at the constant voltage of 0.2V were 51, 76, 103, 96 and 94mAcm^{-2}, respectively with the maximum power density of 10, 15, 21, 19 and 18mWcm^{-2}. However, the thermal stability was significantly reduced. Pasupathi et al. [**132**] synthetized a non-perfluorinated membrane by casting SPEEK and PBI solution into a glass plate. A SPEEK/PBI membrane enhanced DMFC performance: the maximum power density obtained (45 mW cm^2) was two times higher than Nafion 117 at 60°C. Moreover, SPEEK/PBI membranes were found to be extremely stable under DMFC operating conditions up to 60 °C. However, their stability dropped considerably at higher temperatures. Experiments are underway to address the stability issue of these membranes at higher temperatures.

Generally, sulfonated aromatic polymer membranes require a high sulfonation level to achieve sufficient proton conductivity resulting from the low acidity of the sulfonic groups in the aromatic rings [**133**]. However, such a high sulfonation level usually makes them excessively swell and even soluble in methanol/water solution, which may lead to a loss in mechanical properties and become unavailable in applications [**134**]. Therefore, they should be modified including organic or inorganic fillers. Jiang et al. [**135**] investigated the performance of a SPEEK/GO membrane in which GO is sulfonated (SGO) to improve the proton conductivity of the membrane. In fact, the SPEEK/GO membranes exhibit lower ion exchange capacity (IEC) and water uptake than Nafion membrane, and the overall proton conductivity of the membranes remains low. This is due to the lack of proton conductive groups on the pristine GO. Therefore, these membranes are still not quite suitable for use as PEMs in DMFCs. However, by using higher contents of sulfonated GO, these SPEEK/SGO membranes showed even higher IEC and proton conductivity compared to Nafion 112, which makes them particularly attractive as PEMs for the DMFC applications. It is worth noting however that the swelling ratio of membranes increased with the increase of the content of the SGO. DMFCs with SPEEK/SGO showed better performance than those with the plain SPEEK or the pristine SPEEK/GO. With the optimized contents of SGO in SPEEK (3% and 5% wt.), the DMFCs exhibited 38 and 17%, respectively, higher

performance than those with Nafion 112 and Nafion 115. Despite having higher IECs and proton conductivity, the membranes with higher content of the SGO exhibited higher methanol permeability leading to a decrease of the fuel utility and the lifetime of the cathode catalysts, thus low performance. In this regard, for practical applications of the SPEEK/SGO membranes, the contents of SGO in the SPEEK matrices should be well controlled.

Sulfonated Poly (arylene ether sulfone) membranes (SPAES) can be useful for methanol fuel cell through the modification of the polymer matrix by introducing inorganic/organic particles such as laponite. Laponite is made of silica tetrahedral and alumina octahedral sheets which have advantageous hygroscopic properties [**136**]. This inorganic compound was used by Kim et al. [**137**] to prepare and evaluate the behaviour of the SPAES membrane. Properties of the hybrid membranes for DMFC, such as methanol permeability and proton conductivity, were investigated. Authors claimed that methanol permeability was lower than that of a SPAES pure membrane and Nafion using membranes with a small content of Laponite. This is because the presence of Laponite improved the barrier property of the membrane to methanol molecules. This was likely due to the tortuosity of layered silicate and the lower aspect ratio of the particles resulting from their exfoliation increasing methanol diffusion paths through the composite membrane. However, the proton conductivity was very low and further research should be conducted to optimise Laponite loading.

Another approach to reduce the undesired swelling property and methanol crossover of sulfonated membrane is to crosslink membranes. This method has been widely investigated by many researchers for crosslinking SPEEK membranes [**138,139**]. These membranes showed decreased swelling ratio and methanol crossover but decreasing proton conductivity. Following this method, Feng et al. [**140**] used sufonated poly (arylene ether)s as PEM materials due to their good thermal stability, high glass transition and excellent mechanical strength. They synthesized sulfonated poly (arylene ether sulfone) copolymers with propenyl groups then crosslinked using benzoyl peroxide varying the crosslinking. Proton conductivity and methanol permeability were evaluated and compared with Nafion 117, and showed that:

- the proton conductivity of the SPAES membranes increased from 0.1 to 0.16 S/cm with the increase of temperature from 30 to 70°C which was quite similar to that of Nafion 117: 0.11 to 0.17 S/cm from 30 to 70 °C [**141**].

- the methanol permeability evaluated was lower than that of Nafion117 (2.07×10^{-6} cm^2/s): the less pronounced hydrophobic/hydrophilic separation of sulfonated polyaryls compared to Nafion corresponded

to narrower, less connected hydrophilic channels and larger separations of the less acidic sulfonic acid functional groups, which affected the permeability of methanol [**142**].

Poly vinyl alcohol (PVA) is usually synthesized from poly vinyl acetate and commonly used for adhesive, food wrapping, and desalination and pervaporation membranes [**143**]. Regarding the possible use of a membrane made of PVA in DMFC, it is known that PVA does not have any negative charged ions, like carboxylic and sulfonic acid groups, so the conductivity is very low if, when compared with Nafion membrane. Therefore, PVA membranes can be used in a fuel cell if negative ions are incorporated within their structure to increase their conductivity [**144**]. Moreover, several studies have shown how PVA polymer membrane leads to a reduced methanol crossover [**145**]. Regarding the reduction of methanol crossover, it was demonstrated that the addition of filler into PVA matrix contributes to mitigate this issue: fillers such as SiO_2 [**146**], polyrataxane [**147**] were reported. Yang et al. [**148**] used montmorillonite (MMT) as a filler and tested ion conductivity, methanol permeability, current density-potential and power density curves of the PVA/MMT composite polymer showing the following properties:

- high ionic conductivity: 0.0368 S cm^{-1}, performed by PVA/10wt.%MMT at 30 °C;
- methanol permeability: 3–4 × 10^{-6} cm^2 s^{-1}, which was lower than that of Nafion 117 membrane of 5.8 × 10^{-6} cm^2 s^{-1};
- maximum peak power density: 6.77 mW cm^{-2} at ambient pressure and temperature with the PtRu anode based on Ti-mesh in a 2M H_2SO_4 +2M CH_3OH solution.

2.2.1 Other Composite Non-Fluorinated Membranes

The modified polyvinylidene fluoride (PVDF) membranes using inorganic additives were prepared with a view of combining the properties of inorganic ion exchanger (high thermal stability and excellent water holding capacity at higher temperatures) and organic support (chemically stability and high mechanical strength). Impregnation of porous polymeric film of PVDF is the method used by Pandey et al. [**149,150**] to synthesize PVDF/silica and PVDF/Zirconium phosphate (ZrP). Single cell DMFC tests were carried out to study the DMFC performance for the synthesized membrane. The membranes showed better thermal stability, water uptake ratio and lower methanol crossover than Nafion 117, however, performance were low because of poor proton conductivity.

PolyFuel Inc. produced polycarbon membrane for passive DMFC [**151**] showing a power density of 80 mW cm^{-2} for thickness of 45µm, lifetime for a nearly constant runtime is 5000 h and back diffusion of water was improved by 30%, which helped mediate the dissolution of the methanol concentration in a passive DMFC.

There are also other composite membranes developed for PEMFC applications which may also have a good prospect for DMFC. These include trifluorostyrene-based membranes developed by Ballard Power System Inc [**152**], a butadiene/stryene rubber-based membrane developed by Hoku Scientific Inc [**153**] and polystyrene sulfonate (PSS) membranes [**154**]. Table 2 summarizes the properties and the pros and cons of composite electrolyte membranes described in this review compared to those of the commercial membrane. In addition, Table 3 summarizes their DMFC best performance.

. Table 2-Summary of DMFC composite membrane properties

Membrane	Preparation method	Pros	Cons
Nafion/PTFE	Impregnation	Low methanol permeability	Decreased conductivity
Nafion/PVA	Casting	Low methanol permeability Easily manipulation with small thickness	Lower proton conductivity
Nafion/PBI	Screen printing	Reduced methanol permeability	High impedance cosa è?
Nafion/Polypyrrole	Electrodeposition-In situ polymerization	Low methanol permeability	Decreased proton conductivity Increased resistances
Nafion/Polyaniline	In situ-polymerization	Decreased methanol permeability Increased selectivity	Decreased conductivity
Nafion/SPAEK	Casting	Low methanol permeability Higher proton conductivity	Easily breakable
Nafion/SPEEK	Casting	Decreased methanol permeability Reasonable thermal properties	Reduced proton conductivity
Nafion/Metal oxides (SiO_2-TiO_2)	Casting	Increased proton conductivity	Accelerated degradation Difficult homogeneity
Nafion/Montmorillonite	Casting	Methanol crossover decreased	Slight proton conductivity decrease

Nafion/Zeolites (Analcime-Mordenite)	Spray	Methanol crossover decreased Slight increased proton conductivity	Low tensile strength
Nafion/Graphene oxide	Casting	Methanol crossover decreased High thermal and mechanical stability	Decreased proton conductivity
SPEEK	Casting	Low methanol crossover	Poor mechanical stability
SPAES/Laponite	Casting	Low methanol crossover Enhanced tensile strength	Low proton conductivity
PVA/Montmorillonite	Casting	Low methanol crossover Cheap High proton conductivity	Filler content should be well controlled Specific operating condition and specific stack material should be used
PVDF/silica-Zirconium	Impregnation	High tensile strength Low methanol crossover	Poor proton conductivity

Table 3-Summary of DMFC best performance using composite membranes

Membrane	**Type of DMFC**	**Voltage (V)**	**Current Density ($A.cm^{-2}$)**	**Power Density ($mW\ cm^{-2}$)**	**Temperature (°C)**	**Methanol Concentration (M)**
Nafion/silica	Active	0.3	0.2	60.0	75	5
Nafion/TiO2	Active	0.3	0.214	64.2	80	1
Nafion/SiO2	Active	0.3	0.204	62.9	80	1
Nafion/sulfonated montmorillonite	Active	0.2	0.336	67.2	40	2
Nafion/GO	Active	0.31	0.46	141.0	70	1
Nafion/SGO	Active	0.40	0.1	43.0	-	1
Sandwich Nafion/GO	Passive	0.17	0.15	25.0	-	5
Nafion/mordenite	Active	0.18	0.06	10.8	70	4
Nafion/analcime	Active	0.18	0.04	7.2	70	4
Nafion/mordenite/GO	Active	0.23	0.12	27.5	70	1

Nafion/polypirrole	Active	0.30	0.15	45.0	60	
Nafion/polyaniline	Active	0.23	0.3	70.0	60	6
Nafion/PVA	Active	0.26	0.5	130.0	70	1
Nafion/PBI	Active	0.36	0.06	21.7	60	2
Nafion/PTFE	Active	0.25	0.35	87.5	70	2
Nafion/PTFE/zirconium phosphate	Active	0.20	0.3	60.0	80	2
Nafion/SPAEK	Active	0.38	0.3	114.0	80	2
Nafion/SPEEK	Active	0.18	0.15	27.0	80	2
SPEEK	Active	0.20	0.076	15.2	60	1
SPEEK/MMT	Active	0.20	0.1	20.0	60	1
SPEEK/GO	Active	0.35	0.21	72.2	65	1
SPEEK/PBI	Active	0.28	0.16	45.0	60	1
PVA/montmorillonite	Active	0.29	0.023	6.8	25	2
PVDF/zirconium phosphate	Active	0.54	0.060	32.3	60	1

According to the data collected into the two tables above, membranes with fillers guarantee the highest performance. This is because the reduced alcohol permeability counterbalances the reduced proton conductivity in the composite membranes. Materials, such as PTFE, PVA, and metal oxide are not proton-conducting materials, and this results in a reduction in the electrolyte proton conductivity, however they increase the tortuosity of the membrane thereby leading a reduced amount of crossover. Two approaches to increase the proton conductivity were adopted to further enhance the performance, namely: optimising the filler content and functionalising the filler (most commonly by incorporating sulphonic groups) to increase the overall electrolyte proton conductivity. Graphene oxide is an outstanding material to blend with different polymers to enhance the processibility, chemical, electrochemical, and mechanical properties of membranes. The literature review systematically highlighted graphene oxide as a promising membrane material for fuel cells; it also summarizes the potential advantages and recent advancement in the synthesis of graphene-based membranes and their effects on the performance of fuel cells. Graphene oxide positively alters the must-have properties for proton exchange membranes in fuel cells such as proton conductivity,

ionic conductivity, water uptake, reduction in methanol permeation, ion exchange capacity, ionic transport, swelling ratio and proton transport. These are the reasons why it was used in this work.

3 Membranes preparation

This chapter discusses the steps to prepare membranes: from the initial solution up to the final product. Nafion and GO single layer membranes were prepared by casting. Casting is the process of formation of a film or membrane on a flat surface by the evaporation of the solvent. The protocol to cast Nafion has been detailly treated in literature [**155-159**]. This process consists, as mentioned above, in an evaporation of a solvent from a solution containing the polymer (Nafion in this case) plus the solvent (ethanol). Throughout this process, to avoid imperfections, such as pin holes, that can lead to an unsuccessful result, a slow evaporation can be adopted. The imperfections are minimum, but the membrane is mechanically weak [**150,151**]. To increase the mechanical stability, a heat treatment can be applied in the following method:

1. boiling solvents (the solvent is removed after it boils)
2. by annealing with the temperature and solvent evaporation.

This approach was used by several authors [**155,156**] that noticed the migration of the sulphonic groups into the internal part of the structure of the polymer, making the structure of the recast Nafion comparable to that of Nafion 211 and 212[**157,158**]. In addition, the fact of annealing the polymer at 120 °C while casting Nafion, makes the membranes stronger and more resistant [**159**].

During the second year of my Ph.D course, I was a visiting student at the School of Chemical Engineering, University of Birmingham (UK) for six months. Here, I learned and deepened the methodology to produce polymeric membranes, to characterize and to test them. The accumulated knowledge gained during that period formed the basis that allowed me to develop this work. The steps to prepare single layer membranes are presented below.

3.1 Nafion single layers

The Nafion solution, a diluted liquid made from chemically stabilized perfluorosulfonic acid (PFSA) / polytetrafluoroethylene (PTFE) copolymer in the acid (H^+) form was purchased from FuelcellStore. A water-based solution at 10 wt% of Nafion was selected.

To prepare a single Nafion layer, a solution of Nafion/ethanol was firstly poured in a vial and put inside a dryer connected to a vacuum pump (Figure 16).

Figure 16- Vials with Nafion solution in the dryer connected with the vacuum pump

Subsequently, the solution was poured into a flat Petri dish and then put in the oven (Figure 17), varying the amount of Nafion proportional to the target thickness of the final membrane.

Figure 17- Petri dishes with Nafion solution in the oven

The amount of ethanol added is equal to half of Nafion quantity. The following table summarises the thickness and the volume of the Nafion solution required.

Table 4- Volume of Nafion solution required to achieve the target thickness.

Nafion membrane	
Nafion quantity (mL)	Thickness(µm)
4,9	50
3,6	40
3	30

The Petri dish with the solution was placed for drying in an oven, undergoing heating cycles plotted in figure 18:

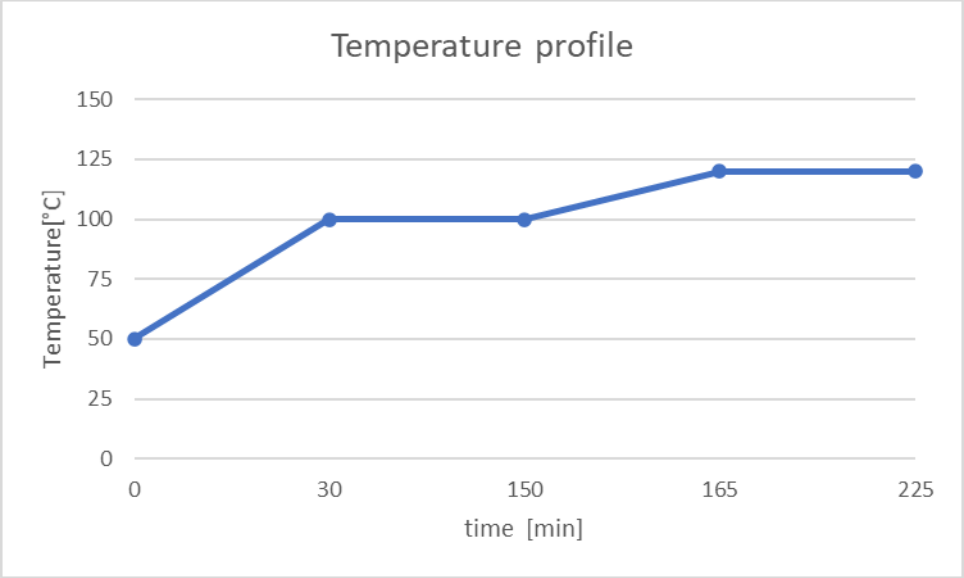

Figure 18-Temperature profile set into the oven

From an initial temperature of 50°C, the oven reaches 100°C after 30 minutes, it works at 100 °C for 2 h. Then, the temperature increases reaching 120°C after 15 minutes and works for further 1 h for annealing the polymer at that temperature. After that, once the oven gets cold, the Petri dishes can be taken off from the oven. The final result is shown in Figures 19-20.

Figure 19- Casted Nafion membrane in the petri dish

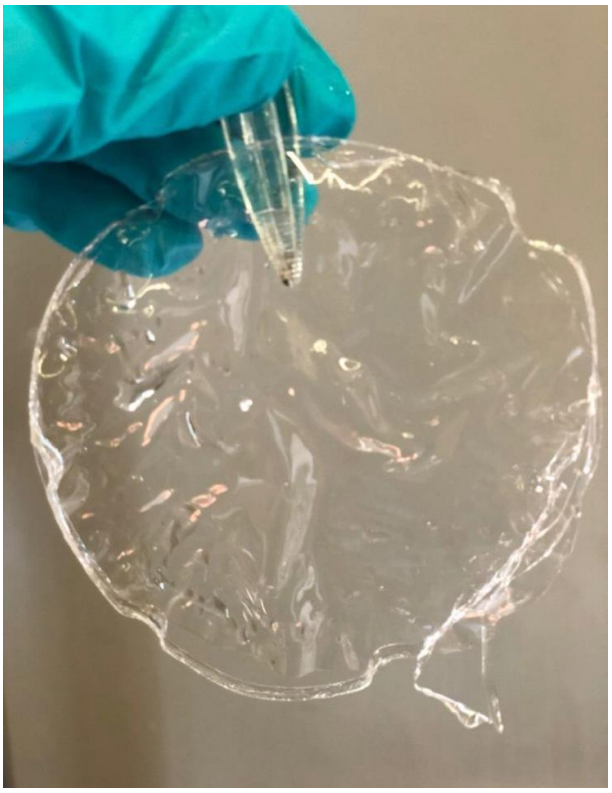

Figure 20- Casted Nafion membrane after peeling off operation

3.2 GO single layer

The protocol to prepare a single GO layer is similar to the one described above: a solution of GO/Nafion/ethanol, after being under the dryer, was poured into a flat Petri dish and then put in the oven, varying the amount of Nafion proportional to the target thickness of the final membrane. The amount of ethanol added is equal to half of Nafion quantity. Table 5 summarises the thickness and the volume of the Nafion solution required.

Table 5- Volume of Nafion solution required to achieve the target thickness.

GO-Nafion composite membranes	
Nafion quantity (mL)	Thickness(µm)
4,2	50
3,2	40
2,4	30

The GO was purchased from Sigma Aldrich. It was in solid phase and in form of sheets. To solubilize the GO, 4 mL of water and GO sheets were ultrasonicated using a probe (Fig. 21), made available from the Department of Chemical engineering, Materials and Environment of La Sapienza. The amount of GO sheets is proportional to the target percentage by weight of GO into the final membrane.

Figure 21- Sonication probe

A solution of water and GO was poured in a vial and subject to the following steps:

- 5 minutes at 40% of amplitude [µm], 5 sec ON and 5 sec OFF
- 4 minutes at 40% of amplitude [µm], 5 sec ON and 1 sec OFF.

Subsequently, this sonicated solution was poured in a Nafion solution then further ultrasonicated for 2 minutes at 20% of amplitude, 5 sec ON and 1 sec OFF. The final solution is poured into a petri dish.

The membranes were successfully prepared using the temperature profile in figure 18. Some of the membranes obtained are shown in figures 22-23.

Figure 22- Nafion/GO membrane

Several membranes were prepared in this work, varying the loading from 0.5% to 4%. In Figure 23 some of the membranes prepared are shown, the loading is 0.5, 1 and 1.5%. As can be seen, the higher the amount of GO was used, the darker the membrane was.

Figure 23- Nafion/GO membranes with 0.5, 1 and 1.5% of loading.

3.3 Membrane activation

The membranes were treated at 80 °C by immersion, using a hotplate (Figure 24) in the following sequence for 1 h each:

1. in deionized (DI) water
2. in 3% hydrogen peroxide, this step is necessary to remove the organic impurities after the casting process
3. in DI water
4. in 0.5 M sulphuric acid, this step is necessary to increase the number of water molecules per sulfonic acid group. The importance of this step will be described in the Chapter V
5. in DI water.

After each step, the membranes were rinsed with DI water before being put into the successive solution. Succeeding the step number 5, the desired membrane sample was immersed in water for at least 24 hours.

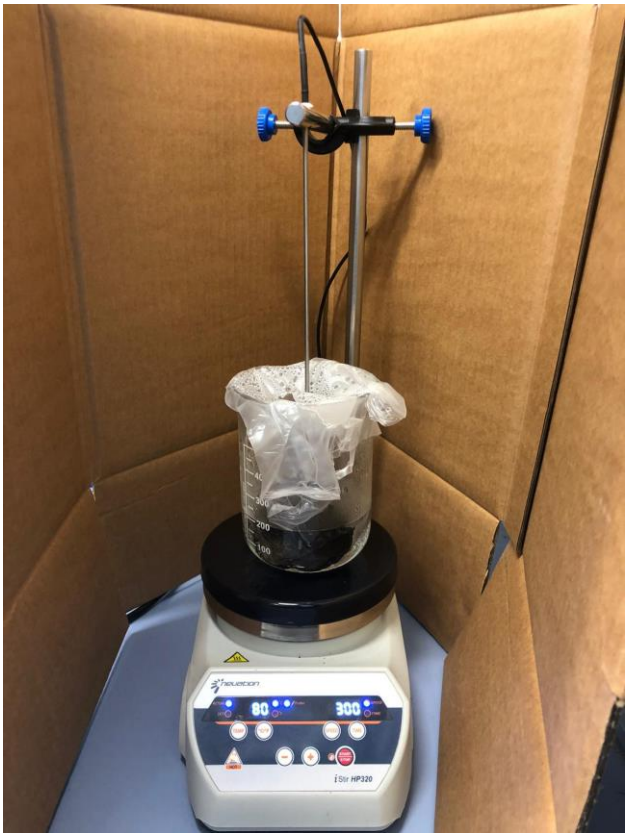

Figure 24- Hot plate for membrane activation

3.4 MEA production

MEAs were fabricated with commercial electrodes. The catalyst of anode and the cathode used supported Pt-Ru/C (from Fuel cell store) and supported Pt/C (from Fuel cell store) respectively. The load of the catalyst for the anode and cathode are all 3mg *cm^{-2}. The GDL were Toray carbon cloth for each electrode. The proton exchange membrane was sandwiched between two electrodes mentioned above and the resulting membrane electrode assembly (MEA) was then hot-pressed for 2 minutes at 135°C using 4 tons of pressure. All MEAs had an active area of 9 cm^2. Some of the produced MEAs are shown in figure 25.

Figure 25- Example of MEAs obtained with commercial Nafion, casted Nafion, GO casted

4.Test bench

In this chapter the test bench configuration is shown, describing the instruments involved and their operating conditions. In addition, processes implemented in the software LabVIEW are discussed and explained. Finally, a brief introduction to the control interface is carried out to introduce the successive analysis.

4.1 Test bench set-up

In this step the entire hardware system was assessed. The main objective was to develop a framework that allows to monitor and control every instrument as a single device in connection with the others, according to the measured parameters (flows, temperatures, pressures, fuel concentration, fuel level, current etc.). LabView software was used to set-up the control system. The test bench showed in Figure 26 is described in the following paragraphs focussing on:

1. Hydraulic circuit used to feed the fuel cell.
2. Electric circuit to have the remote control of fuel cell, auxiliary systems and sensors.
3. Electronic load connection.

Figure 26-The test bench

4.2 Hydraulic system

The hydraulic system (Figure 27) mainly consists in two branches that allow the appropriate cell operation for the anode side, from the fuel feedings to the discharge of reaction products.

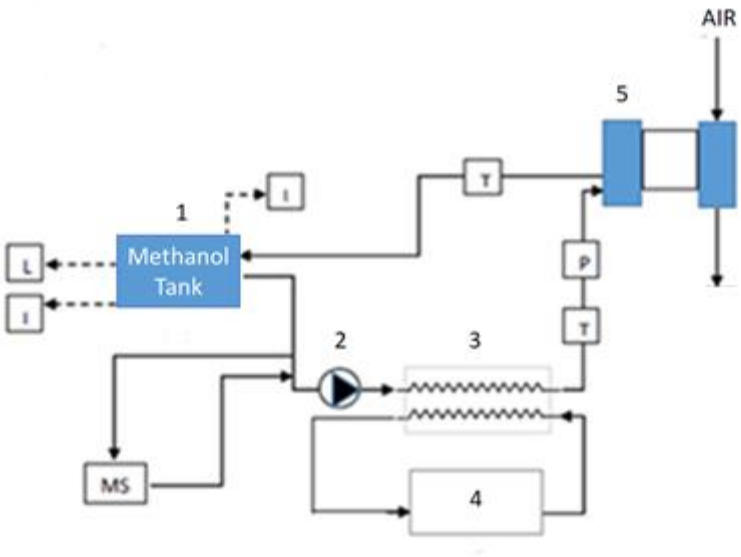

Figure 27- Hydraulic System

In the following paragraphs material and information flows are explained, using the identification numbers provided in Figure 27 as references.

4.2.1 Anode side

The anode system central core is located in the mixing tank (n. 1), containing the proper chemical methanol-water solution. Starting from here, a pump (n. 2), able to elaborate low flow rates (0.4-180 mL/min), leads the chemical blend into a heat exchanger (n. 3) fed by a thermostatic bath (n. 4) in order to increase the fluid temperature until the desired level. At the end, the fuel arrives to the cell anode (n. 5) and the outgoing discharging products are unloaded back to the mixing tank, so that the circuit is closed. Within this system, some sensors are used to monitor operating parameters in the cycle as the chemical concentration (MS), temperatures (T) and the inlet pressure (P).

4.2.2 Cathode side

In the cathode system, the design of the cell is set up to have the open flow field in an up and down orientation in order to take advantage of natural convection as the cell warms.

4.3 Data acquisition and electric circuit

The electric system allows receiving and sending operating signals between the software interface and the test bench components. A National Instrument chassis is the main responsible for this task, using different exchange modules to differentiate the type of information needed (Figure 28).

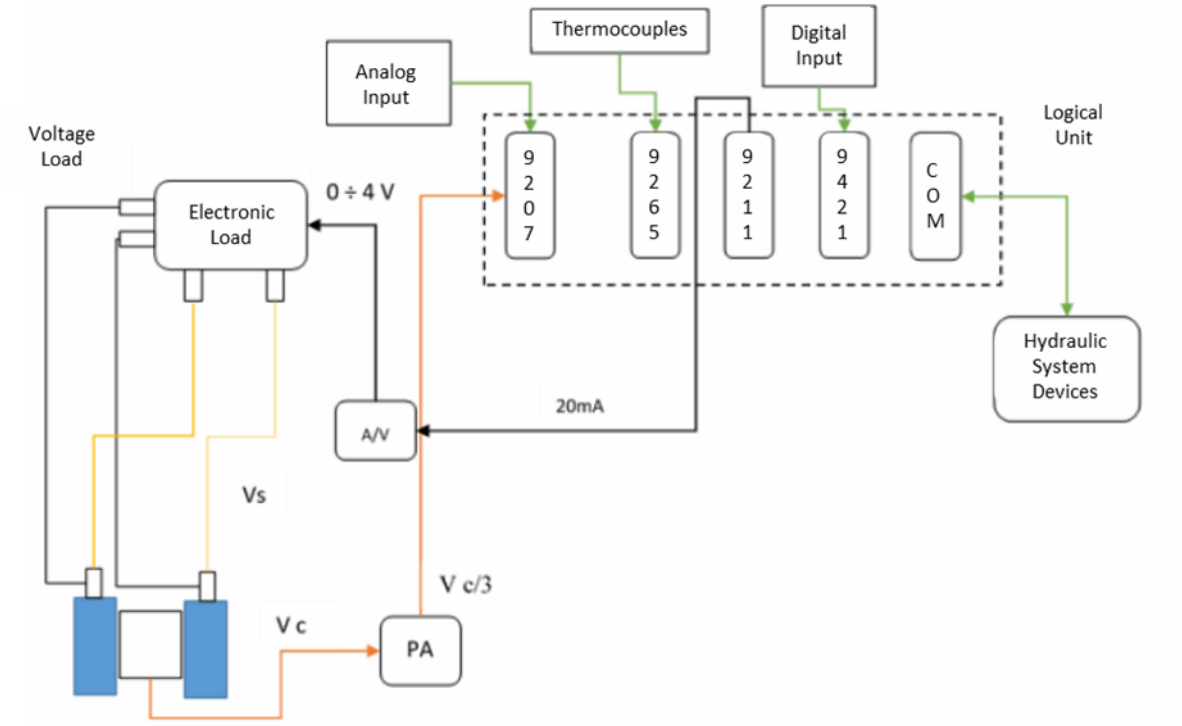

Figure 28--Data acquisition system and electric circuit

In this sense, the logical unit includes:

- Module 9421: it receives a digital voltage input equal to 0 or 5 V corresponding, respectively, to the level sensors on or off states.

- Module 9211: it sends analogical signals in electrical current between 0 and 20 mA. It translates the software input to the electrical load.
- Module 9265: it continuously receives signals from every thermocouple.
- Module 9207: it receives the whole set of analogical measures from pressure transducers and voltmeter.

In addition to these devices, connections of hydraulic system components through serial ports (pumps, thermostatic bath, etc.) must be enclosed within the COM module of the logical unit, assigning a unique name and progressing number to each one of them.

4.3.1 Electronic Load

The electronic load, LD300 Aim TTi, (Figure 29) is the instrument used to simulate a load connected to the cell. Its main component is a variable electrical resistance placed in parallel with the stack in order to modify the induced current according to the needs.

Current range [A]	0 - 80
Voltage range [V]	0 - 80
Nominal power [W]	300

Figure 29- Electronic Load LD300 and nominal data

The electric connection to the cell is realized through four wires that must put physically in contact the variable load resistance with the stack and the electronic load with the CPU hardware. This last link is crucial since it allows to control the device voltage output from the LabVIEW interface.

4.3.2 Control and measure devices set-up

Once the test bench has been configured, each component must be calibrated and registered.

Dosing Pump

The dosing pump (Figure 30) control is implemented using procedures provided by their producers, supplying specific command strings to be transmitted to send different flow rates requests.

Flow rate [ml/min]	Min	0.4
	Max	180
Rotation speed [rpm]	Min	40
	Max	1800
Input	6.4mm external diameter pipes	

Figure 30- Dosing pump ISMATEC REGLO-CPF Digital and nominal data

In addition to the standard process, two supplemental controls are enabled:

1. Minimum flow rate: the instrument works at this minimum pre-set flow rate level, even if it receives the input to elaborate a flow rate below it.
2. Zero flow rate: if the instrument receives the order to feed a null flow rate, it instantaneously stops its procedure.

These additional parameters allow to completely control the dosing pumps without any hardware operation.

Refractometer

The refractometer KNAUER RI DETECTOR 2300 (Figure 31) is the instrument selected to measure methanol concentrations in the chemical solution entering in the stack.

Cell volume [µL]	15
Refractive Index [RIU]	1 – 1.75
Max flow rate [ml/min]	5
Sensitivity [RIU]	$3 \cdot 10^{-8}$

Figure 31- Refractometer KNAUER RI DETECTOR 2300 and nominal data

The operating principle of this device is based on the refractive index variation between two cells filled with two different fluids and crossed by the same light beam. According to the Snell's law (Eq. 15), during a light transfer from a medium 1 to a medium 2, the angle of incidence (α1) and the angle of refraction (α2) are related to each other depending on the chemical and physical properties of the mediums (Figure 32). In this sense, the refractometer basically compares the light flux motion between a reference cell filled with a known fluid and the measuring cell filled with the target solution.

$$\frac{sin\alpha_1}{sin\alpha_2} = \frac{n_1}{n_2} = n \qquad (15)$$

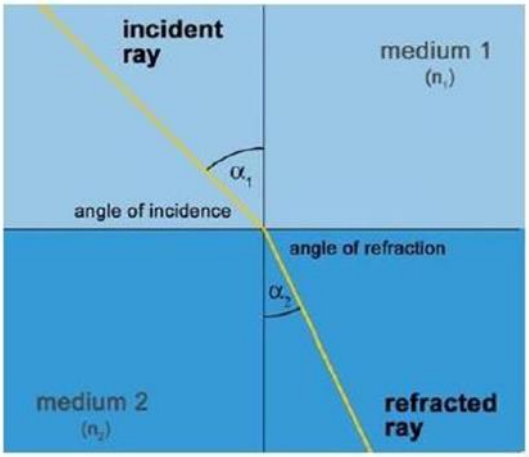

Figure 32- Light beam path while passing through two different mediums [KNAUER, "RI Detector 2300 Datasheet".]

In Figure 33, the light beam path within the instrument environment is shown.

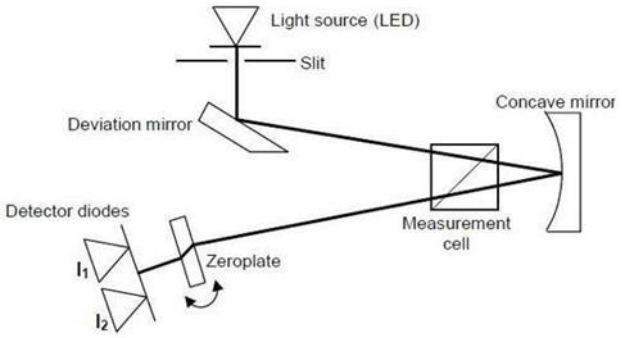

Figure 33- Light beam path within instrument environment [KNAUER, "RI Detector 2300 Datasheet".]

The light is emitted by a LED and diverted by a series of mirrors in order to cross the measurement cell and then to arrive to two final detector diodes. These two devices record the light angles and calculate the difference between measured refractive indexes and the reference one set to zero. The calibration process related to this device is extremely important to associate the Refractive Index Unit (RIU) value with the right chemical concentrations and the following paragraphs represent the steps performed.

Reference cell setting

This process is performed to set double-distilled water as reference fluid so that its RIU value will be the "zero" compared to other compounds. Since the device has only one input and one output channel, in normal operations the liquid is pushed to flow into the measurement cell and to be driven out at the end of the path. To manually inject double-distilled water inside the reference cell, it is necessary to change the instrument mode using the FLUSH function. While "flushing", the device allows the user to send fluid to the reference cell through a dropper, setting it to 0 mRIU and employing it as the base of each comparison test.

Refractometer scale calibration

The experimental relation that links the output value expressed in mRIU by the equipment with its related molarity value is now determined. The objective is to start from solutions with known temperatures and molarities and to measure the refractometer figures associated to them. Table 6 summarizes the results.

Table 6- Refractometer measurements for different concentrations

Molarity [M]	mRIU		
	20°C	**60°C**	**70°C**
0	0	0	0
0.3	0.263	0.25	0.233
0.6	0.467	0.46	0.447
0.9	0.70	0.682	0.676
1.2	0.938	0.93	0.925

From these values it is possible to report the linear approximation of the relation with a graphical outcome as shown in Figure 34.

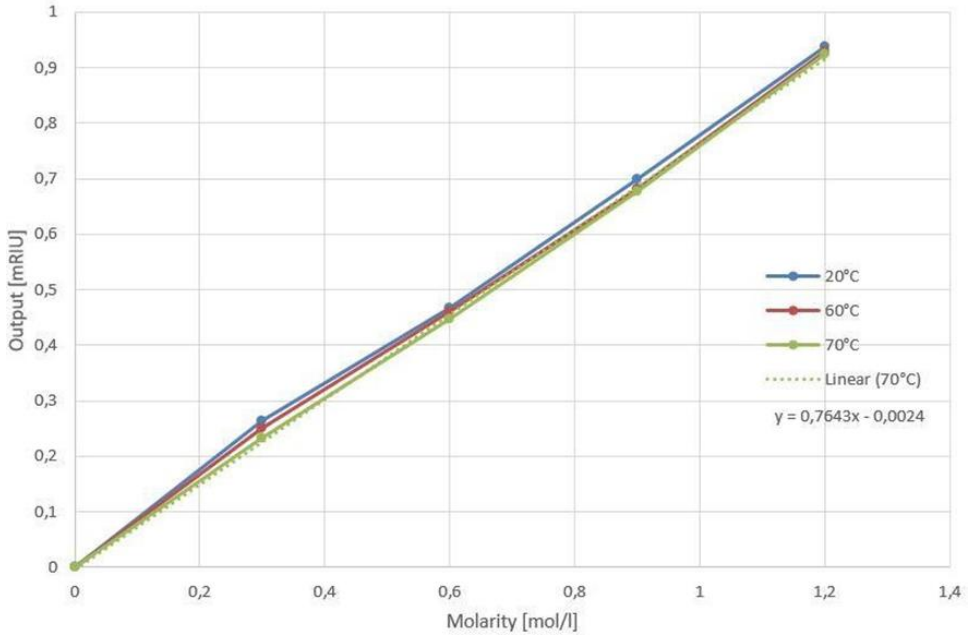

Figure 34- mRIU output depending on molarity

Once this correlation has been obtained, it is important to associate it with the signal sent from the device to the logic unit, which is a voltage indication in the range of 0V and 1V proportional with the refractive index. To have the instantaneous value of the molarity on the LabVIEW interface, it is necessary to interpolate

another experimental relation between concentrations and voltages measured at the device's ends. Table 7 shows the obtained products.

Table 7- Voltages values output

Molarity [M]	Voltage		
	20°C	**60°C**	**70°C**
0	0	0	0
0.3	0.053	0.044	0.039
0.6	0.099	0.089	0.08
0.9	0.14	0.131	0.125
1.2	0.182	0.171	0.16
2	0.313	0.29	0.281
3	0.448	0.434	0.429

These outcomes are represented in Figure 35, which gives the linear trend relation too.

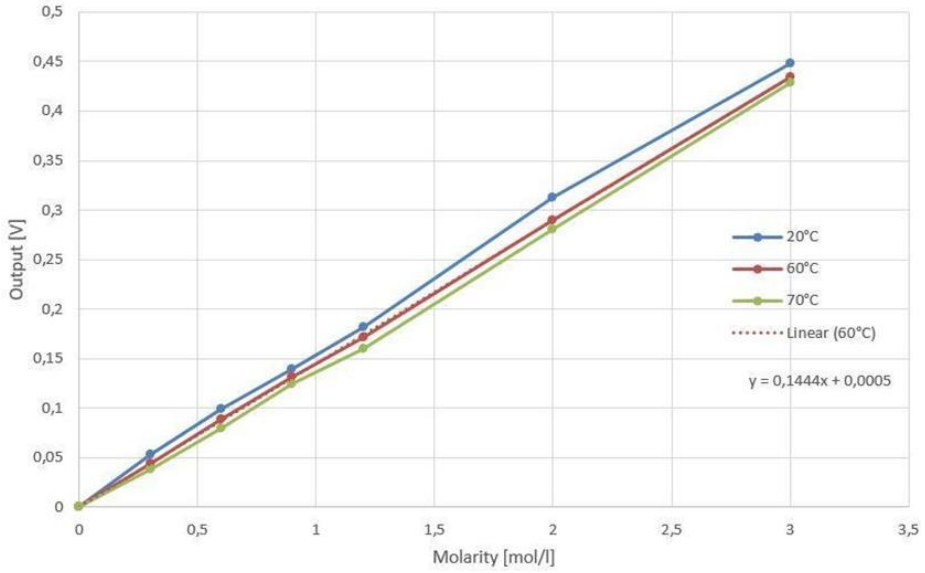

Figure 35- Voltage output depending on molarity

Introducing this scale into the LabVIEW interface, it is possible to keep track of every molarity variation during the tests, allowing to analyse the behaviour of the cell in different concentration conditions.

Thermocouples

Temperature is one of the most affecting parameters among the cell operating conditions. To monitor this factor within the system, two thermocouples (Figure 36) are installed in proximity of the crucial points of the anode input and the anode output.

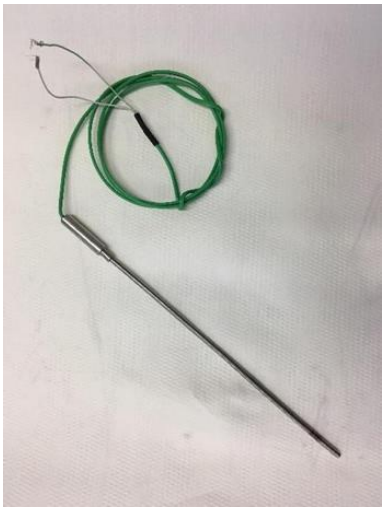

Figure 36- Thermocouple installed

The voltage analogic signal is then acquired by the software through the Nidaq module and reported by the LabVIEW interface.

Pressure transducers

To monitor the pressure differences across the anode inlet and outlet, two pressure sensors are installed and calibrated (Figure 37 and Figure 38).

Pressure [bar]	Min	0
	Max	0.25
Output [A]	Min	0.004
	Max	0.02
Temperature range [°C]	Min	0
	Max	60

Figure 37- BARKSDALE UPA2DMP343 pressure transducer and nominal data

Pressure [bar]	Min	0
	Max	4
Output [A]	Min	0.004
	Max	0.02
Temperature range [°C]	Min	-40
	Max	100

Figure 38- OMEGA PX482A-060GI pressure transducer and nominal data

The output signal (A) is acquired analogically and linearly scaled to represent the pressure magnitude in bar. This last step is performed using the producer's indications reported in Figure 39 and Figure 40, entered LabVIEW.

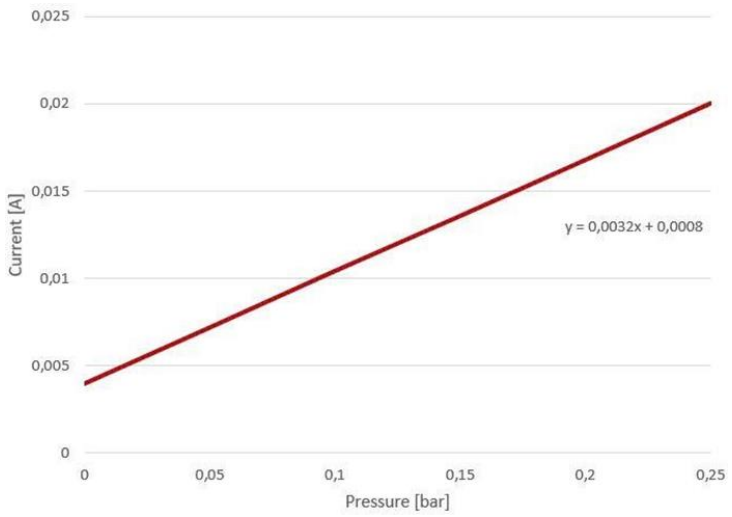

Figure 39- BARKSDALE scale

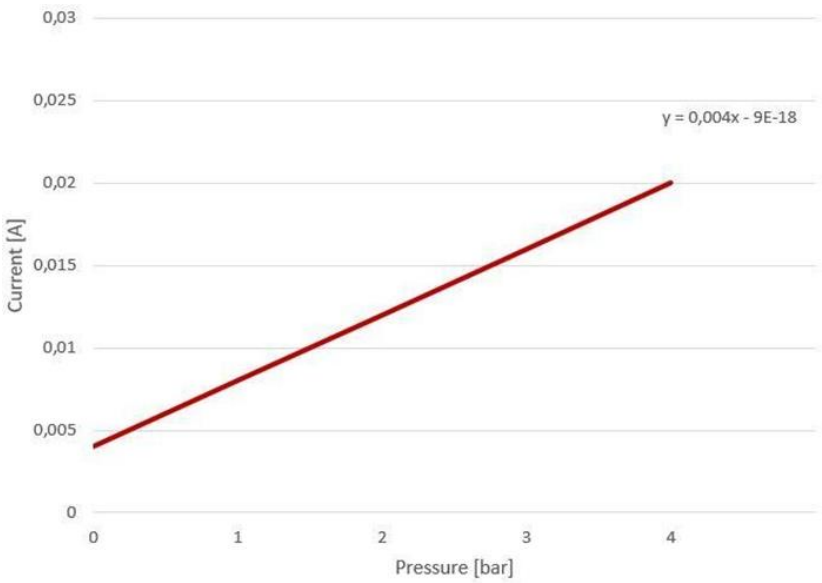

Figure 40-OMEGA scale

Thermostatic bath

The thermostatic bath (Figure 41) relates to a counter-current heat exchanger. In one direction it is present the recirculation pump flux, while on the other one the flow is pumped up until the inlet of the fuel cell.

Working temperature range [°C]	Min	20
	Max	200
Room temperature range [°C]	Min	5
	Max	40
Measurement accuracy	±0.3K and ±5% relative measurement	

Figure 41- LAUDA ECO SILVER thermostatic bath and nominal data

The aim of this instrument is to heat the chemical solution and to keep constant its temperature during the fuel cell operation.

4.4 Software interface (LabVIEW model)

This section is focused on the software side of the activity, analysing the main features of LabVIEW (Laboratory Virtual Instrument Engineering Work) environment and its exploitation within this work. The

primary application of this program is to develop an electronic management and data acquisition from the installed tools, receive their signals and evaluate their meaning. The environment that allows this kind of programming is the “G language”, which consists in a graphical block diagram representation of the target system. The essential component of this framework is the Virtual Instrument (VI) and the whole domain is composed of many of them linked to each other. A Virtual Instrument allows the interaction between a computer and a device, providing, at the same time, a clear communication panel to the control user. In this way, the operator can communicate with every tool (Instrument) through a structure directly located in the software (Virtual) that represents the real composition of the hardware scheme.

4.4.1 Instrumentation setting

It is the main control interface linked to every measurement and feeding instrument. In Figure 42, the graphical aspect of this feature, representing the most important commands is shown. To set the correct device associated to each VI, it is crucial to introduce the proper serial port number (COM) that gives the hardware connection between computer and device. In this way, it is possible to send any signal requested by the user and translate it as an input for the equipment.

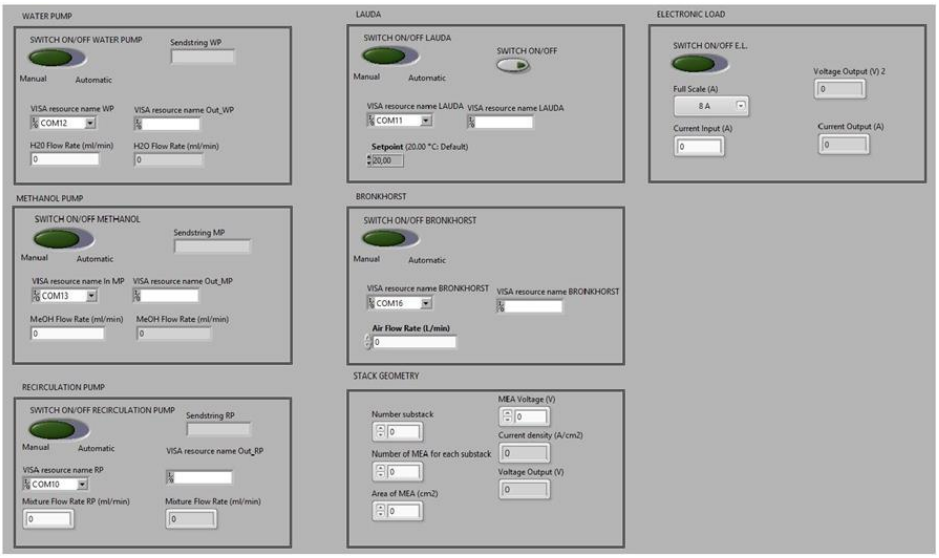

Figure 42- Instrumentation setting framework

There are two different regulation paths for each instrument, allowing to select a manual or automatic management.

- Manual regulation: the user selects manually the required activity, basically varying operating conditions and current density.
- Automatic regulation: the software receives inputs from a pre-set file that allows to fix various operating times and the working parameters associated to them. In this way, the test goes on without any intervention from the operator.

4.4.2 Test development

Once the testing system has been properly set up, it is possible to start carrying on the analyses. The aim of these procedures is to check the variations in terms of available power and efficiency when changing the cell operating conditions.

For each analysis it has been performed a basic preparation procedure to initialize the environment:

- Mixing tank filling: the mixing tank is filled with a solution with known concentration.
- Input datasheet realization: for every different operating process, it is necessary to generate an appropriate input file communicating the correct parameters to LabVIEW.
- Timeframes selection: in order to realize each polarization curve, the cell is tested in open circuit (OCV) condition for 60 seconds before increasing the current value by 5mA every time interval (60s). The end of the analysis is automatically set to the point where the cell voltage reaches 0.1V. This limit is fixed to avoid the dissolution of ruthenium atoms on the anode electrode catalyst layer: with an excessively high electric field these molecules would be dragged through the membrane causing a crossover and a deposition on the cathode electrode that would result in an inevitable MEA deterioration [**160**].

Moreover, the experimental nature of the whole framework leads to have a deviation even in results with the same parameters, making necessary to repeat every test three times (triplicate proofs). This kind of method ensures more accurate results and a minimization of possible measurement mistakes.

5 Influence of GO on the Membrane properties

The characterization of the GO membranes developed and produced during the thesis project are discussed. The membranes were prepared by casting process with three different GO loading: 0.5, 1 and 1.5% wt. The main properties, such as water uptake (WU), ion exchange capacity (IEC), proton conductivity, microscopic structure and tensile strength, were evaluated. WU, proton conductivity and IEC are relevant tests to characterize a membrane as proton exchange membrane due to the influence of water on the proton transport. Microscopic structure and tensile strength measurement were carried out to understand the dispersion of GO in the Nafion matrix and the improvement of mechanical properties. For a better comprehension, all the data are compared with that of the commercial membrane and a casted Nafion. In some tests, it was necessary to produce membranes with higher GO loading, 3 and 4%, to get a better understanding of the influence of GO in the polymeric matrix.

5.1 Water uptake

Considering the chemical reactions that occur in the cell (1), (2) and (3), water and CO_2 are generated. The water balance in the stack is one of the greatest challenges associated with PEMFCs. The polymeric membrane has an ionic conductivity depending on temperature and relative humidity.

In order to have a high ionic conductivity, the membrane relative humidity should be between 85 and 98%. Under this range, the membrane is dry, and it loses its conductive properties. At 100%, the membrane reaches a humidity level too high, and the cathode CL is filled with water giving life to the flooding phenomenon, that hinders reactants diffusion through the GDL and CL, decreasing the cell catalyst activity and the cell efficiency. Therefore, the water content in the polymer membrane affects the proton conductivity and activation overpotentials. If the MEA is not adequately humidified, the protonic conductivity decreases, meaning that the cell resistance increases.

Water uptake (WU) was determined gravimetrically by recording the wet and dry mass of the membranes using the following steps (repeated three times): the membranes were placed in water at room temperature for 24 h, and then their wet weight was measured. To measure the wet weight, the water on the surface was absorbed using dry filter paper. After this, the wet membrane samples were dried at 100 °C (until no more

weight variation was detected) and their dry weight was recorded. The water uptake (WU) was measured using the Equation 16, where WE_w and WE_d denote the wet weight and the dry weight, respectively.

$$WU = \frac{WE_w - WE_d}{WE_d} \quad (16)$$

The results are reported in Table 8:

Table 8-Water uptake of Nafion 117, casted Nafion and casted Go membranes

Membrane	Water uptake [%]	Increase with Nafion casted %
Nafion 117	38	18.75
Nafion casted	32	/
GO membrane 0.5%	35	9.38
GO membrane 1%	35.3	10.31
GO membrane 1.5%	35.5	10.93

The addition of GO led to an improvement of water uptake. A small addition of GO, 0.5%, led to an increase of WU of around 9.4% compared to the casted Nafion. WU increases with GO content reaching an increment of almost 11% at 1.5% wt. Since the enhancement was very slow, the WU was evaluated also for membranes with 3 and 4% of GO loading to properly assess this trend. The results obtained were 36% and 38.4%, for a Nafion/GO at 3 and 4% respectively. In Figure 43, all the results were plotted.

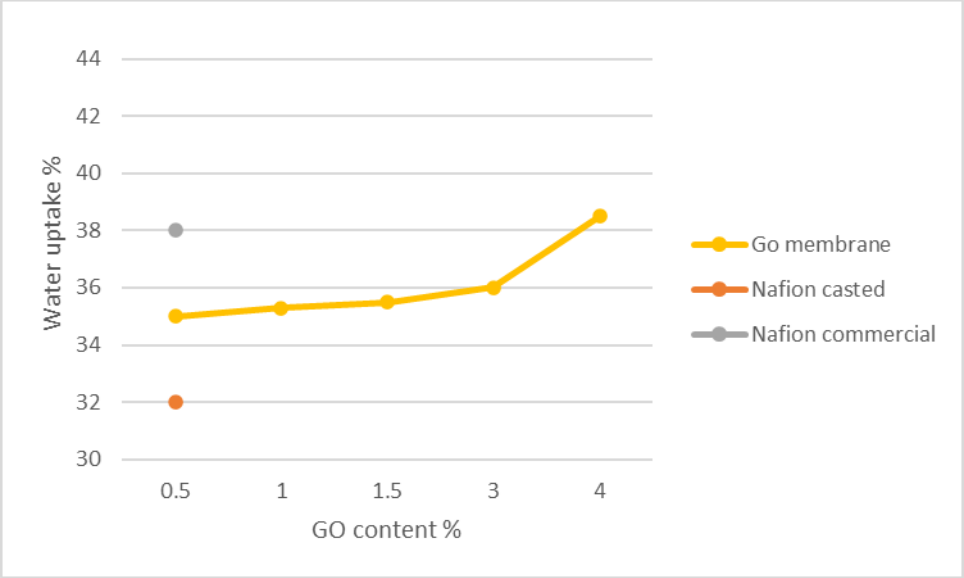

Figure 43-Water uptake of Nafion 117, casted Nafion and casted Go membranes

As can be seen from the figure 43, the water uptake of Nafion/GO composite membranes was always higher than that of casting Nafion membrane. The WU slightly increased with hydrophilic GO content up to 4%. The increase in GO from 0.5 to 4% resulted in an improvement approx. of 10%, comparing the WU of the GO membranes, and a maximum improvement of 20% if compared with the Nafion casted. Needless to say, the WU of the commercial membrane is higher of all composite membranes except for a GO content of 4%. This trend is due to the hydrophilic nature of GO. A further increase in the GO content, higher than 4%, does not lead to an increase in the WU because of the amphiphilic nature of the Nafion membrane.

A similar trend was also reported by Peng et al. [**161**] who prepared single layer composite membranes of Nafion/GO-Nafion with different loadings of GO-Nafion. The authors considered 0.05-0.15% of GO content and found that the WU increases when increasing GO in the Nafion matrix. However, for the highest content, the WU started decreasing, because of the non-homogeneous dispersion of GO. The presence of water is essential to the proton transport, since the proton transport mechanisms, hopping and diffusion, are water dependant. However, high WU can cause severe dimensional changes in the membrane during the FC operation. This can affect the membrane performance and properties, like mechanical resistance and proton conductivity. The thicker the membrane, the higher is the protonic resistance. Thus, if water content considerably increases the thickness, it reduces the proton conductivity. For such reason, it can be considered that the best conditions are obtained at a GO content from 0.5 to 1.5% wt.

5.2 Ion exchange capacity

The ion exchange capacity (IEC), expressed as milliequivalent of ion exchange groups per gram of the membrane (meq/g), is an important parameter because the ionic transport properties depend on the amount of the ion exchange groups. The IEC and WU are usually correlated: an increase of IEC induces high water content, but the mechanical strength of the membrane drops [**162**].

Membranes Ion Exchange Capacity was evaluated by acid-base titration method [**118**]. The desired membrane was soaked in 0.1 M HCl for 24 h. After thoroughly rinsing the membrane with water, it was immersed in saturated NaCl for 72 h to exchange the H+ ions for Na+ ions. Then, the proton release was evaluated by titrating the solution with 0.01 M NaOH at room temperature with phenolphthalein as indicator. The IEC was obtained by using the Equation 17:

$$IEC = \frac{VOL_{NaOH}\, x\, M_{NaOH}}{WE_d} \quad (17)$$

Where, VOL_{NaOH} is the volume of NaOH titrated, M_{NaOH} is the molar mass of NaOH and WE_d is the sample dry weight.

The IEC values of the membranes are shown in Table 9.

Table 9-Ion exchange capacity of analysed membranes

Membrane	IEC [meq/g]	Increase with Nafion casted %
Nafion 117	0.91	9.64
Nafion casted	0.83	/
Go membrane 0.5%	0.92	10.84
Go membrane 1%	0.99	19.27
Go membrane 1.5%	1.07	28.91

The beneficial effect of GO on the IEC is controversial. Some authors [**118**] claimed that the IEC decreased with the addition of GO, when compared to the recast Nafion, for two possible reasons:

- the GO composite membranes have less Nafion.

- the incorporation of GO leads to a reduction in ionic channels.

However, other authors [**109**] claimed that the addition of GO contribute to improve the IEC, as achieved in this work. Therefore, it was preferred to investigate this behaviour testing the GO membranes at 3 and 4%, as done for the WU. The results obtained were 1.18 e 1.29, for the 3 and 4% respectively. The trend was plotted in figure 44.

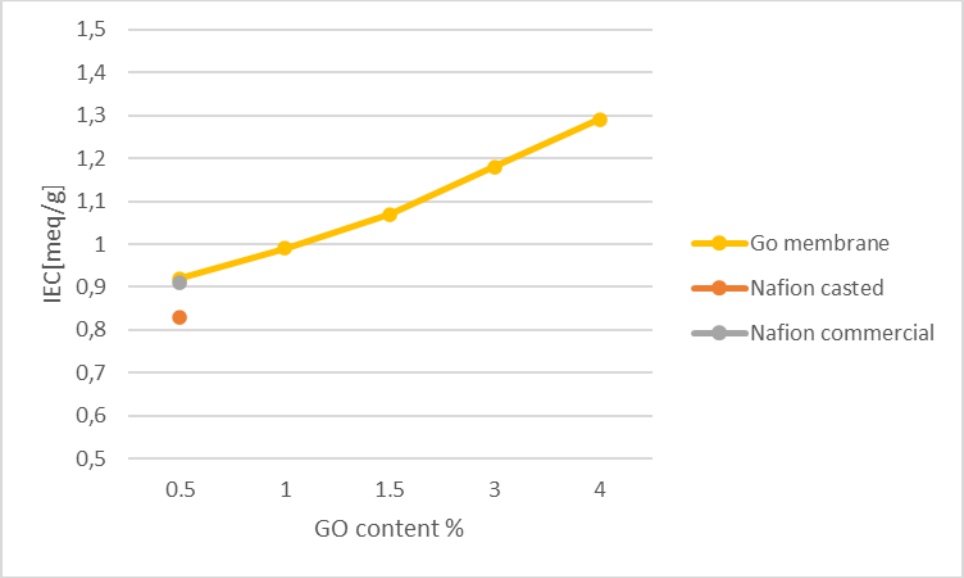

Figure 44-Ion exchange capacity of analysed membranes

The IEC increases with the increase of the GO content. The higher value, 1.29, was obtained with a GO content of 4%, reaching a maximum enhancement of 55%. The values obtained are always better than that of Nafion casted membrane. There are several possible causes to explain this deviation:

- A non-uniformity in the graphene oxide dispersion within the composite membrane, in fact for this type of test, just a small piece of membrane was used (3 samples, 1x1 cm). A non-uniform dispersion with agglomerates could potentially have a higher IEC as less ionic channels are obstructed by the graphene oxide.

- The Nafion solution used to prepare the membranes is 10% wt. in water, but that might not be the amount of Nafion contained into the samples (e.g. it could be 9% or 11%). This is due to the density difference between Nafion and water. This can be applicable also for the WU.

- The titration stopped when the solution turned a bright pink, so some errors due to the human eye may be occurred.

The trend observed for IEC is like that of WU: high GO content leads high IEC. However, considering the observations made in the previous section, the best conditions are obtained for the range 0.5-1.5%. Moreover, multiple tests on more membranes than those used in this study (two) are necessary to prevent any visual mistakes.

5.3 Proton conductivity

Proton conductivity is a form of electrical conductivity where positive hydrogen ions carry the charge, as opposed to electrons. It is a key parameter that strongly affects the performance, high proton conductivity means high voltage per current density. The proton conductivity of composite membranes was measured [**163**] using a potentiostat integrated to 850e High Temperature Scribner Associates Incorporated Test Stand. The test was carried out over six hours at stable condition (120°C and 50% of relative humidity) and varying the amount of GO loading from 0.5 to 5%. That study measured a higher proton conductivity for pristine recast Nafion membrane (40 mS/cm) than for the GO membranes (32 and 30 mS/cm for the 3 and 5% of loading respectively). This behaviour is expected, due to the barrier effect of GO and in accordance with the work of Choi et al. [**106**], even if their measurements were carried out at 25°C.

Table 10 lists the results obtained for both works and Figure 45 shows the proton conductivities of composite membranes as a function of the GO loading.

Table 10-Ion exchange capacity of analysed membranes

Membrane	Proton conductivity [S cm-1] Hattenberg [163]	Decrease with Nafion casted %	Proton conductivity [S cm-1] Choi et al. [106]	Decrease with Nafion casted %
Nafion casted	0.040	/	0.042	/

Go membrane 0.5%	0.034	15	0.040	4.76
Go membrane 1%	Missing	/	0.033	21.43
Go membrane 1.5%	Missing	/	0.026	38.09
Go membrane 2%	Missing	/	0.023	45.24
Go membrane 3%	0.032	20	Missing	
Go membrane 5%	0.030	25	Missing	

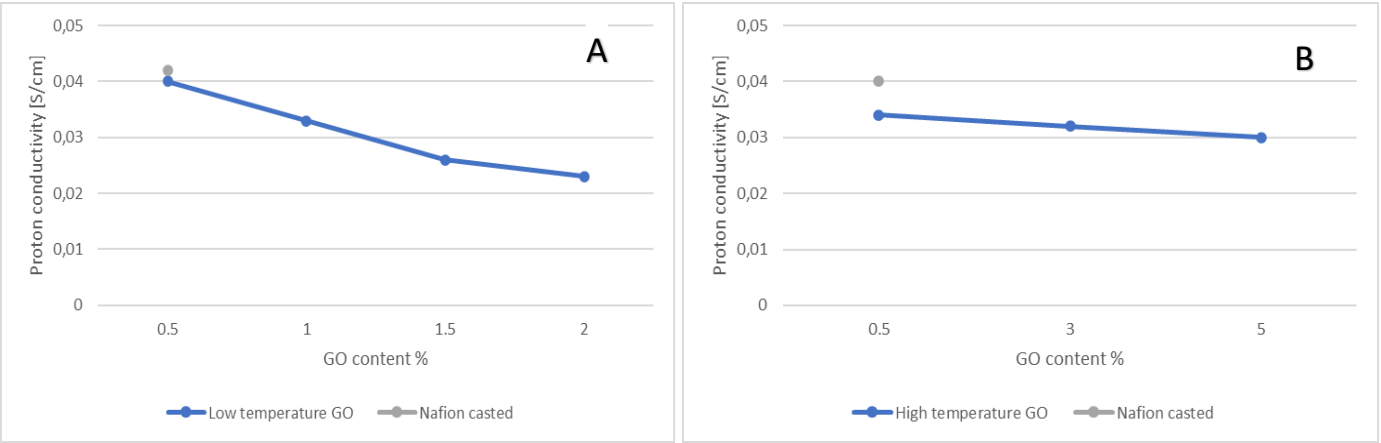

Figure 45-Proton conductivity of casted Nafion and casted Go membranes at low (A) and high temperature (B)

The proton conductivities of the composite membranes decreased with GO addition. Since, it was only at the relatively high temperatures where that doped membranes showed increased conductivity, at lower temperature the drop in proton conductivity is more evident. In fact, the loss in proton conductivity, measured at 25°C, is about 45% at 2% of GO loading, while is roughly 25% at 120°C with a content of 5%. In

this work, but in general for all the DMFC applications, operating temperature is low, therefore it must be taken in consideration the behaviour depicted in figure 45A where the decline in proton conductivity is more pronounced when increasing the GO, even tough the trend highlighted in figure45A and B are similar.

5.4 Morphology

Scanning electron microscope (SEM) was used to record surface morphology information of the sample by recording secondary electrons emitted from the material due to inelastic scattering [**164**]. Using this method, the primary electron beam is scanned across the sample, exciting the electrons on the surface, which are then detected to produce 3D images. SEM can successfully be used to investigate particle distribution throughout the thickness of the membranes at both nanometre and micrometre scale. The analysis is carried out through Electron microscopy analyzer using a Zeiss EM10 SEM, in the following operating conditions: 20 kV acceleration voltage, beam current between 6 and 14 pA and BSD detector with four elements, gain +3.

By analysing the cross sections of the composite membranes by SEM, the distribution of the filler particles could be evaluated. Figures 46-47-48 show the dispersion of GO sheets for some GO composite membranes.

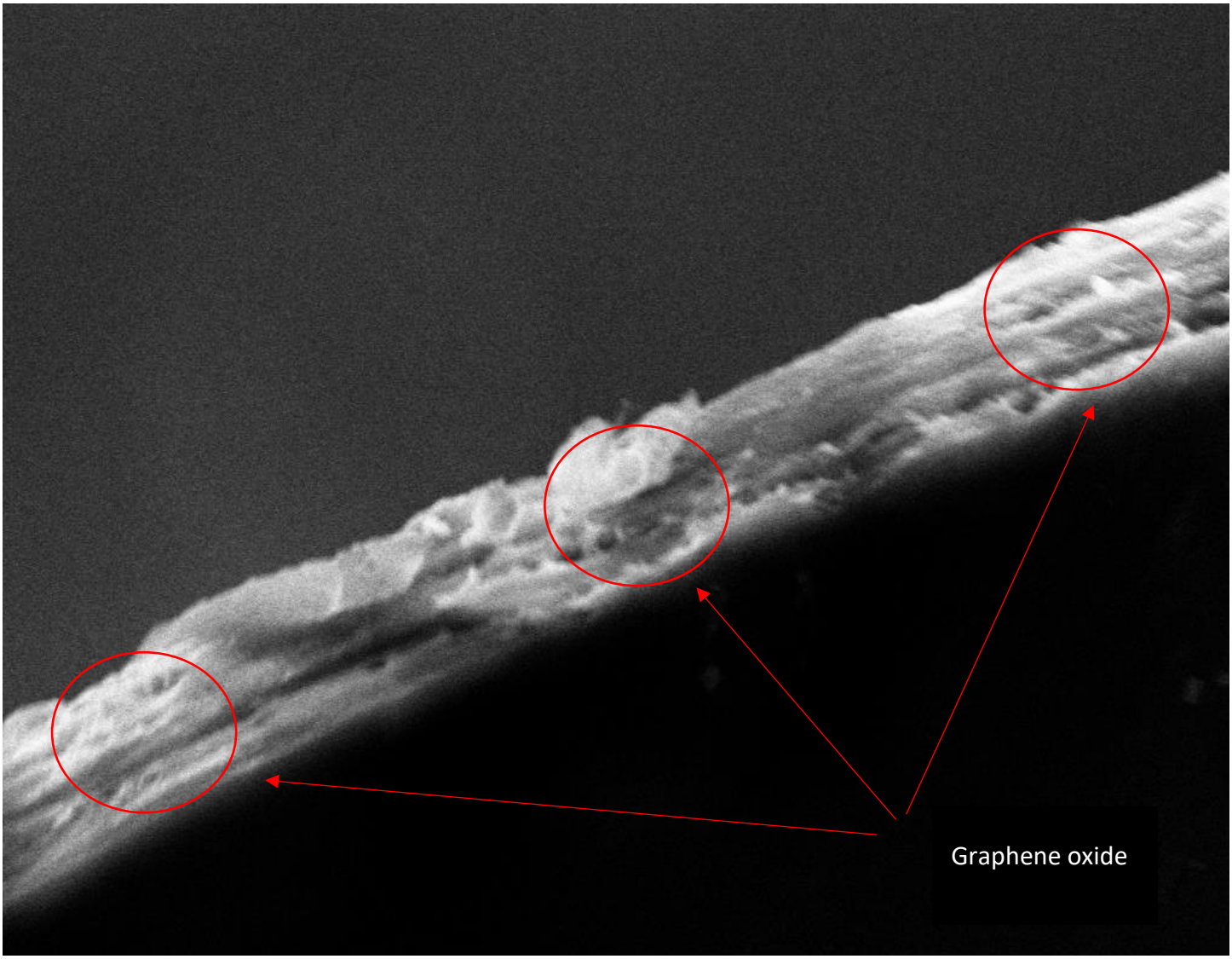

Figure 46-Cross section of GO membrane at 0.5% of GO content

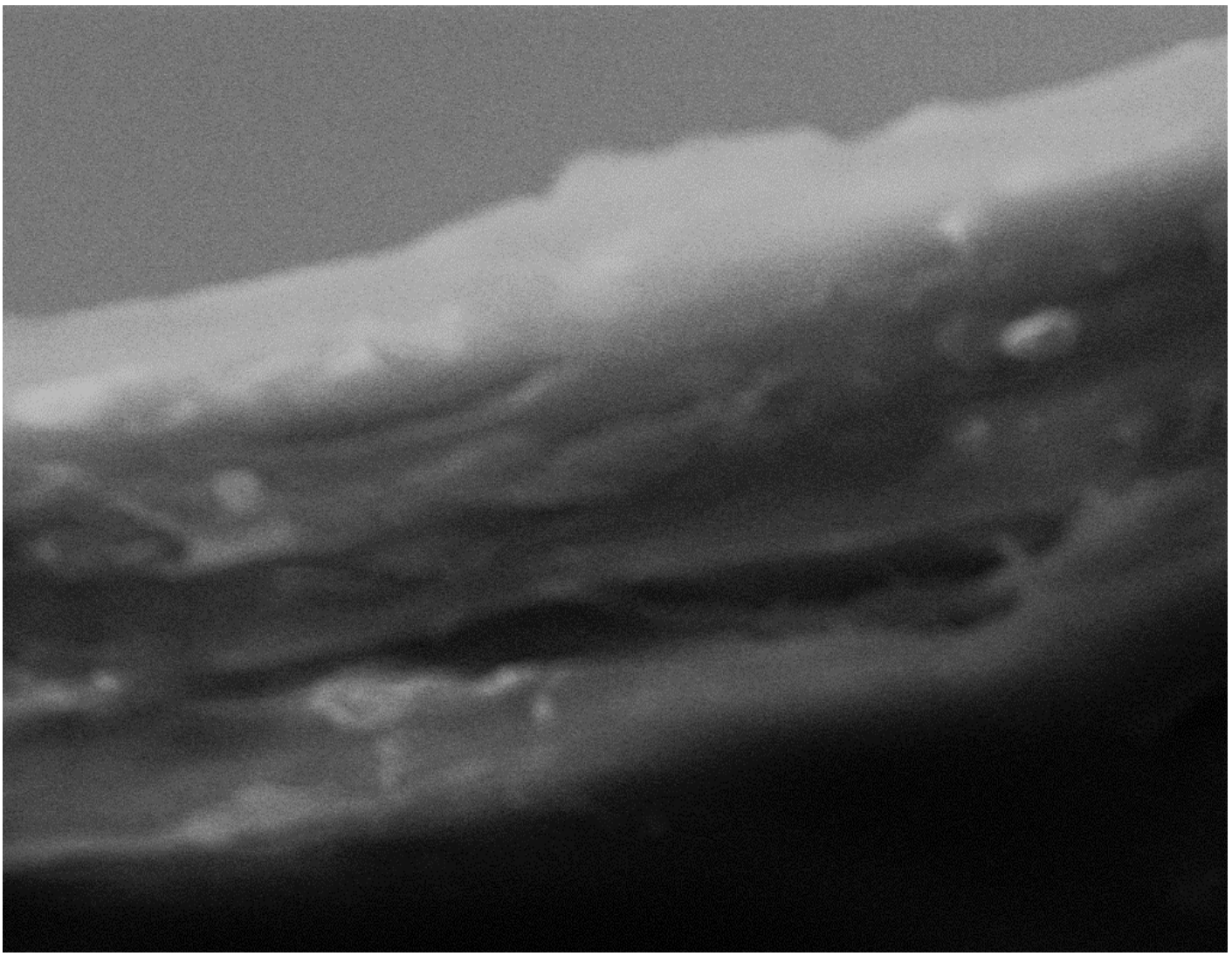

Figure 47-Particular of GO membrane at 0.5% of GO content

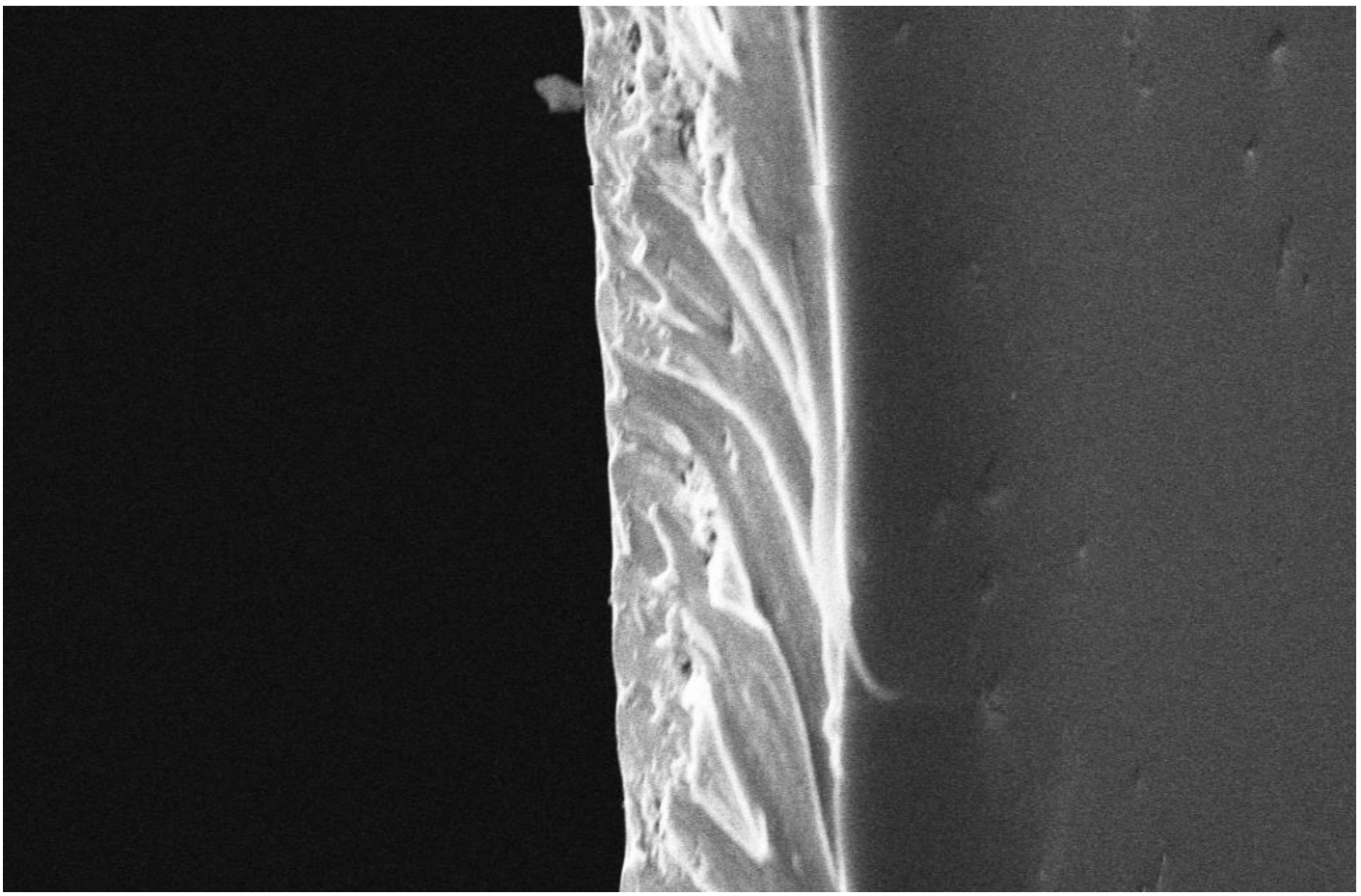

Figure 48-Cross section of GO membrane at 1% of GO content

It is clear from these images, that the filler particles were evenly distributed into the Nafion matrix (the blank one) through the thickness of the membrane, but that a large degree of agglomeration had occurred. The particles were consistently orientated horizontally to the through-plane dimension creating a sort of "sheets". This analysis showed what the addition of GO creates: a more difficult path for the methanol to cross the membrane, reaching the cathode side creating parasite current, so lowering the power output.

Moreover, using the SEM Zeiss EVO MA 10 and the EDS Bruker Quantax 200, the morphological analysis and microanalysis of particles and matrices of the composite membranes were carried out, in order to estimate the composition of the samples qualitatively and quantitatively. As soon as a chemical element is identified by the instrument, it is depicted in the form of a spot. Each chemical element is associated with one colour: the red identifies Carbon (C), green for Oxygen (O), dark blue for Fluorine (F), light blue for Aluminium (Al), purple for Sulfur (S) and yellow for Silicon (Si). This kind of test was carried out on figure 47 and figure 49. Results were shown in figures 50 and 51.

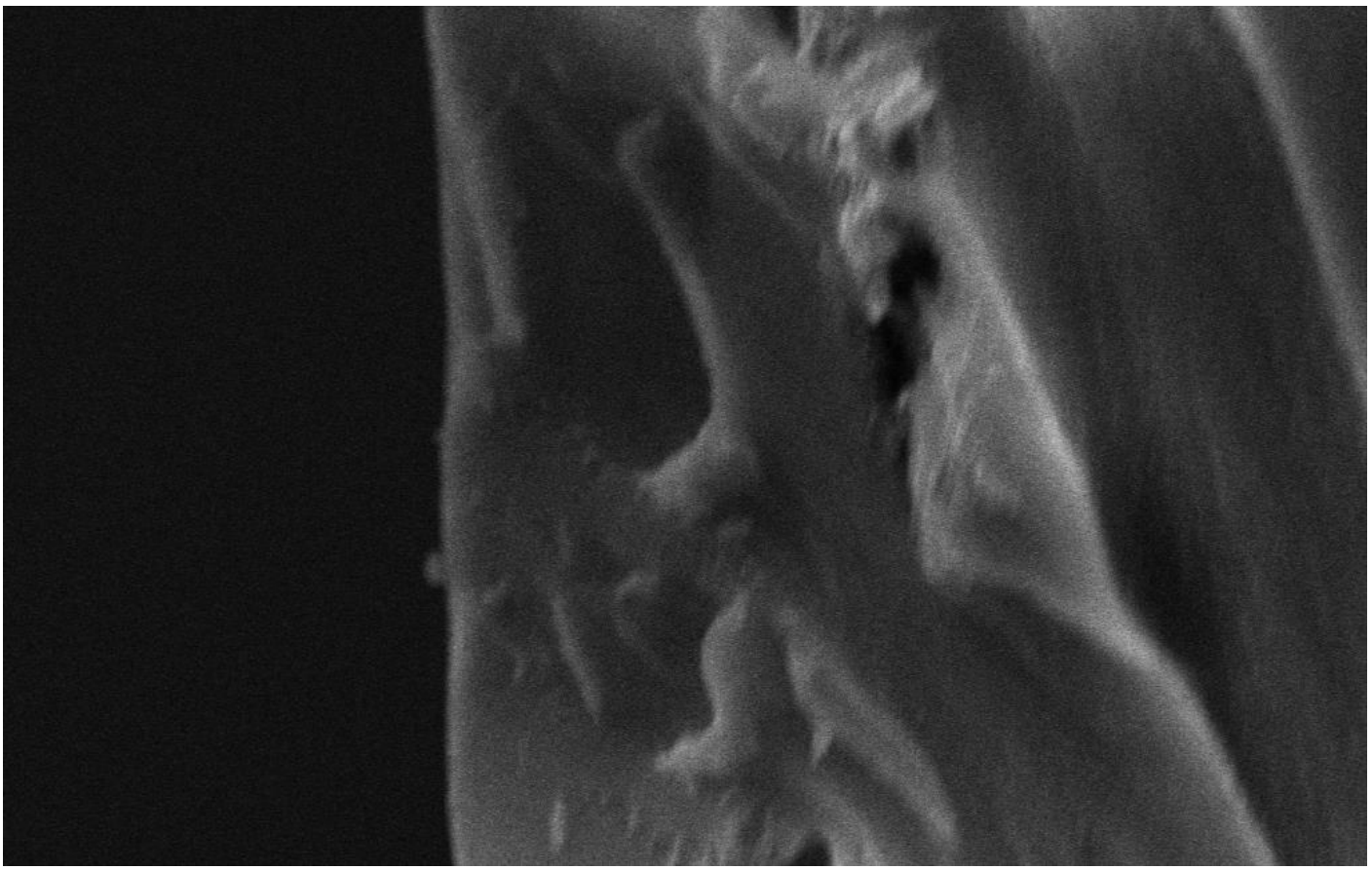

Figure 49-Particular of GO membrane at 1% of GO content

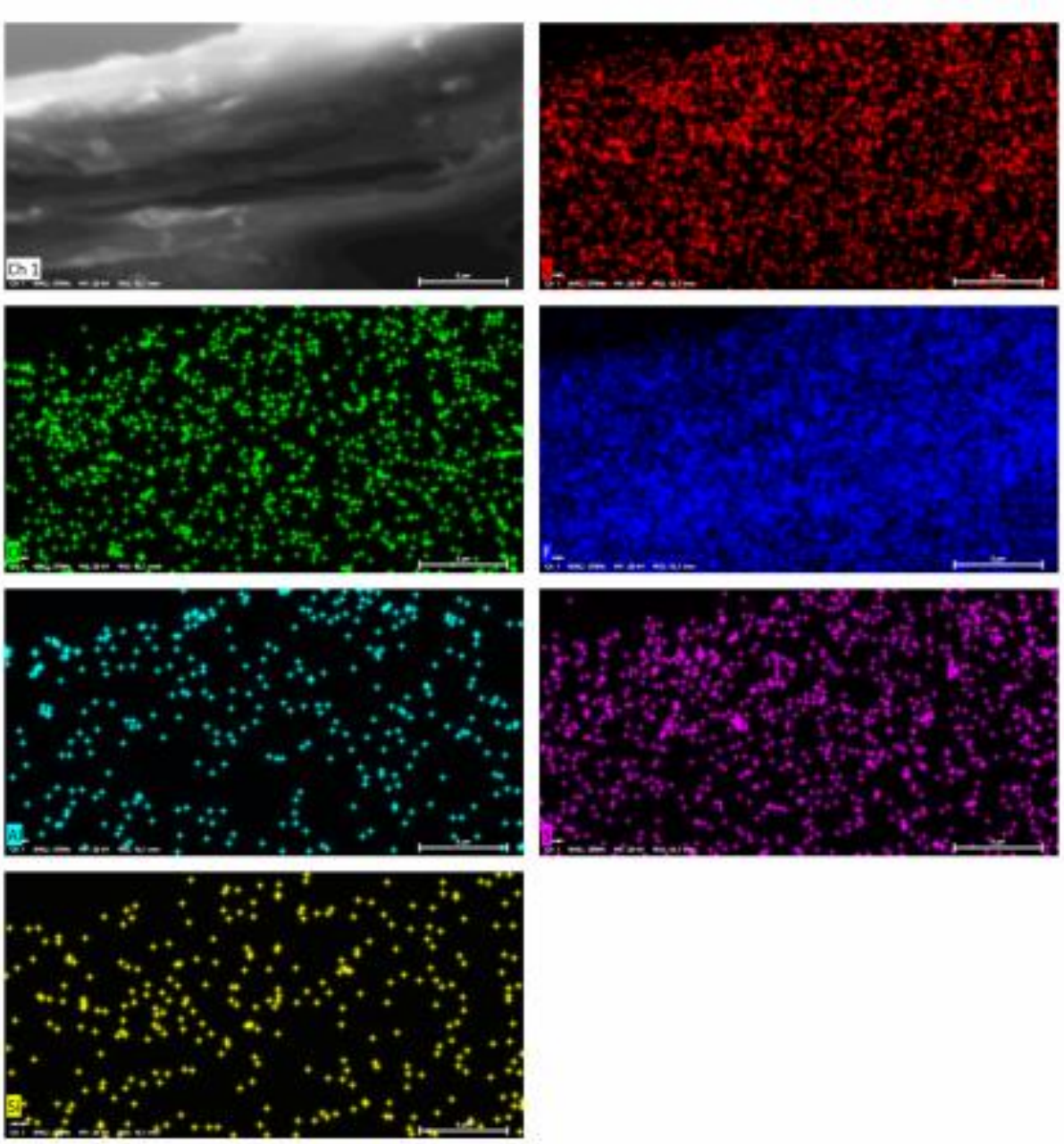

Figure 50-Component analysis at 0.5% of GO content [red for Carbon (C), green for Oxygen (O), dark blue for Fluorine (F), light blue for Aluminium (Al), purple for Sulfur (S) and yellow for Silicon (Si)]

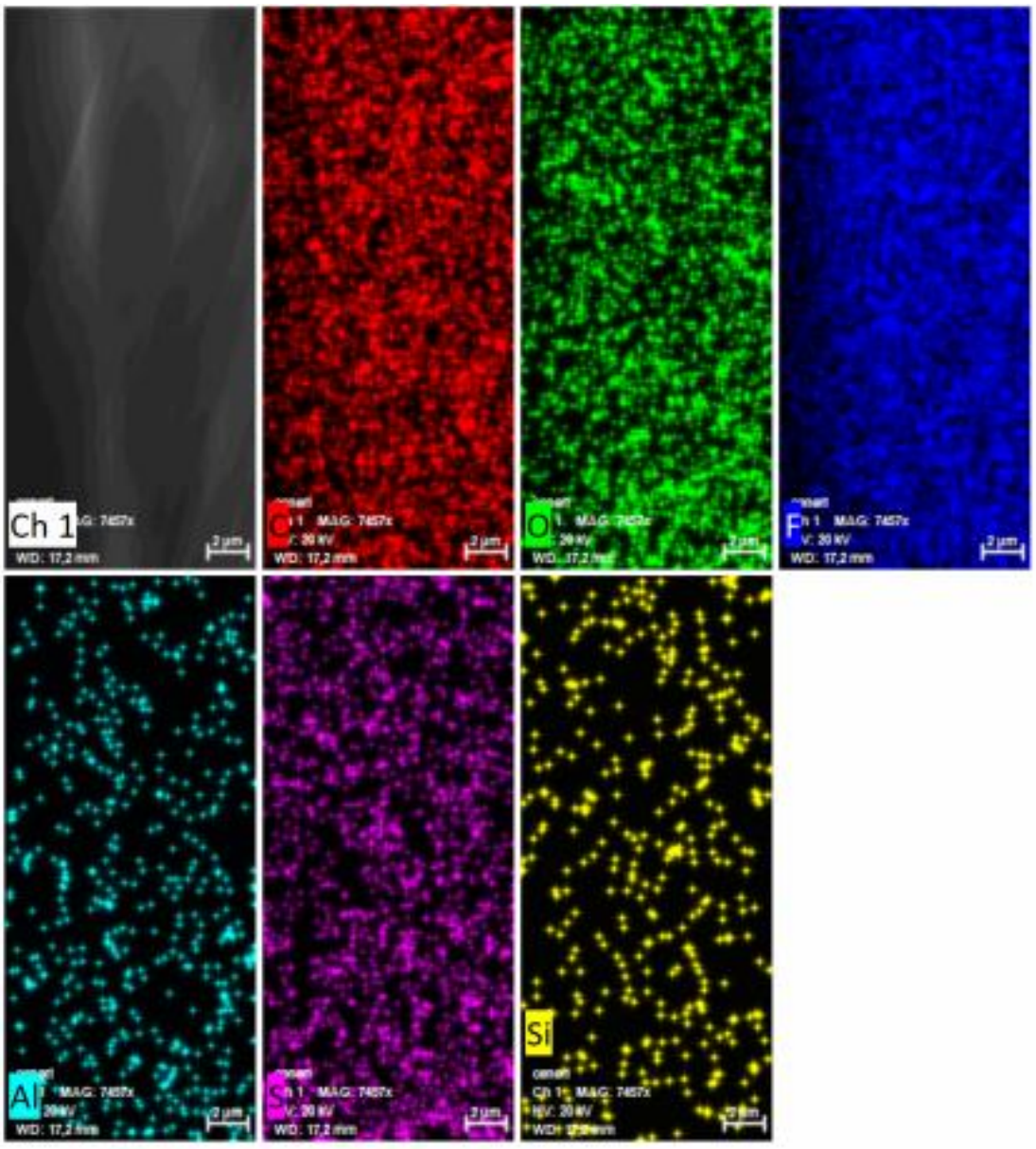

Figure 51-Component analysis at 1% of GO content [red for Carbon (C), green for Oxygen (O), dark blue for Fluorine (F), light blue for Aluminium (Al), purple for Sulfur (S) and yellow for Silicon (Si)]

As mentioned above, Nafion contains a hydrophobic fluorocarbon backbone and perfluoroether side chains terminating in a super acidic, hydrophilic ionic pendant group, sulfonic acid, so it is expected that the chemical elements with the highest concentration are Fluorine (F), Sulphur (S) and Oxygen (O). The addition of graphene oxide into the Nafion matrix, implies the implementation of other chemical components: Carbon principally, Oxygen and Hydrogen. It can be noticed, merely observing and comparing figures 50 and 51, that the content of oxygen and carbon is greater with increasing the GO content in the membrane. This is highlighted in tables 11 and 12 where the mass fractions of all the chemical components are reported.

Table 11-Mass fraction of the chemical components for a 0.5% GO membrane

Map

Element	At. No.	Netto	Mass [%]	Mass Norm. [%]	Atom [%]	abs. error [%] (1 sigma)	rel. error [%] (1 sigma)
Fluorine	9	27046	65,45	65,45	56,47	8,22	12,55
Carbon	6	3657	25,69	25,69	35,07	4,36	16,97
Oxygen	8	2061	7,65	7,65	7,83	1,50	19,60
Sulfur	16	1382	1,05	1,05	0,53	0,08	7,75
Aluminium	13	180	0,13	0,13	0,08	0,04	34,49
Silicon	14	58	0,03	0,03	0,02	0,01	34,23
		Sum	**100,00**	**100,00**	**100,00**		

Table 12-Mass fraction of the chemical components for a 1% GO membrane

Map

Element	At. No.	Netto	Mass [%]	Mass Norm. [%]	Atom [%]	abs. error [%] (1 sigma)	rel. error [%] (1 sigma)
Fluorine	9	6851	59,44	59,44	50,83	8,94	15,03
Carbon	6	1193	27,52	27,52	37,22	6,06	22,03
Oxygen	8	828	10,36	10,36	10,52	2,56	24,76
Sulfur	16	809	1,84	1,84	0,93	0,14	7,59
Silicon	14	204	0,46	0,46	0,27	0,08	17,59
Aluminium	13	120	0,38	0,38	0,23	0,09	22,29
		Sum	**100,00**	**100,00**	**100,00**		

The results are in line with the expectations: the mass fraction of carbon and oxygen increased introducing more GO in the composite membrane. The presence of Aluminium and Silicon, together with a small amount of carbon, is due to the preparation protocol for this test that required the use of a clamping system.

5.5 Tensile strength

Tensile strength and elongation are both important mechanical properties regarding polymeric membrane because they indicate the maximum stress to which a material can resist before breaking. This test was performed using a Zwick/Roel Z010 (Figure 52) following the standard method D882-02.

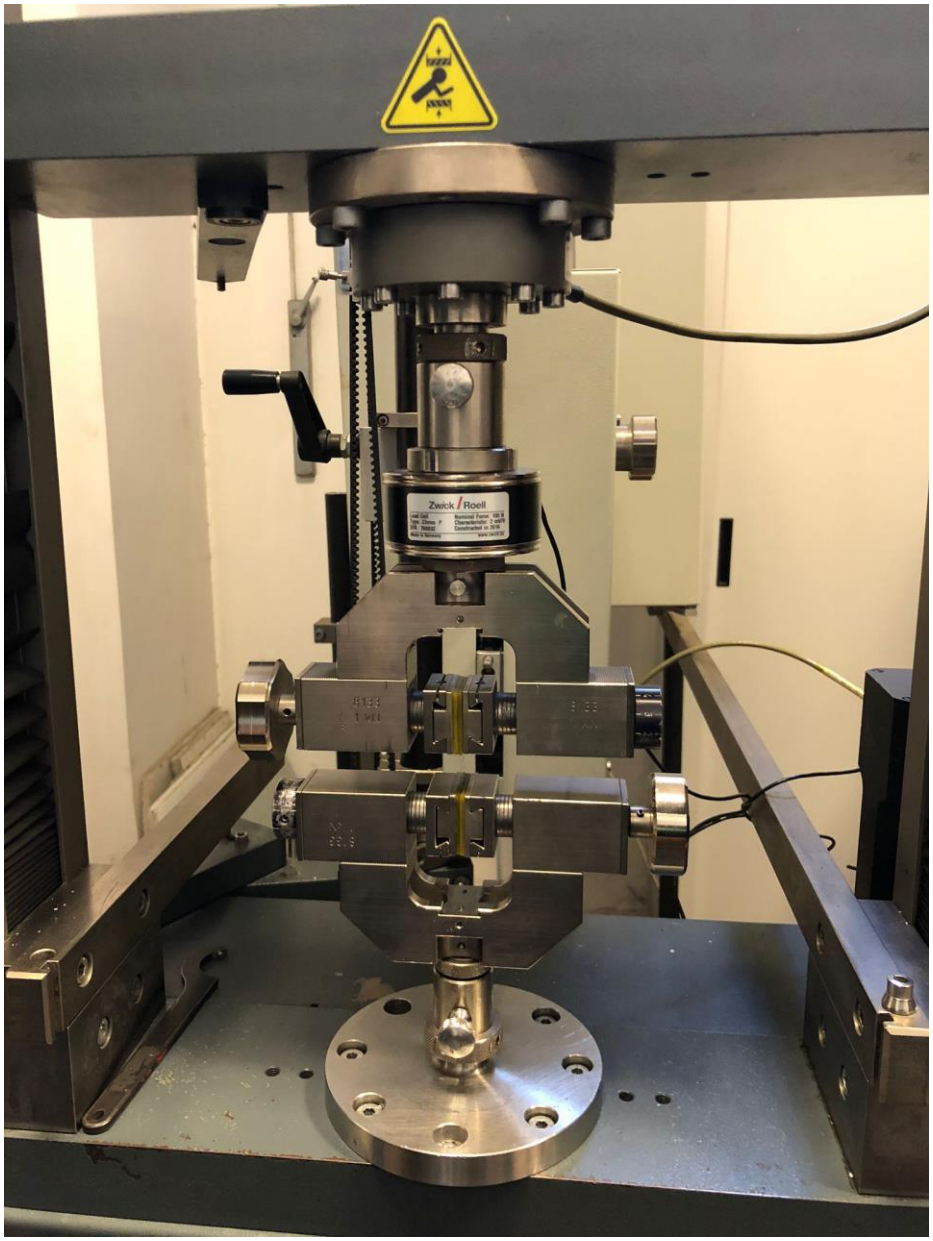

Figure 52-Zwick/Roel Z010 for tensile strength test

5 samples were cut in strips of uniform width, 11 mm, placed in the grips of the machine and tested at a strain rate of 1 mm/min. Table 13 displays the tensile strength and the elongation ratio of the composite membranes of varying loading.

Table 13-Tensile strength and elongation ratio of composite membrane and Nafion casted

Membrane	Tensile strength [Mpa]	Increase with Nafion casted %	Elongatio ratio %	Decrease with Nafion casted %
Nafion casted	11.5	/	75	/
Nafion/GO 0.5%	22	91.3	65	13.3
Nafion/GO 1%	25	117.39	50	33.33
Nafion/GO 1.5%	12	4.34	40	46.66

Tensile strength tests (Table 13) showed that a general increase of tensile strength is obtained. Only the membrane with 1.5% showed a tensile strength slightly higher than that of the bare Nafion membrane due to the inclusion of GO into the perfluorosulfonic matrix. The result obtained for the membrane at 1.5% was unexpected because GO enhances the mechanical characteristic of the membrane, so the more GO is included in the membrane, the higher tensile strength is expected as stated by several authors [**165,166**] as obtained for the membranes at 0.5 and 1% wt. However, the results of Table 13, represent the average of 5 tests performed on the membranes peeled off from the petri dish. The non-uniform dispersion of GO between the edge and the centre of the membrane maybe influenced the test. In fact, the standard deviation calculated for all the membranes are 0.4, 0.73, 0.86 and 3, for the casted Nafion, 0.5 % GO, 1% GO and 1.5% GO respectively. However, as can be observed, the elasticity of the GO membrane is very low compared to Nafion. The maximum elongation of the GO membrane before breaking is 65, 50 and 40% for 0.5% of GO, 1% and 1.5%, which is 13, 33 and 47% lower than that of recast Nafion. This result is in agreement with literature. In fact, Bayer et al. [**166**] claimed that the elongation of the GO membrane before rupture is only 22 ± 1%, compared with 411 ± 14% in Nafion, so the introduction of GO results in a decrease in elongation.

5.6 Final consideration

Properties of Nafion/GO composite membranes were discussed in the previous sections. The SEM analysis revealed how the GO is disposed into the Nafion matrix. The tortuosity created, due to the presence of GO, hinders the passage of methanol through the membrane thus lowering the crossover of this fuel. The tensile strength is a parameter related to the mechanical resistance of the membrane. The addition of GO benefits

the tensile strength of the membrane at the expense of the elongation. In this study, the tensile strength has less impact than WU, IEC and proton conductivity, as it is a property relevant especially at high temperature operation. In the present applications, the tests are carried out at low temperature. Water uptake, IEC and proton conductivity are key parameters that directly influence the performance of a fuel cells. The behaviour of those parameters with the increasing of GO content is the opposite: the water uptake and the IEC values were enhanced while the proton conductivity decreased. Figure 53 highlights the trend of WU and proton conductivity (53A), IEC (53B) and tensile strength and elongation ratio (53C) at different GO loading.

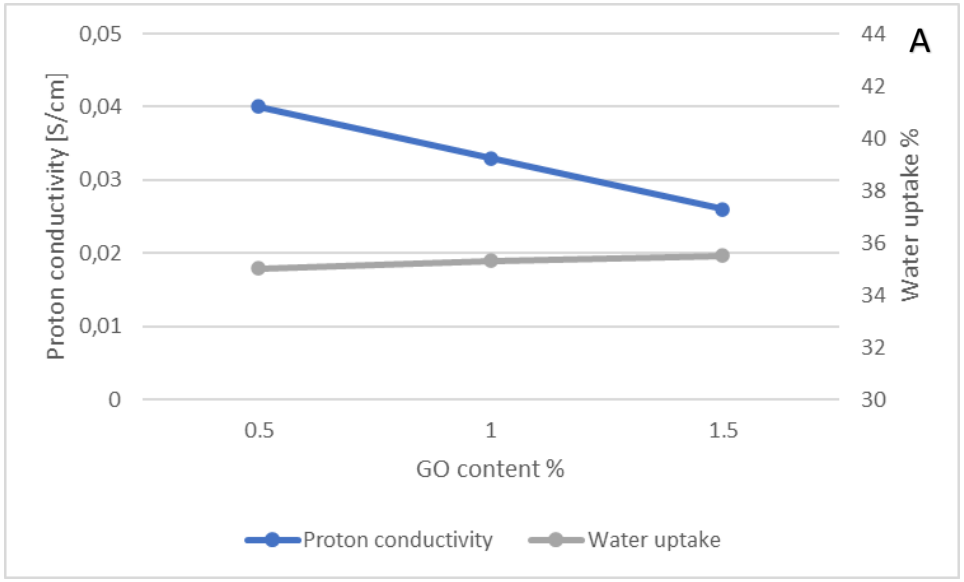

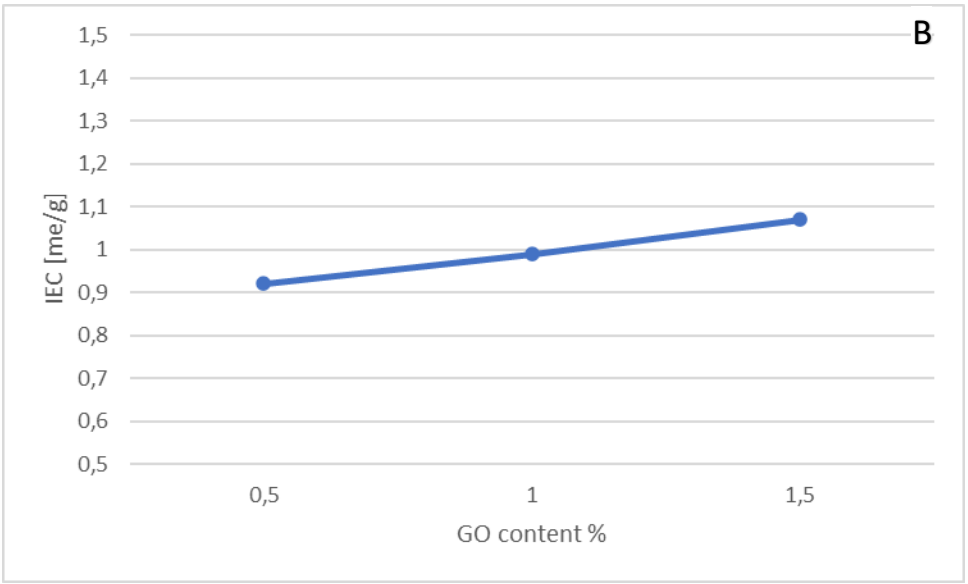

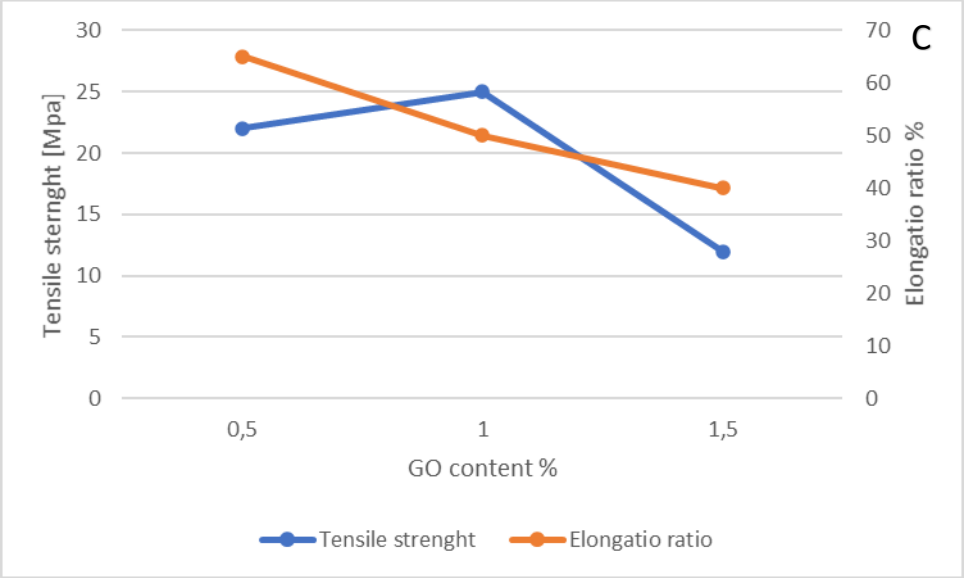

Figure 53-Trend of WU and proton conductivity (53A), IEC (53B), tensile strength and elongation ratio (53C) at different GO loading.

g

The benefits that are obtained at elevated GO content do not justify the increase of the material used. We can conclude that the meaningful interval ranges between 0.5 and 1.5%. Table 14 shows the percentage deviation of WU, proton conductivity, IEC, tensile strength and elongation, taking the casted Nafion as reference. Regarding the proton conductivity, as depicted in figure 45, the reduction is narrowing by adding more GO in the Nafion matrix when increasing the temperature. Since some values were missing at high temperature (at 1 and 1.5%), those were excluded from table 14 but the trend depicted in figure 45B was considered in the final evaluation.

Table 14-Deviation of proton conductivity, IEC and WU of Nafion/Go membranes at different GO loading from the Nafion casted

GO content	Water uptake	IEC	Proton conductivity at 25°C	Tensile strenght	Elongation rate
0.5%	+9.38%	+10.84%	-4.76%	+91.3%	-13%
1%	+10.31%	+19.27%	-21.43%	+117.39%	-33%
1.5%	+10.93%	+28.91%	-38.09%	+4.34%	-47%

A good compromise between a gain obtained from the water uptake, IEC, and tensile strength and the loss of the proton conductivity and of the elongation rate, is obtained by using the membranes with 0.5 and 1% of GO loading, which represent the optimum range. This conclusion was achieved also from Choi et al. [**106**] where the authors claimed that the best physical and transport properties were obtained by a Nafion/GO composite membrane with 0.5% of GO loading, in a range 0.5-2% wt. The membrane with 0.5% showed the highest selectivity (the ratio between proton conductivity and methanol permeability) but the difference

with the other one at 1% was only 10%. Even though the membrane with 1% had lower methanol permeability, the proton conductivity reduced also. Lee et al. [**111**], analysed the performance obtained from a direct methanol fuel cell, using Nafion/GO membranes at 0.5, 3 and 4.5%. The reduced methanol crossover enhanced the performance of the composite membrane, but, at 4.5%, the drop in proton conductivity was too high despite having low methanol permeability; the optimum was 3%. These two papers underline how vital is reducing the crossover of the fuel, also sacrificing the proton conductivity, to improve the performance of the fuel cell. This aspect has an important implication for a future application, as for instance for the mobile technologies, because reducing the methanol crossover signifies that, for a specific power density, the DMFC works with lower flow rates, thus reducing the size of the device [**167**]. The morphological analysis pointed out how the GO is more dispersed in the membrane with 1% rather than that at 0.5%, contributing to block the passage of methanol through the membrane. Therefore, taking into account all the results listed in table 14, examining the behaviour of proton conductivity in figure 45, pondering both the great impact of methanol crossover on the performance and the SEM analysis, in this work, MEAs were fabricated using GO membranes with 1% of loading.

6 Single cell tests

The single cell tests were carried using the test bench described in the chapter 4. Bipolar plates were composed of graphite with single serpentine flow channels to favour the reactants distribution. MEAs had an active area of 9 cm^2. The gas diffusion electrodes (GDE) with carbon cloth support and the catalyst were purchased from Fuelcell store with a catalyst loading of 3 mg Pt-Ru/cm^2 at the anode and 3 mg Pt/cm^2 at the cathode. The MEAs were tested in the fuel cell single cell sample holder. The I-V curve was recorded 3 times for each sample. The tests are organized as follow: firstly, tests were carried out to assess the influence of membrane activation. Then tests were carried out varying the anode flow rate, temperature and methanol concentration, to study the effect of the operating condition on the performance of the composite membrane. All the results were compared with that obtained from the Nafion membrane, by using both the casted and commercial version.

6.1 Chemical pre-treatment of the membrane

The performance of a fuel cell mainly depends on the water management which is controlled by the humidification of the membrane. Temperature and water content (in particular, the ratio of water and sulfonic acid groups) affect the ionic conductivity of the polymer electrolyte membranes that are used in the fuel cells. Furthermore, the temperature and the hydration of a membrane influence the ionic conductivity. Many researchers showed that a chemical pre-treatment procedure strongly influences the water content and hence the resulting ionic conductivity of the membrane [**168**]. During pre-treatment, the type of proton-donating acid, the acid concentration as well as the applied temperature governs the ionic conductivity. Therefore, the chemical pre-treatment is a necessary step to increase the performance of a fuel cell. It has been proved that an acid treatment is able to increase the number of water molecules per sulfonic group, therefore activating the membrane. Napoli et al. [**169**] performed the acid treatment using several acids and varying their concentration. They observed no important difference. The pre-treatment of the membranes used in this study, was described in section 3.3. All the membranes were treated using a solution of 0.5M of sulfuric acid. In figure 54, the results of a test carried out for a non-activated and an activated membrane are compared. To distinguish the performance of the non-activated membrane from the activated, a solid and a dotted line are used respectively.

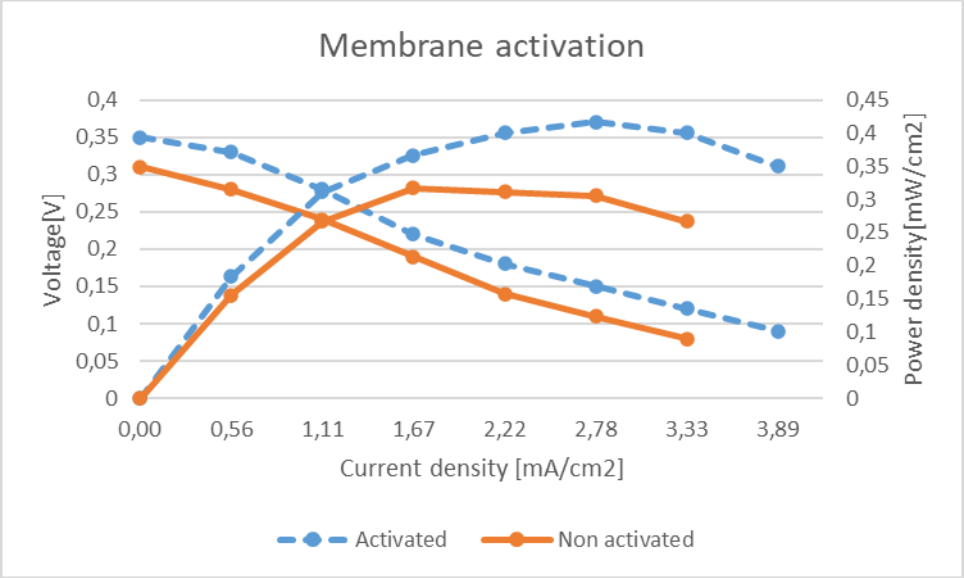

Figure 54-Activation effect of a membrane [Anode flow:5 ml/min- T=40°C- 1M of methanol solution]

As expected, the performance of the activated membrane is better. The power output was increased of nearly 31% and the operating range was enhanced of almost 17%. The acid treatment increases the proton number in the membrane that are available for facilitating of transfer protons from the anode to the cathode leading to higher proton conductivity so higher performance.

6.2 Operating conditions optimization

The aim of these procedures is to check the variations in terms of available power when changing the cell operating conditions.

The operating conditions object of the study are:

- Anode flow rate
- Temperature
- Molarity

All tests were carried out for Nafion commercial and casted membrane and GO membranes.

6.2.1 Anode flow rate

The influencing factors of methanol flow rate to the DMFC performance are mass transport of methanol, methanol crossover, the removal of product CO_2 as well as the heat exchange between the methanol solution and the catalyst layer. The other operating conditions are fixed to:

- Temperature: 40°C
- Methanol Concentration: 1M

With this design, three different anode flow rates (AFRs) have been proved: 4ml/min, 7ml/min and 15ml/min. Table 15 summarizes the operating conditions used to test the effect of AFR:

Table 15 Operating conditions to test the effect of AFR

Operating condition	Value
Temperature °C	40
Methanol concentration M	1
Anode flow rate mL/min	4-7-15

Figure 55, Figure 56 and Figure 57 show the power density and polarization curves for the commercial Nafion, casted Nafion and GO composite membrane with 1% of GO loading. To distinguish the different operating conditions, a solid line, a dotted and a dash-dot line are used for 4, 7 and 15 mL/min respectively.

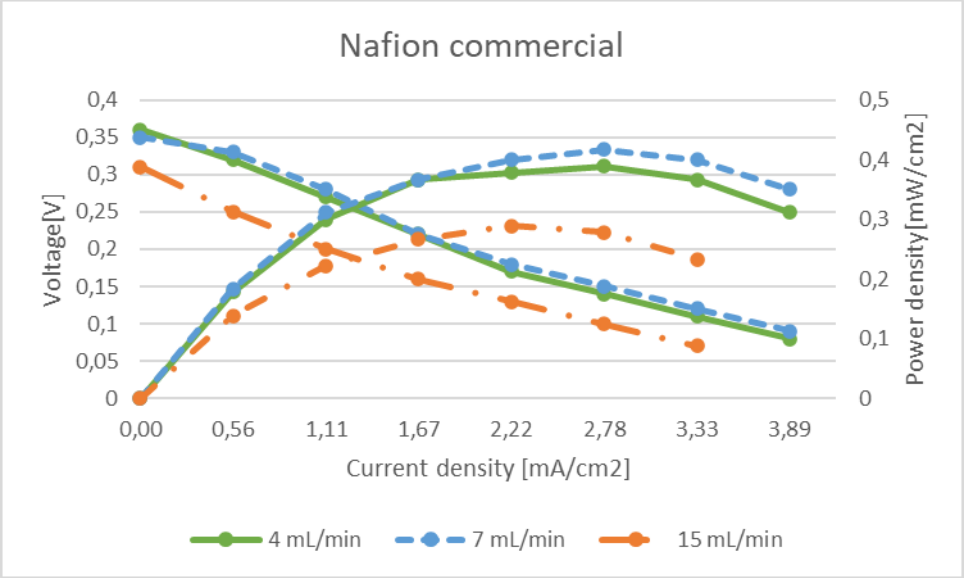

Figure 55-Effect of anode flow rate on Nafion commercial membrane

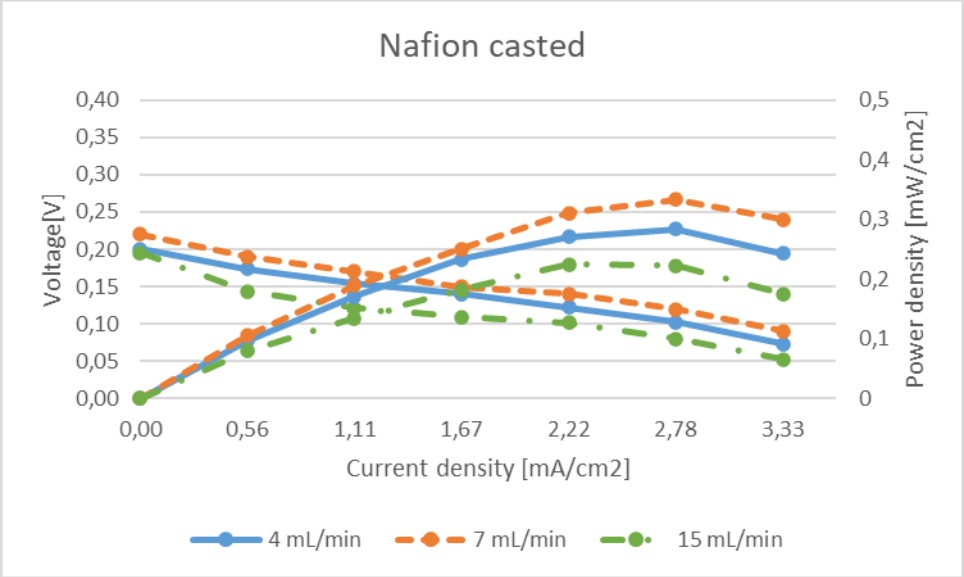

Figure 56-Effect of anode flow rate on Nafion casted

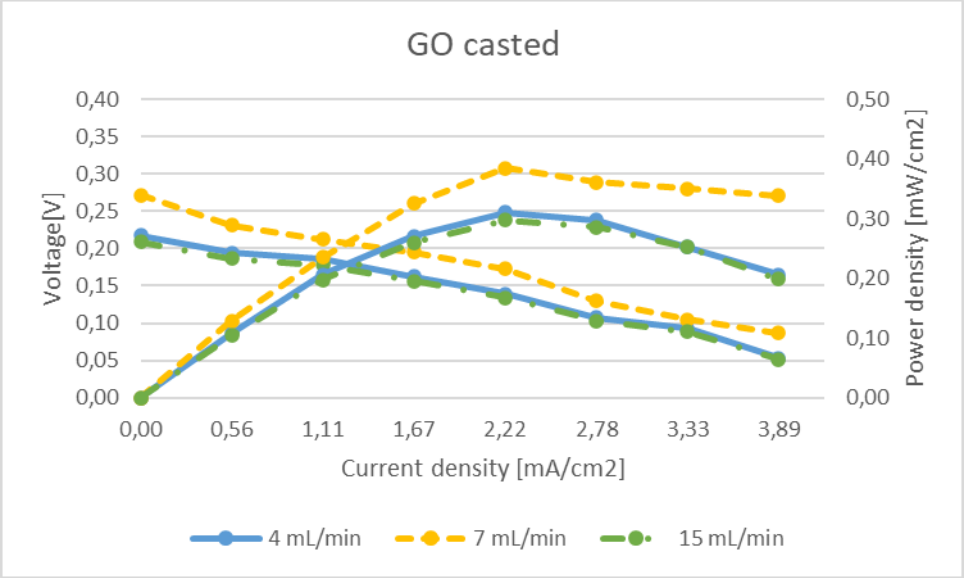

Figure 57-Effect of anode flow rate on GO composite membrane

All the figures show how the DMFC performance first increases but then decreases with increasing anode flow rates. The optimal DMFC performance is achieved at a methanol flow rate of 7 mL/min. There is a rapid decrease in the DMFC performance when the methanol flow rate further increases to 15 mL/min. In fact, although high methanol flow rate can facilitate the mass transport of methanol and the removal of CO_2, it also results in more methanol crossover. In addition, the methanol solution at high flow rate would cool down the temperature of catalyst surface, and hence decrease the activity of the Pt-Ru catalyst. In this study, the appropriate range of methanol flow rate is 4-7 mL/min, the optimum is obtained at 7 mL/min.

6.2.2 Methanol concentration

The methanol molarity expresses the number of methanol moles present in the solution, representing a measure of the quantity of fuel available for a determined compound flow. Isolating the variation of this factor, keeping the others unchanged, allows to analyze the behavior of the cell related to it. In this case the operating conditions are set to:

- Anode Flow Rate: 7 ml/min
- Temperature: 40°C

In this arrangement, three different levels of concentration were tested: 0.5M, 1M and 1.5M.

Table 16 summarizes the operating conditions used to test the effect of methanol concentration:

Table 16 Operating conditions to test the effect of molar concentration

Operating condition	Value
Temperature °C	40
Methanol concentration M	0.5-1-1.5
Anode flow rate mL/min	7

Figure 58, Figure 59 and Figure 60 show the power density and polarization curves associated to the cell under this configuration. To distinguish the different operating conditions, a solid line, a dotted and a dash-dot line are used for 0.5, 1 and 1.5 M respectively.

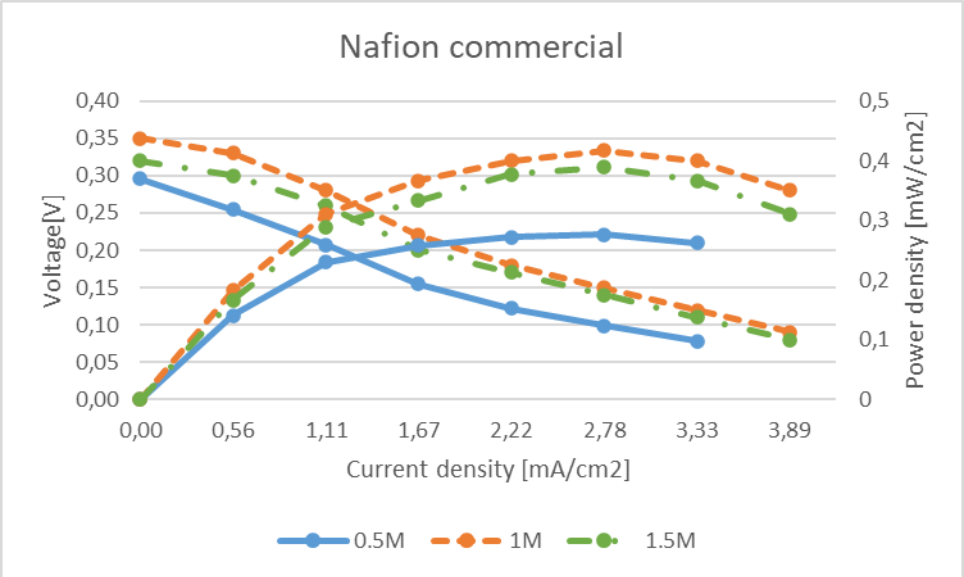

Figure 58-Effect of methanol concentration on Nafion commercial membrane

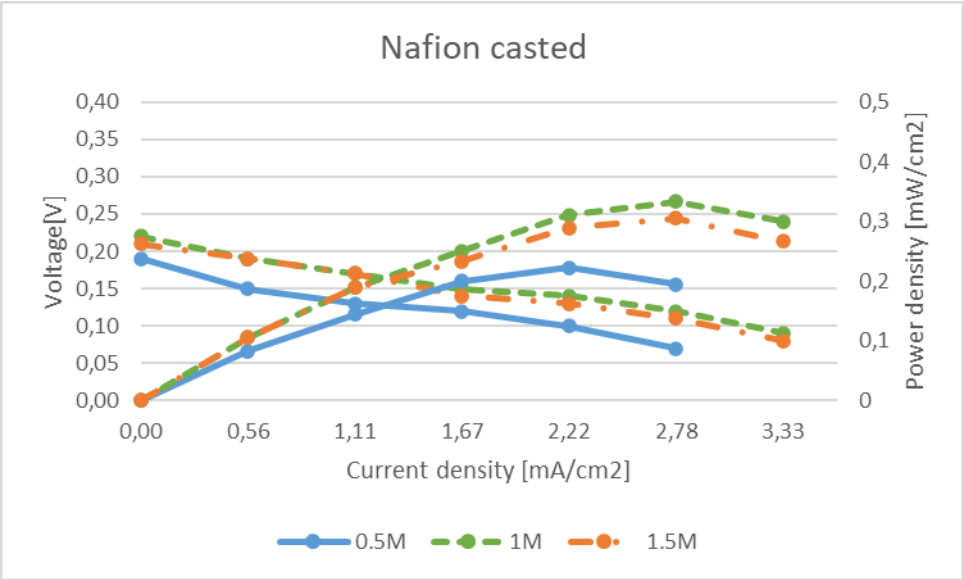

Figure 59-Effect of methanol concentration on Nafion casted

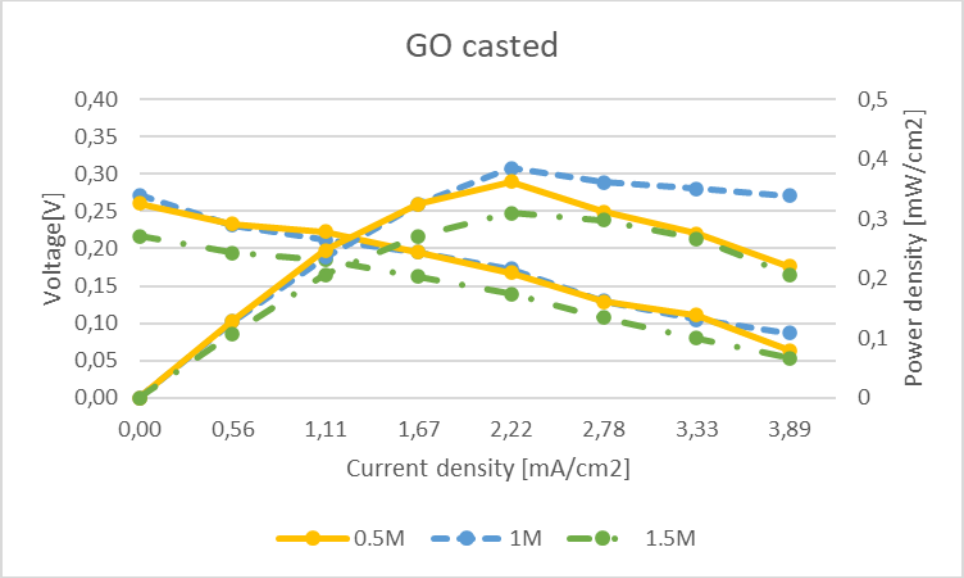

Figure 60-Effect of methanol concentration on GO membrane

All the figures show that a molarity variation leads to well-designed deviation in the achieved results. High methanol concentration enhances the reaction rate in the anode, but at the same time increases the methanol crossover to the cathode. The methanol in the cathode will be oxidized over Pt catalyst to produce mixed potential, thus decreases the DMFC performance. The open circuit voltages drop in all the membranes when the concentration of the solution is 1.5M. The open circuit voltages generally decrease with the increase of methanol

concentration because the methanol crossover also increases with increasing methanol concentration, which will result in higher crossover current and hence lower the open circuit voltage. When the methanol concentration is 0.5 M, the performance is pretty low because of the less methanol concentration. However, at higher methanol concentration, the DMFC performance increases rapidly and then dropped when the concentration of the reactant is too high. The DMFC performance decreases at the high loading current density region because the concentration of methanol solution of 0.5 M is too low. This behavior is more evident using the pure Nafion membrane. In this study, the appropriate methanol concentration is 1M. This trend agrees well with that obtained by Jung et al. [**170**].

6.2.3 Temperature

Temperature is one of the most relevant parameters affecting cell performance. The influence of this factor is assessed by fixing the other parameters and varying the temperature conditions during a certain timeframe. The selected environment is set as follows:

- Anode Flow Rate: 7 ml/min
- Chemical Concentration: 1M

In this configuration, three different levels of temperatures have been proved: 20°C, 40°C and 60°C.

Table 17 summarizes the operating conditions used to test the effect of temperature:

Table 17 Operating conditions to test the effect of temperature

Operating condition	Value
Temperature °C	20-40-60
Methanol concentration M	1
Anode flow rate mL/min	7

Figure 61, Figure 62 and Figure 63 show the power density and polarization curves associated to the cell under this arrangement. To distinguish the different operating conditions, a solid line, a dotted and a dash-dot line are used for 20, 40 and 60°C respectively.

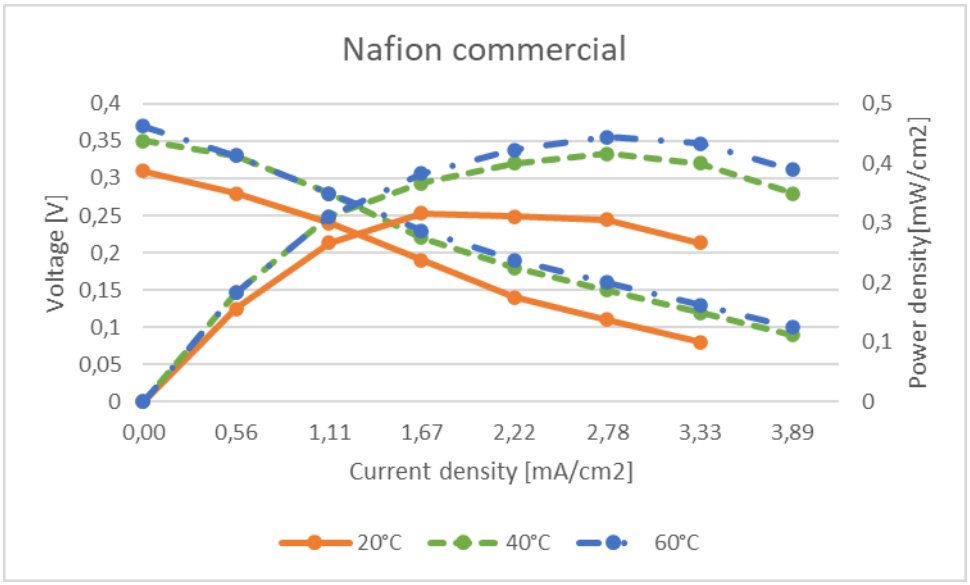

Figure 61-Effect of temperature on Nafion commercial membrane

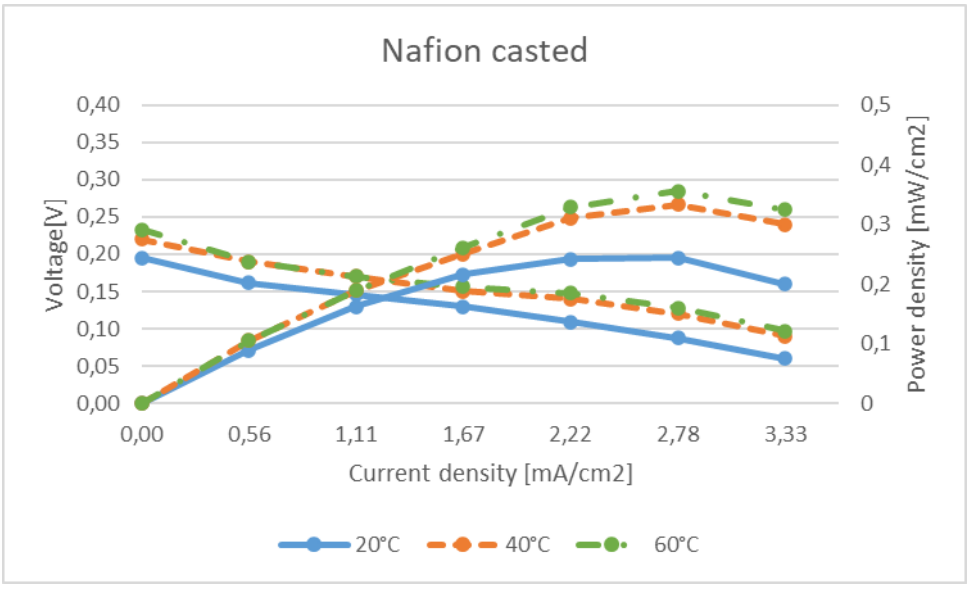

Figure 62-Effect of temperature on Nafion casted membrane

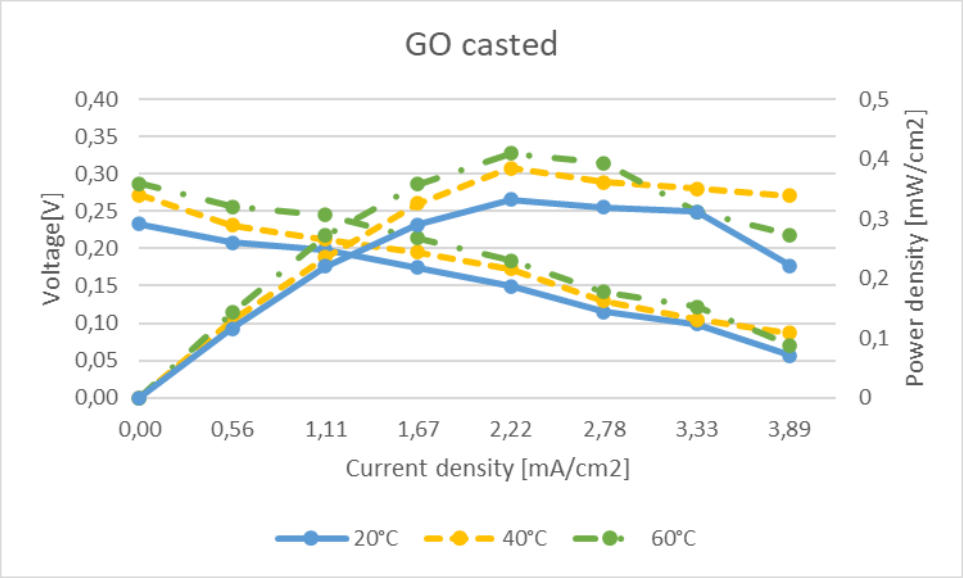

Figure 63-Effect of temperature on GO composite membrane

It can be seen from figure 61 to figure 63, that the DMFC performance increases significantly with an increase in cell temperature. These results agree well with those obtained by Govindarasu et al. [**171**]. The temperature could have been increased beyond 60°C, however, the methanol boiling point is 64.7°C so the temperature never got over 60°C to both exploiting the heat generation by the exothermic global reaction and avoiding methanol boiling.

The enhanced DMFC performance at increasing cell temperatures can be attributed to the following two processes:

- The increase of the catalytic activities for methanol electro-oxidation and oxygen reduction with increasing cell temperature.
- The ion conductivity of Nafion membrane or Nafion ionomer in the catalyst layers decreases with an increase in cell temperature, so the ohm polarization loss decreases.

At low temperature, the methanol electro-oxidation rate is slow, the CO_2 in the anode and the water in the cathode cannot be removed in time, which will block the diffusion of methanol and oxygen to the catalyst surface. When the cell temperature increases, the reactant diffusion and the product removal increase, so the electrochemical reaction is faster. In addition, high cell temperature enhances the ion conductivity of the membrane and catalyst layer, therefore the cell resistance is reduced. All these processes contribute to the enhanced DMFC performance at high cell temperature.

6.2.4 Final consideration

The effect of operating conditions on the performance of a DMFC with Pt-Ru as the anode catalyst has been investigated. Extending the anode flow rate and methanol concentration has a dual effect: increasing the flow of the reactant allows to obtain higher performance despite enhancing the methanol crossover and losses. At one point, the loss will be no longer counterbalanced, and performance starts decreasing. The appropriate operating conditions of the target DMFC are 1M methanol at the flow rate of 7 mL/min. The greatest DMFC performance increase is attributable to an increase in cell temperature, which can be ascribed to the enhancement of the catalytic activities as well as the ion conductivity in the MEA. The optimum is obtained at 60°C.

6.3 The influence of GO in the performance of the cell

The I-V characteristics obtained from single cell test and the relative power curves for Nafion casted and GO casted membrane (loading 1%) are shown in Figures 64 to Figure 69. To highlight the impact of GO in the Nafion matrix, a comparison between the Nafion casted membrane and the composite one was made for each operating condition. The comparison with the commercial Nafion is neglected because due to the different thickness of the membrane and the different manufacture. Below the results obtained varying the anode flow rate (figure 64 to figure 66) and the methanol concentration (figure 67 to figure 69). To distinguish the GO membrane from Nafion casted, a solid and a dotted line are used respectively.

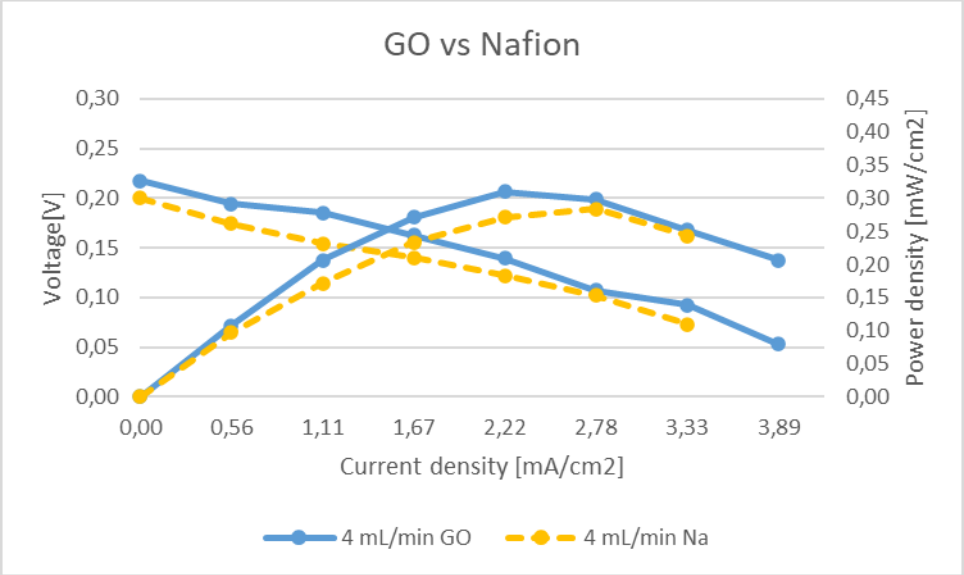

Figure 64- Comparison between casted Nafion and Go at 4 mL/min of AFR

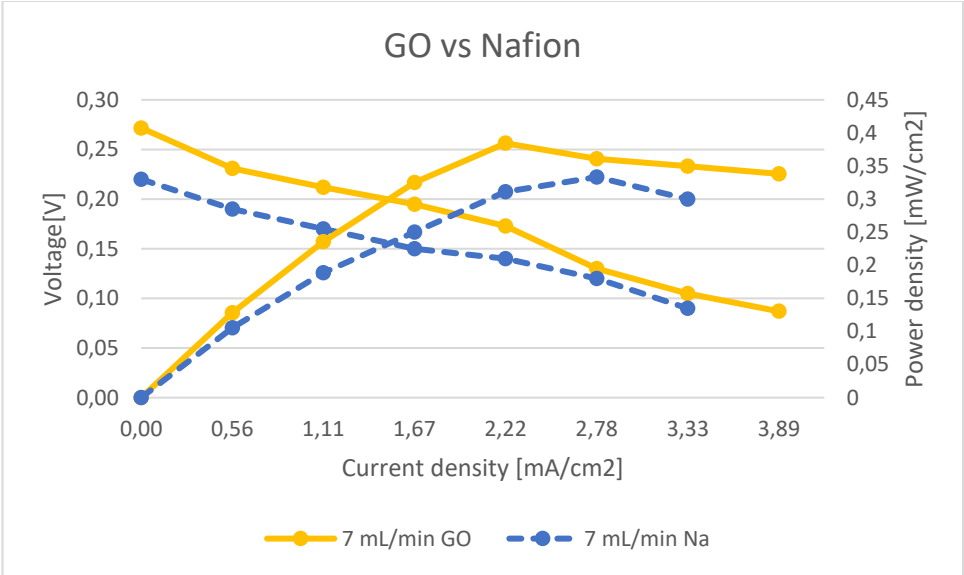

Figure 65- Comparison between casted Nafion and Go at 7 mL/min of AFR

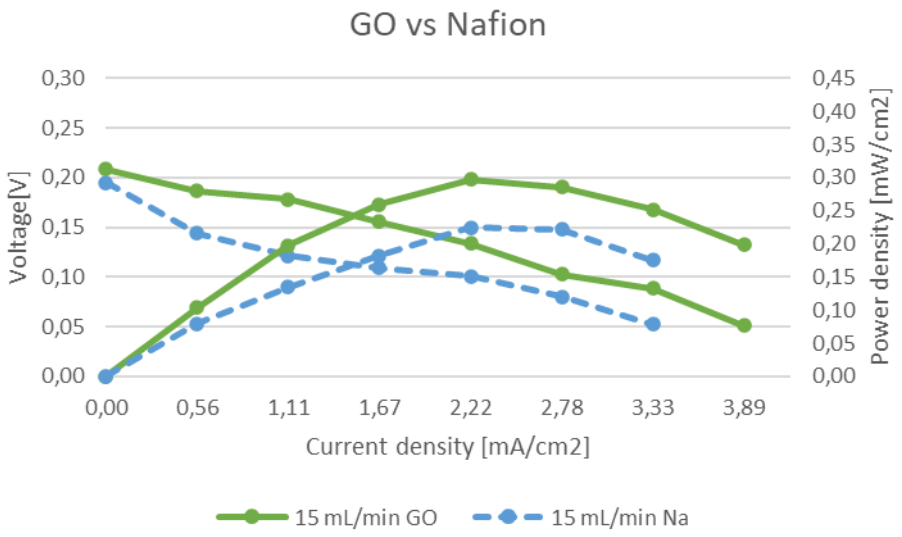

Figure 66- Comparison between casted Nafion and Go at 15 mL/min of AFR

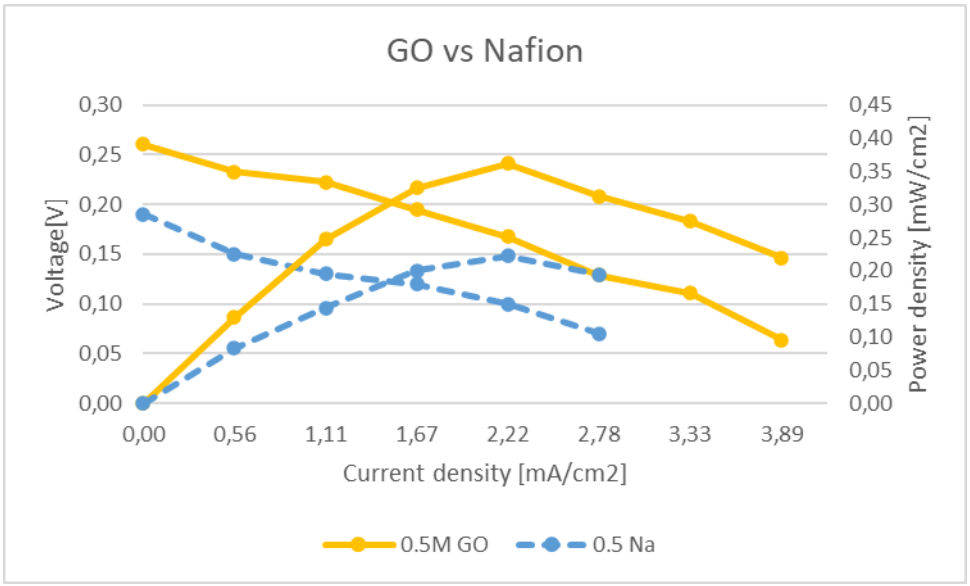

Figure 67-Comparison between casted Nafion and GO at 0.5 M

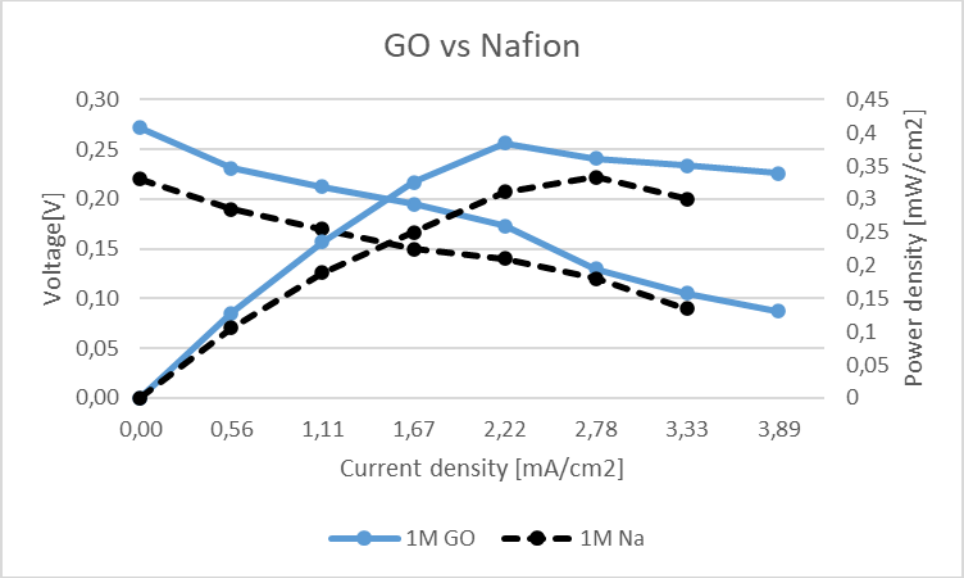

Figure 68-Comparison between casted Nafion and GO at 1M

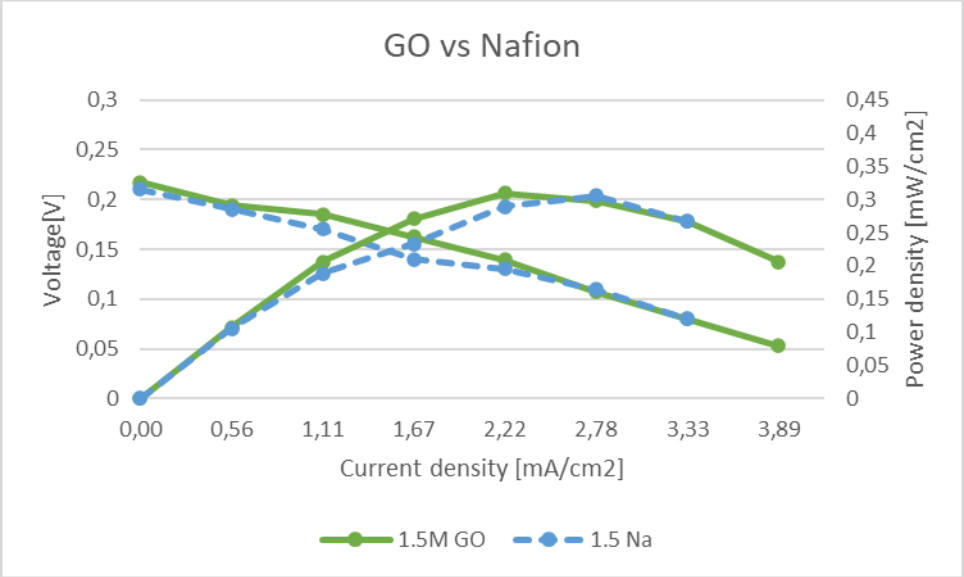

Figure 69-Comparison between casted Nafion and GO at 1.5M

The improvement in DMFCs' performance was remarkable with GO-based composite membranes compared to Nafion casted membrane in controlled operating conditions. Table 18 summaries the percentage deviation of OCV, best power output and operating range of the composite membrane as against the casted Nafion membrane.

Table 18-Rate of improvement of GO membrane with respect to Nafion

Operating condition	OCV	Maximum Power output	Operating range
4 mL/min	+10%	+11%	+17%
7 mL/min	+23%	+15.3%	+17%
15 mL/min	+10%	+32.5%	+17%
0.5 M	+36.8%	+63%	+40%
1 M	+24%	+15.6%	+17%
1.5 M	+5%	+4%	+17%

The performance of bare Nafion is always lower, this behavior is emphasized at low methanol concentration and using an intermediate anode flow rate. All the three parameters considered, the maximum power output, OCV and operating range, increased in each test. Notably, the impact of GO is remarkable at 0.5M where the maximum increment is obtained: 36.8% for the OCV, 63% for the best power output and the operating range was enhanced of 40%. The evolution of the performance is the result of what has been illustrated in the chapter 5: the introduction of GO in the polymeric matrix contributed to enhance the retention of water and reduce the fuel cell crossover, to the detriment of proton conductivity. Even if the methanol permeability or the methanol crossover current density was not tested, the beneficial effect of the GO on the crossover is remarked from the values of the open circuit voltage.

In every test, the OCV of the composite membrane is higher and this is principally due to the structure of GO (showed in the SEM analysis) included into the Nafion that hinders the passage of methanol to the cathode side. In addition, it is evident the correlation between OCV, methanol crossover and power output: from table 18, the higher is the increment in OCV, the higher is the power output in spite of the fact the proton conductivity of the composite membrane is lower. As stated before, the methanol crossover is the major issue of the DMFC and affects the overall performance of the cell. The graphene oxide allows to reduce this type of loss.

7 SUMMARY AND PERSPECTIVES

The aim of this study was to assess the potential of GO in improving DMFC performance. In fact, even if the beneficial effect of GO in improving PEMs was well known, it was not extensively optimized on DMFCs. Here, the first extensive analysis is reported with reference to the influence of the most relevant parameters.

The membrane preparation method by casting was discussed and was successfully conducted. Besides the composite membrane preparation, the study developed under two objectives which are discussed below. Graphene oxide has been considered as an appropriate element that offers promising results in terms of water uptake and mechanical properties. In fact, the WU of the composite membranes are all higher than the Nafion one, due the high amount of oxygen groups presents in the structure. A similar trend is also reported for the IEC. However, the proton conductivity follows the opposite behavior due to the barrier effect of GO. The mechanical test showed that the elongation ratio of the composite membrane decreased and only the membrane with 1.5% of loading showed lower tensile strength. A detailed discussion of the results obtained has led to the conclusion that the optimum GO loading is 1%. The performance in the cell were evaluated to investigate the effect of the chemical pre-treatment of the membrane and of operating conditions. The acid treatment of the membrane is necessary to protonate the membrane to ease the flow of proton. The increase of DMFC performance with the temperature can be ascribed to the enhancement of the catalytic activities as well as the ion conductivity in the MEA. Although high methanol flow rate and high methanol concentration facilitates the mass transport of methanol, it also results in more methanol crossover. The best operating condition were 1M and 7 mL/min. Comparing with Nafion, GO has increased the OCV and the best power output of the cell because GO increased the tortuosity of the membrane and then reduced the fuel crossover. This is more evident at low methanol concentration. The drop in proton conductivity is counterbalanced by the drop in methanol crossover, that is highlighted by the enhance in OCV. This result was expected and underlined by the SEM analysis that depicted the blocking structure of graphene oxide. The performances in the fuel cell prototype demonstrated the potential of these membranes but this study is a start point to develop GO membranes. Further investigation shall be carried out to deepen the influence of GO on some properties. In fact, although the trend observed for WU, proton conductivity and elongation ratio totally agree with works reported in literature, IEC and the tensile strength for high GO loading requires any additional examinations. Moreover, more single cell tests shall be conducted to confirm what it is achieved in this work and to investigate on the effect of GO at higher methanol concentration. Successive research activities will be focused on other types of composite membranes and, alternatively,

sulphonated polymers that have recently been studied to substitute Nafion membranes. Nevertheless, there is a strong concern regarding the solubility of sulphonated polymers in water, and a consequent drop in the water dependent proton conductivity. An approach adopted recently to minimize these effects is the use of multilayer membranes. This approach is expected to help keep the best properties of each layer/component intact while overcoming the drawbacks of each by using and combining layers of different membranes/polymer materials. So, the combination of the characteristics of Nafion and GO could be a new way to produce the membrane. However, the preparation is very complex because it involves different materials that could be handled in different ways. During my internship in Birmingham, a multilayer Nafion/GO/Nafion membrane was prepared using the casted method. The performance obtained were encouraging, in fact they were marginally better to that of Nafion commercial membrane: this is principally due to the reduced methanol crossover that was around 30% lower.

References

1. Barbir, F.; Gomez, T. Efficiency and economics of proton exchange membrane (PEM) fuel cells. Int. J. Hydrog. Energy **1996**, 21, 891–901.
2. EG&G Technical Services Inc. Fuel Cell Handbook, 7th ed.; U.S. Department of Energy/Office of Fossil Energy/National Energy Technology Laboratory: Morgantown, WV, USA, **2004**.
3. Thomas, S.; Zalbowitz, M. The Polymer Electrolyte Membrane Fuel Cell; Fuel Cells Green Power/Los Alamos National Laboratory U.S.: Los Alamos, NM, USA, **2000**.
4. Kamarudina, S.; Achmada, F.; Dauda, W. Overview on the application of direct methanol fuel cell (DMFC) for portable electronic devices. Int. J. Hydrog. Energy **2009**, 34, 6902–6916.
5. Shimizu, T.; Momma, T.; Mohamedi, M.; Osaka, T.; Sarangapani, S. Design and fabrication of pumpless small direct methanol fuel cells for portable applications. J. Pow. Sour. **2005**, 150, 277-283.
6. Dutczak, J. Issues related to fuel cells application to small drones propulsion. IOP Conference Series Materials Science and Engineering **2018**, 421(4)
7. Sundmacher, K.; Schultz, T.; Zhoua, S.; Scott, K.; Ginkel, M.; Gilles, E.D. Dynamics of the direct methanol fuel cell (DMFC): experiments and model-based analysis. Chemical Engineering Science, 2001, 56(2), 333-341
8. Larminie, J.; Dicks, A. Fuel System Explained; John Wiley & Sons Ltd.: Chichester, UK, **2009**.
9. Silvestroni, P. Fondamenti di chimica, Roma: Libreria Eredi Virgilio Veschi, **1953.**
10. Sahu, I.P.; Krishna, G.; Biswas, M.; Das, M.K. Performance study of PEM fuel cell under different loading conditions. Energy Procedia **2014**, 54, 468-478
11. Seo, S.H.; A.; Lee, C.S. A study on the overall efficiency of direct methanol fuel cell by methanol crossover current. Applied Energy. **2010**, 87(8), 2597-2604
12. Huang, X.; Zhang, Z.; Jiang, J. Fuel Cell Technology for Distributed Generation: An Overview. IEEE International Symposium **2006**, vol. 2
13. Bard, A.; Faulkner, L.; Electrochemical methods- Fundamentals and Applications. John Wiley &Sons, Inc, **2001**, New York, NY, USA
14. Barbis, F. PEM fuel cells: Theory and practice. Elsevier, Inc, **2005**, San Diego, USA
15. Kulikovsky, A. Fuel cell basics. Analytical Modeling of Fuel cells (Second Edition) **2019**
16. Haverkort, J.W. A theoretical analysis of the optimal electrode thickness and porosity. Electrochemical Acta **2019**, 295, 846-860
17. Saleh, I.M.M.; Ali, R.; Zhang, H. Simplified mathematical model of proton exchange membrane fuel cell based on horizon fuel cell stack. Journal of Modern Power Systems and Clean Energy **2016**, 4, 668-679.
18. Al-Baghdadi, M.; Shahad, H. Parametric and optimization study of a PEM fuel cell performance using three-dimensional computational fluid dynamics model. Renewable Energy **2007**, 32, 1077-1101.
19. Akimoto, Y.; Okajima, K. Semi-Empirical Equation of PEMFC Considering Operation Temperature. Energy Technology & Policy **2014**, 1, 91-96
20. Gerteisen, D. Transient and steady-state analysis of catalyst poisoning and mixed potential formation in direct methanol fuel cells. J. Pow. Sour. **2010**, 195, 6719-6731.
21. Qi, Z.; Kaufman, A. Open circuit voltage and methanol crossover in DMFCs. J. Pow. Sour. **2002**, 110, 177-185
22. An, M.; Mehmood,A; Ha, H.Y. A sensor-less methanol concentration control system based on feedback from the stack temperature. Applied Energy, **2014**, 131, 257-266.
23. Casalegno, A.; Marchesi, R.; Grassini, P. Experimental analysis of methanol crossover in a direct methanol fuel cell. Applied Thermal Engineering **2007**, 27, 748-754.
24. Kulikovsky, A. A model for mixed potential in direct methanol fuel cell cathode. Electrochimica Acta **2012**, 62, 185-191.
25. Dutta K. Direct methanol fuel cell Technology, 1st Edition. Elsevier, Inc, 2020, San Diego, USA

26. Kulikovsky, A. Bubbles in the anode channel and performance of a DMFC: asymptotic solutions. Electrochimica Acta **2006**, 51, 2009-2011
27. Calabriso, A.; Borello, D.; Romano, G.P.; Cedola, L.; Del Zotto, L.; Santori G.S. Bubbly flow mapping in the anode channel of a direct methanol fuel cell via PIV investigation. Applied Energy **2017**, 185 (2), 1245-1255
28. Rosli, N.; Loh, K.; Wong, W.; Yunus, R.; Lee, T.; Ahmad, A.; Chong, S. Review of Chitosan-Based Polymers as Proton Exchange Membranes and Roles of Chitosan-Supported Ionic Liquids. Int. J. Mol Sci **2020**, 21 (2), 632.
29. Wang, L.; He, M.; Hu, Y.; Zhang, Y.; Liu, X.; Wang, G. A. "4-cell" modular passive DMFC (direct methanol fuel cell) stack for portable applications. Energy **2015**, 82, 229-235
30. Park, T.; Lee, Y.; Cha, S. Fabrication of Bipolar Plates Based on Graphite Sheet via Stamping Method. ECS Transactions **2013**, 50, 795-804
31. Liu, H.; Li, P.; Juarez-Robles, D.; Wang, K.; Hernandez- Guerrero, A. Experimental study and comparison of various designs of gas flow fields to PEM fuel cells and cell stack performance. Front. Energy Res. **2014**
32. Carrette, L.; Friedrich, K.A.; Stimming, U. Fuel cells -Fundamentals and Applications. Fuel cells **2001**,1
33. Garcia-Diaz, B.L.; Sethuraman, V.; Weidner, J.; White R.E. Mathematical Model of a Direct Methanol Fuel Cell. Journal of Fuel Cell Science and Technology **2004**, 1
34. Shrivastava, N.; Harris, T.A.L. Direct Methanol Fuel Cells. Reference Module in Earth Systems and Environmental Sciences **2017**
35. Zuo, Z.; Fu, Y.; Manthiram, A. Novel Blend Membranes Based on Acid-Base Interactions for Fuel Cells. Polymers **2012**, 4, 1627-1644
36. Pasupathi, S.; Maiyalagan, T. Components for PEM Fuel cells An Overview. Materials Science Forum **2012**, 657, 143-189
37. Curtin, D.E.; Lousenberg, R.D.; Henry, T.J.; Tangeman, P.C.; Tisack, M.E. Advanced materials for improved PEMFC performance and life. J. Power Sources **2004**, 131, 41–48.
38. Liu, J.G.; Zhao, T.S.; Liang, Z.X.; Chen, R. Effect of membrane thickness on the performance and efficiency of passive direct methanol fuel cells. J. Power Sources **2006**, 153, 61–67.
39. Heinzel, A.; Barragàn, V.M. A review of the state-of-the-art of the methanol crossover in direct methanol fuel cells. J. Power Sources **1999**, 84, 70–74.
40. Han, J.; Liu, H. Real time measurements of methanol crossover in a DMFC. J. Power Sources **2007**, 164, 166–173.
41. Ahmed, M.; Dincer, I. A review on methanol crossover in direct methanol fuel cells: Challenges and achievements. Int. J. Energy Res. **2011**, 35, 1213–1228.
42. Kickelbick, G. Hybrid. Materials: Synthesis, Characterization, and Applications; Wiley—VCH: Weinheim, Germany, 2007; ISBN 978-3-527-31299-3. Molecules **2020**, 25, 1712 36 of 44
43. Trogadas, P.; Parrondo, J.; Ramani, V. Degradation Mitigation in Polymer Electrolyte Membranes Using Cerium Oxide as a Regenerative Free-Radical Scavenger. Electrochem. Solid State Lett. **2008**, 11, 113–116.
44. Bracco, C.M.; Sharma, S.; De Camargo Forte, M.M.; Steinberger-Wilckens, R. New approaches towards novel composite and multilayer membranes for intermediate temperature-polymer electrolyte fuel cells and direct methanol fuel cells. J. Power Sources **2016**, 316, 139–159.
45. Dhanapal, D.; Xiao, M.; Wang, S.; Meng, Y. A Review on Sulfonated Polymer Composite/Organic-Inorganic Hybrid Membranes to Address Methanol Barrier Issue for Methanol Fuel Cells. Nanomaterials **2019**, 9, 668.
46. Karimi, M.B.; Mohammadi, F.; Hooshyari, K. Recent approaches to improve Nafion performance for fuel cell applications: A review. Int. J. Hydrog. Energy **2019**, 44, 28919–28938.
47. Liu, X.; Fang, S.; Ma, Z.; Zhang, Y. Structure Design and Implementation of the Passive-DMFC. Micromachines **2015**, 6, 230–238.
48. Lin, H.L.; Yu, T.L.; Huangb, L.N.; Chena, L.C.; Shen, K.S.; Jung, G.B. Nafion/PTFE composite membranes for direct methanol fuel cell applications. J. Power Sources **2005**, 150, 11–19.
49. Nouel, K.M.; Fedkiw, P.S. Nafion®-based composite polymer electrolyte membranes. Electrochim. Acta **1998**, 43, 2381–2387.
50. Yu, T.L.; Lin, H.L.; Shen, K.S.; Chang, Y.C.; Jung, G.B. Nafion/PTFE Composite Membranes for Fuel Cell Applications. J. Polym. Res. **2004**, 11, 217–223.
51. Chen, L.C.; Yu, T.L.; Lin, H.L.; Yeh, S.H. Nafion/PTFE and zirconium phosphate modified Nafion/PTFE

composite membranes for direct methanol fuel cells. J. Membr. Sci. **2008**, 307, 10–20.
52. Vijayakumar, V.; Kim, K.; Nam, S.Y. Recent Advances in Polybenzimidazole (PBI)-based Polymer Electrolyte Membranes for High Temperature Fuel Cell Applications. Appl. Chem. Eng. **2019**, 30, 643–651.
53. Wong, C.Y.; Wong, W.Y.; Loh, K.S.; Daud, W.R.W.; Lim, K.L.; Khalid, M.; Walvekar, R. Development of Poly(Vinyl Alcohol)-Based Polymers as Proton Exchange Membranes and Challenges in Fuel Cell Application: A Review. Polym. Rev. **2020**, 60, 171–202.
54. Shao, Z.G.;Wang, X.; Hsing, I.M. Composite Nafion/polyvinyl alcohol membranes for the direct methanol fuel cell. J. Membr. Sci. **2002**, 210, 147–153.
55. Mollà, S.; Compan, V. Performance of composite Nafion/PVA membranes for direct methanol fuel cells. J. Power Sources **2011**, 196, 2699–2708.
56. Shao, Z.G.; Hsing, I.M. Nafion Membrane Coated with Sulfonated Poly (vinyl alcohol)-Nafion Film for Direct Methanol Fuel Cells. Electrochem. Solid State Lett. **2002**, 5, 185.
57. Lin, H.L.;Wang, S.H.; Chiu, C.K.; Yu, T.L.; Chen, L.C.; Huang, C.C.; Cheng, T.H.; Lin, J.M. Preparation of Nafion/poly(vinyl alcohol) electro-spun fiber composite membranes for direct methanol fuel cells. J. Membr. Sci. **2010**, 365, 114–122.
58. Mollà, S.; Compan, V. Polyvinyl alcohol nanofiber reinforced Nafion membranes for fuel cell applications. J. Membr. Sci. **2011**, 372, 191–200.
59. Hobson, L.J.; Nakano, Y.; Ozu, H.; Hayase, S. Targeting improved DMFC performance. J. Power Sources **2002**, 104, 79–84.
60. Ainla, A.; Brandell, D. Nafion®–polybenzimidazole (PBI) composite membranes for DMFC applications. Solid State Ion. **2007**, 178, 581–585.
61. Ausejo, J.G.; Cabedo, L.; Gamez-Perez, J.; Molla', S.; Giménez, E.; Compañ, V. Modification of Nafion Membranes with Polyaniline to Reduce Methanol Permeability. J. Electrochem. Soc. **2015**, 162, 325–333.
62. Ben Jadi, S.; El Guerraf, A.; Bazzaoui, E.A.; Wang, R.; Martins, J.I.; Bazzaoui, M. Synthesis, characterization, and transport properties of Nafion-polypyrrole membrane for direct methanol fuel cell (DMFC) application. J. Solid State Electrochem. **2019**, 23, 2423–2433.
63. Penner, R.M.; Martin, C.R. Electronically Conductive Composite Polymer Membranes. J. Electrochem. Soc. **1986**, 133, 310.
64. Sata, T.; Funakoshi, T.; Akai, K. Preparation and Transport Properties of Composite Membranes Composed of Cation Exchange Membranes and Polypyrrole. Macromolecules **1996**, 29, 4029–4035.
65. Zhu, J.; Sattler, R.R.; Garsuch, A.; Yepez, O.; Pickup, P.G. Optimisation of polypyrrole/Nafion composite membranes for direct methanol fuel cells. Electrochim. Acta **2006**, 51, 4052–4060.
66. Wang, C.H.; Chenc, C.C.; Hsud, H.C.; Dud, H.Y.; Chend, C.P.; Hwangd, J.Y.; Chend, L.C.; Shihb, H.C.; Stejskal, J.; Chena, K.H. Low methanol-permeable polyaniline/Nafion composite membrane for direct methanol fuel cells. J. Power Sources **2009**, 190, 279–284.
67. Escudero-Cid, R.; Montiel, M.; Sotomayor, L.; Loureiro, B.; Fatás, E.; Ocón, P. Evaluation of polyaniline-Nafion® composite membranes for direct methanol fuel cells durability tests. Int. J. Hydrog. Energy **2015**, 40, 8182–8192.
68. Huanga, Q.M.; Zhanga, Q.L.; Huanga, H.L.; Li, W.S.; Huanga, Y.J.; Luoc, J.L. Methanol permeability and proton conductivity of Nafion membranes modified electrochemically with polyaniline. J. Power Sources **2008**, 184, 338–343.
69. Wang, B.; Hong, L.; Li, Y.; Zhao, L.;Wei, Y.; Zhao, C.; Na, H. Considerations of the Effects of Naphthalene Moieties on the Design of Proton-Conductive Poly(arylene ether ketone) Membranes for Direct Methanol Fuel Cells. ACS Appl. Mater. Interfaces **2016**, 8, 24079–24088.
70. Kim, T.; Choi, J.; Kim, S. Blend membranes of Nafion/sulfonated poly (aryl ether ketone) for direct methanol fuel cell. J. Membr. Sci. **2007**, 300, 28–35.
71. Bauer, B.; Jones, D.J.; Rozière, J.; Tchicaya, L.; Alberti, G.; Casciola, M.; Massinelli, L.; Peraio, A.; Besse, S.; Ramunni, E. Electrochemical characterisation of sulfonated polyetherketone membranes. J. New Mat. Elect. Syst. **2000**, 3, 93–98.

72. Fu, T.Z.; Wang, J.; Ni, J.; Cui, Z.M.; Zhong, S.L.; Zhao, C.J.; Na, H.; Xing, W. Sulfonated poly(ether ether ketone)/aminopropyltriethoxysilane/phosphotungstic acid hybrid membranes with non-covalent bond: Characterization, thermal stability, and proton conductivity. Solid State Ion. **2008**, 179, 2265–2273.
73. Ru, C.; Gu, Y.; Duan, Y.; Zhao, C.; Na, H. Enhancement in proton conductivity and methanol resistance of Nafion membrane induced by blending sulfonated poly (arylene ether ketones) for direct methanol fuel cells. J. Membr. Sci. **2019**, 573, 439–447.
74. Tsai, J.; Cheng, H.; Kuo, J.; Huang, Y.; Chen, C. Blended Nafion®/SPEEK direct methanol fuel cell membranes for reduced methanol permeability. J. Power Sources **2009**, 189, 958–965.
75. Ye, G.; Hayden, C.A.; Goward, G.R. Proton Dynamics of Nafion and Nafion/SiO2 Composites by Solid State NMR and Pulse Field Gradient NMR. Macromolecules **2007**, 40, 1529–1537.
76. Peighambardoust, S.J.; Rowshanzamir, S.; Amjadi, M. Review of the proton exchange membranes for fuel cell applications. Int. J. Hydrog. Energy **2010**, 35, 9349–9384.
77. Mishra, A.K.; Bose, S.; Kuila, T.; Kim, N.H.; Lee, J.H. Silicate-based polymer-nanocomposite membranes for polymer electrolyte membrane fuel cells. Prog. Polym. Sci. **2012**, 37, 842–869.
78. Junoh, H.; Jaafar, J.; Nordin, N.A.H.M.; Ismail, A.F.; Othman, M.H.D.; Rahman, M.A.; Aziz, F.; Yusof, N.; Salleh,W.N.W. Porous Proton Exchange Membrane Based Zeolitic Imidazolate Framework-8 (ZIF-8). J. Membr. Sci. Res. **2019**, 5, 65–75.
79. Lufrano, F.; Baglio, V.; Di Blasi, O.; Staiti, P.; Antonucci, V.; Arico, A.S. Design of efficient methanol impermeable membranes for fuel cell applications. Phys. Chem. Chem. Phys. E PCCP **2012**, 14, 2718.
80. Ren, S.; Sun, G.; Li, C.; Liang, Z.; Wu, Z.; Jin, W.; Qin, X.; Yang, X. Organic silica/Nafion® composite membrane for direct methanol fuel cells. J. Membr. Sci. **2006**, 282, 450–455.
81. Shao, Z.G.; Xu, H.; Li, M.; Hsing, I.M. Hybrid Nafion–inorganic oxides membrane doped with heteropolyacids for high temperature operation of proton exchange membrane fuel cell. Solid State Ion. **2006**, 177, 779–785.
82. Hammami, R.; Ahamed, Z.; Charradi, K.; Beji, Z.; Assaker, I.B.; Naceur, J.B.; Auvity, B.; Squadrito, G.; Chtourou, R. Elaboration and characterization of hybrid polymer electrolytes Nafion–TiO2 for PEMFCs. Int. J. Hydrog. Energy **2003**, 38, 11583–11590.
83. Kim, J.H.; Kim, S.K.; Namb, K.; Kim, D.W. Composite proton conducting membranes based on Nafion and sulfonated SiO_2 nanoparticles. J. Membr. Sci. **2012**, 415, 696–701.
84. Ercelik, M.; Ozden, A.; Devrim, Y.; Colpan, C.O. Investigation of Nafion based composite membranes on the performance of DMFCs. Int. J. Hydrog. Energy **2017**, 42, 2658–2668.
85. Paul, D.R.; Robeson, L.M. Polymer nanotechnology: Nanocomposites. Polym. Nanotechnol. **2008**, 49, 3187–3204.
86. Wu, X.;Wu, N.; Shi, C.; Zheng, Z.; Qi, H.;Wang, Y. Proton conductive montmorillonite-Nafion composite membranes for direct ethanol fuel cells. Appl. Surf. Sci. **2016**, 388, 239–244.
87. Song, M.; Park, S.; Kim, Y.; Kim, K.; Min, S.; Rhee, H. Characterization of polymer-layered silicate nanocomposite membranes for direct methanol fuel cells. Electrochim. Acta **2004**, 50, 639–643.
88. Rhee, C.; Kim, H.; Chang, H.; Lee, J. Nafion/Sulfonated Montmorillonite Composite: A New Concept Electrolyte Membrane for Direct Methanol Fuel Cells. Chem. Mater. **2005**, 17, 1691–1697.
89. Lin,Y.; Yen, C.; Hung, C.; Hsiao,Y.; Ma, C. A novel composite membranes based on sulfonated montmorillonite modified Nafion® for DMFCs. J. Power Sources **2007**, 168, 162–166.
90. Liebau, F. Zeolites and clathrasils—Two distinct classes of framework silicates. Zeolites **1983**, 3, 191–193.
91. Smith, J. Definition of a zeolite. Zeolites **1984**, 4, 309–310.
92. Kešelj, D.; Lazi´c, D.; Škudri´c, B.; Penavin-Škudri´c, J.; Peruši´c, M. The possibility of hydrothermal synthesis of nay zeolite using di_erent mineral acids. Int. J. Latest Res. Sci. Technol. **2015**, 4, 37–41.
93. Sun, X.; Yang, C.; Xia, Z.; Qi, F.; Sun, H.; Sun, Q. Molecular sieve as an effective barrier for methanol crossover in direct methanol fuel cells. Int. J. Hydrog. Energy **2020**, 45, 8994–9003.
94. Tricoli, V.; Nannetti, F. Zeolite–Nafion composites as ion conducting membrane materials. Electrochim. Acta **2003**, 48, 2625–2633.
95. Makertihartha, I.G.B.N.; Zunita, M.; Rizki, Z.; Dharmawijaya, P.T. Recent advances on zeolite modification for direct alcohol fuel cells (DAFCs). AIP Conf. Proc. **2017**, 1818.

96. Prapainainara, P.; Dua, Z.; Kongkachuichaya, P.; Holmes, S.M.; Prapainainar, C. Mordenite/Nafion and analcime/Nafion composite membranes prepared by spray method for improved direct methanol fuel cell performance. Appl. Surf. Sci. **2017**, 421, 24–41.
97. Prapainainara, P.; Pattanapisutkun, N.; Prapainainar, C.; Kongkachuich, P. Incorporating graphene oxide to improve the performance of Nafion-mordenite composite membranes for a direct methanol fuel cell. Int. J. Hydrog. Energy **2019**, 44, 362–378.
98. Tiwari, S.K.; Sahoo, S.; Wang, N.; Huczko, A. Graphene research and their outputs: status and prospect. Journal of Science: Advanced Materials and Devices **2020**, 5(1), 10-29.
99. Pumera, M. Electrochemistry of graphene, graphene oxide and other graphenoids: Review. Electrochem. Commun. **2013**, 36, 14–18.
100. Dikin, D. A.; Stankovich, S.; Zimney, E.J.; Piner, R.D.; Dommett, G.H.B.; Evmenenko, G.; Nguyen, S.T.; Rodney, S.; Ruoff, R.S. Preparation and characterization of graphene oxide paper. Nature volume **2007**, 448, 457–460
101. Cheng, M.; Huang, L.; Wang, Y.; Tang, J.; Wang, Y.; Zhao, Y.; Liu, G.; Zhang, Y.; Kipper, M.J.; Belfioreb, L.A.; Ranilc, W.S. Recent developments in graphene-based/nanometal composite filter membranes. RSC Adv. **2017**, 7, 47886
102. Robinson, J.T.; Zalalutdinov, M.; Baldwin, J.W.; Snow, E.S.;Wei, Z.; Sheehan, P.; Houston, B.H. Wafer-scale. Reduced Graphene Oxide Films for Nanomechanical Devices. Nano Lett. **2008**, 8, 3441–3445.
103. Wang, J.; Zhang, P.; Liang, B.; Liu, Y.; Xu, T.;Wang, L.; Cao, B.; Pan, K. Graphene Oxide as an Effective Barrier on a Porous Nanofibrous Membrane for Water Treatment. ACS Appl. Mater. Interfaces **2016**, 8, 6211–6218.
104. Pham, V.H.; Cuong, T.V.; Hur, S.H.; Shin, E.W.;Kim, J.S.; Chung, J.S.;Kim, E.J. Fast and simple fabrication of a large transparent chemically-converted graphene film by spray-coating. Carbon, **2010**, 48, 1945–1951.
105. Ma, J.; Ping, D.; Dong, X. Recent Developments of Graphene Oxide-Based Membranes: A Review .Membranes **2017**, 7(3).
106. Choi, B.; Huh, Y.; Park, Y.; Jung, D.; Hong, W.; Park, H. Enhanced transport properties in polymer electrolyte composite membranes with graphene oxide sheets. Carbon **2012**, 50, 5395–5402.
107. Chien, H.; Tsai, L.; Huang, C.; Kang, C.; Lin, J.; Chang, F. Sulfonated graphene oxide/Nafion composite membranes for high-performance direct methanol fuel cells. Int. J. Hydrog. Energy **2013**, 38, 13792–13801.
108. Yan, X.H.; Wu, R.; Xu, J.B.; Luo, Z.; Zhao, T.S. Ku—Nafion sandwich membrane for direct methanol fuel cells. J. Power Sources **2016**, 311, 188–194.
109. Kumar, R.; Xu, C.; Scott, K. Graphite oxide/Nafion composite membranes for polymer electrolyte fuel cells. RSC Adv. **2012**, 2, 8777–8782.
110. Sahu, A.K.; Ketpang, K.; Shanmugam, S.; Kwon, O.; Lee, S.; Kim, H. Sulfonated Graphene-Nafion Composite Membranes for Polymer Electrolyte Fuel Cells Operating under Reduced Relative Humidity. J. Phys. Chem.C **2016**, 120, 15855–15866.
111. Lee, D.C.; Yang, H.N.; Park, S.H.; Kim, W.J. Nafion/graphene oxide composite membranes for low humidifying polymer electrolyte membrane fuel cell. J. Membr. Sci. **2014**, 452, 20–28.
112. Lee, D.C.; Yang, H.N.; Park, S.H.; Park, K.W.; Kim, W.J. Self-humidifying Pt–graphene/SiO2 composite membrane for polymer electrolyte membrane fuel cell. J. Membr. Sci. **2015**, 474, 254–262.
113. Yang, H.N.; Lee, W.H.; Choi, B.S.; Kim, W.J. Preparation of Nafion/Pt-containing TiO2/graphene oxide composite membranes for self-humidifying proton exchange membrane fuel cell. J. Membr. Sci. **2016**, 504, 20–28.
114. Kim, Y.; Ketpang, K.; Jaritphun, S.; Park, J.S.; Shanmugam, S. A polyoxometalate coupled graphene oxide-Nafion composite membrane for fuel cells operating at low relative humidity. J. Mater. Chem. A **2015**, 3, 8148–8155.
115. Staiti, P.; Minutoli, M.; Hocevar, S. Membranes based on phosphotungstic acid and polybenzimidazole for fuel cell application. Journal of Power Sources **2000**, 90 (2), 231-235
116. Maiti, J.; Kakati, N.; Woo, S.P.; Yoon, Y.S. Nafion® based hybrid composite membrane containing GO and dihydrogen phosphate functionalized ionic liquid for high temperature polymer electrolyte membrane fuel cell. Compos. Sci. Technol. **2018**, 155, 189–196.
117. Branco, C.M. Multilayer Membranes for Intermediate Temperature. Ph.D. Thesis, University of Birmingham, Birmingham, UK, **2017**.

118. Ibrahim, A.; Hossain, O.; Chaggar, J.; Steinberger-Wilckens, R.; El-kharouf, A. GO-Nafion composite membrane development for enabling intermediate temperature operation of polymer electrolyte fuel cell. Int. J. Hydrog. Energy **2019**, 45, 5526–5534.
119. Zakil, F. A.; Kamarudin, S.K.; Basri, S. Modified Nafion membranes for direct alcohol fuel cells: An overview. Renewable and Sustainable Energy Reviews **2016**, 65, 841-852.
120. Fathima, N.N.; Aravindhan, R.; Lawrence, D.; Yugandhar, U.; Moorthy, T.S.R.; Nair, N.U. SPEEK polymeric membranes for fuel cell application and their characterization: A review. J. of scientific / industrial research **2007**, 66,209.
121. Li, L.; Zhang, J.; Wang, Y. Sulfonated polyether ether ketone membranes cured with different methods for direct methanol fuel cells. Journal of materials science letters **2003**, 22, 1595.
122. Zaidi, S.M.; Mikhailenko, S.D.; Robertson, G.P.; Guiver, M.D.; Kaliaguine, S. Proton conducting composite membranes from polyether ether ketone and heteropolyacids for fuel cell applications. J.Membr. Sci. **2000**, 173 ,17.
123. Li, X.; Liu, C.; Xu, D.; Zhao, C.; Wang, Z.; Zhang, G.; Na, H.; Xing, W. Preparation and properties of sulfonated poly(ether ether ketone)s (SPEEK)/polypyrrole composite membranes for direct methanol fuel cells. J. Power Sources **2006**, 162,1.
124. Cai, H.; Shao, K.; Zhong, S.; Zhao, C.; Zhang, G; X. Li, X.; Na, H.. Properties of composite membranes based on sulfonated poly(ether ether ketone)s (SPEEK)/phenoxy resin (PHR) for direct methanol fuel cells usages. Journal of Membrane Science **2007**, 297, 162.
125. Di Vona, M.L.; D'Epifanio, A.; Marani, D.; Trombetta, M.; Traversa, E.; Licoccia, S. SPEEK/PPSU-based organic–inorganic membranes: proton conducting electrolytes in anhydrous and wet environments. J Membr Sci **2006** ,279, 186.
126. Zaidi, S.M.J.; Ahmad, M.I. Novel SPEEK/heteropolyacids loaded MCM-41 composite membranes for fuel cell applications. J Membr Sci **2006**, 279(1-2), 548-557.
127. Nagarale, R.K.; Gohil, G.S.; Shahi, V.K. Sulfonated poly(ether ether ketone)/polyaniline composite proton-exchange membrane. J Membr Sci **2006**,280, 389.
128. Zhang, H.; Fan, X.; Zhang, J.; Zhou, Z. Modification research of sulfonated PEEK membranes used in DMFC. Solid State Ionics **2008**, 179, 1409.
129. Sengul, E.; Erdener, H.; Akay, R.G.; Yucel, H.; Bac, N.; Eroglu, I. Effects of sulfonated polyether-etherketone (SPEEK) and composite membranes on the proton exchange membrane fuel cell (PEMFC) performance. Int J Hydrogen Energ **2009**, 34, 4645.
130. Bhattad, S.S.; Mahanwar, P.A. Preparation and Physical Characterization of Sulfonated Poly (Ether Ether Ketone) and Polypyrrole Composite Membrane. Journal of Membrane Science & Research **2019**, 5, 49-54.
131. Gosalawit, R.; Chirachanchai, S.; Shishatskiy,S.; Nunes S.P. Sulfonated montmorillonite/sulfonated poly(ether ether ketone) (SMMT/SPEEK) nanocomposite membrane for direct methanol fuel cells (DMFCs). Journal of Membrane Science **2008** ,323 ,337.
132. Pasupathi, S.; Bernard, S.; Bladergroen, J.; Linkov, V. High DMFC performance output using modified acid–base polymer blend. International Journal of Hydrogen Energy **2008**, 33(12),3132.
133. Li, W.; Manthiram, A. Sulfonated poly(arylene ether sulfone) as a methanol-barrier layer in multilayer membranes for direct methanol fuel cells. Journal of Power Sources **2012**, 195 ,962.
134. Lee, C.H.; Park, H.B.; Chung, Y.S.; Lee, Y.M.; Freeman, B.D. Water Sorption, Proton Conduction, and Methanol Permeation Properties of Sulfonated Polyimide Membranes Cross-Linked with N,N-Bis(2-hydroxyethyl)-2-aminoethanesulfonic Acid (BES). Macromolecules **2006**, 39, 755.
135. Jiang, Z.; Zhao, X.; Manthiram, A. Sulfonated poly(ether ether ketone) membranes with sulfonated graphene oxide fillers for direct methanol fuel cells. International Journal of Hydrogen Energy **2013**, 38,5875.
136. Greaves, C.R.; Bond, S.P.; McWhinne, W.R. Conductivity studies on modified laponites. Polyhedron **1995**, 14,3635.
137. Kim, D.; Hwang, H.; Jung, S.; Nam, S. Sulfonated poly(arylene ether sulfone)/Laponite-SO3H composite membrane for direct methanol fuel cell . Journal of Industrial and Engineering Chemistry **2012**, 18,556.
138. Mikhailenko, S.D., Robertson, G.P.; Guiver, M.D.; Kaliaguine, S. Properties of PEMs based on cross-linked sulfonated poly(ether ether ketone) . J. Membr. Sci. **2006**, 285, 306.

139. Zhong, S.; Cui, X.; Cai, H.; Fu, T.; Zhao, C.; Na, J. Crosslinked sulfonated poly(ether ether ketone) proton exchange membranes for direct methanol fuel cell applications. Power Sources **2007**, 164, 65.
140. Feng, S.; Shang, Y.; Xie, X.; Wang, Y.; Xu, J. Synthesis and characterization of crosslinked sulfonated poly(arylene ether sulfone) membranes for DMFC applications. Journal of Membrane Science **2009**, 335,13.
141. Prapainainar, C.; Holmes, S.M. Sustainability in Energyand Buildings: Research Advances. Proton conductivity of Nafion® membrane in actual direct methanol fuel cell Operation. Special Edition - Mediterranean Green Energy Forum **2013** (MGEF-13), 2, 31–35
142. Kreuer, K.D. On the development of proton conducting polymer membranes for hydrogen and methanol fuel cells . J. Membr. Sci. **2001** ,185, 29.
143. Moritani,T.; Kajitani, K.. Functional modification of poly(vinyl alcohol) by copolymerization: 1. Modification with car□ylic monomers. Polymer **1997**, 38 (12),2933.
144. Rhim, J.; Park, H.; Lee, C.; Jun, J.; Kimb, D.; Lee Y. Crosslinked poly(vinyl alcohol) membranes containing sulfonic acid group: proton and methanol transport through membranes. Journal of Membrane Science **2004**, 238 ,143.
145. Kang, M.; Choi, Y.; Moon, S. Water-swollen cation-exchange membranes prepared using poly(vinyl alcohol) (PVA)/poly(styrene sulfonic acid-co-maleic acid) (PSSA-MA). J. Membr. Sci. **2002**, 207, 157.
146. Panero, S.; Fiorenza, P.; Navarra,M.A.; Romanowska, J.; Scrosati, B. Silica-Added, Composite Poly(vinyl alcohol) Membranes for Fuel Cell Application. J. Electrochem. Soc. **2005**, 152 (12), 2400.
147. Son, J.H.; Kang, Y.S.; Won, J. Poly(vinyl alcohol)-based polymer electrolyte membranes containing polyrotaxane. J. Membr. Sci. **2006**, 281, 345.
148. Yang, C.; Lee, Y.; Yang, J. Direct methanol fuel cell(DMFC) based on PVA/MMT composite polymer membranes. Power Sources **2009**, 188, 30.
149. Pandey, J.; Shukla A. PVDF supported silica immobilized phosphotungstic acid membrane for DMFC application. Solid State Ionics **2014**, V262, 811.
150. J.Pandey, M.Seepan, A. Shukla. Zirconium phosphate based proton conducting membrane for DMFC application. International Journal of Hydrogen Energy 2015, Volume 40, Issue 30, 9410.
151. Neburchilov, V.; Martin, J.; Wang, H.; Zhang J. A review of polymer electrolyte membranes for direct methanol fuel cells. Journal of Power Sources **2007**, 169, 221.
152. Stone, C.; Steck, A.E.; Choudhury, B. US Patent 6,723,758 (September 26, **2004**).
153. Taft, K.M.; Kurano, M.R. US Patent 6,630,265 (October 7, **2003**).
154. Chen, S.L.; Krishnan, L.; Srinivasan, S.; Benziger, J.; Bocarsly A.B. Ion exchange resin/polystyrene sulfonate composite membranes for PEM fuel cells. J.Membr. Sci. **2004**, 243, 327.
155. Vengatesan, S.; Cho, E.; Kim H.-J.; Lim T.-H. Effects of curing condition of solution cast Nafion® membranes on PEMFC performance. Korean Journal of Chemical Engineering, **2009**, 26(3), 679-684.
156. Zook, L.A.; Leddy, J. Density and Solubility of Nafion: Recast, Annealed, and Commercial Films. Analytical Chemistry, **1996**, 68(21), 3793-3796.
157. Moore, R.B.; Martin,C.R.; Chemical and Morphological Properties of Solution-Cast Perfluorosulfonate Ionomers. Macromolecules, **1988**, 21, 1334-1339.
158. Gebel, G.; Aldebert, P.; Pineri,M.; Structure and Related Properties of Solution-Cast Perfluorosulfonated Ionomer Films. Macromolecules, **1987**, 20, 1425-1428.
159. Jung, H.-Y.; Cho, K.-Y.; Lee, Y.M.; Park, J.-K.; Choi J.-H.; Sung Y.-E. Influence of annealing of membrane electrode assembly (MEA) on performance of direct methanol fuel cell (DMFC). Journal of Power Sources, **2007**, 163(2),952-956.
160. Malkow, T.; Jahnke, G.; Futter, G.; Tsotridis, T. Protocols for stack characterization improved durability and cost-effective components for new generation solid polymer electrolyte direct methanol fuel cells. DURAMET Deliverable Report D2.4, **2017**.
161. Peng, K.-J.; Lai, J.-Y.; Liu, Y.-L. Nanohybrids of graphene oxide chemically bonded with Nafion: Preparation and application for proton exchange membrane fuel cells. Journal of Membrane Science, **2016**, 51486-94.
162. Yasukawa, M.; Suzuki, T.; Higa, M. Chapter 1 - Salinity Gradient Processes: Thermodynamics, Applications, and Future Prospects. Membrane-Based Salinity Gradient Processes for Water Treatment and Power Generation, **2018**, 3-56

163. Hattenberg, M. Composite proton exchange membranes for intermediate temperature fuel cells. Ph.D Thesis. University of Birmingham, **2015**.
164. Leng, Y.; Materials Characterization. **2008**, Singapore: John Wiley & Sons (Asia) Pte Ltd.
165. Wang, L.; Kang, J.; Nam, J.; Suhr, J.; Prasad, A.; Advani, S. Composite Membrane Based on Graphene Oxide Sheets and Nafion for Polymer Electrolyte. ECS Electrochemistry Letters, **2015**, 4(1)
166. Bayer, T.; Bishop, S.R.; Nishihara, M.; Sasaki, K.; Lyth, S.M. Characterization of a graphene oxide membrane fuel cell. Journal of power sources, **2014**, 272, 239-247.
167. Hosseinpour, M.; Sahoo, M.; Page, M.; Baylis, S.; Patel, F.; Holmes, S. Improving the performance of direct methanol fuel cells by implementing multilayer membranes blended with cellulose nanocrystals. International Journal of Hydrogen Energy **2019**, 44(57), 30409-30419.
168. Lavorante, M.J.; Scalise, B.; López, C.; Sanguinetti, A.; Franco, J.; Fasoli, H. Study of the Nafion 117 hydration using different concentrarions of Sulfuric Acid. Escuela Superior Técnica del Ejército, General Manuel N. Savio, Pontificia Universidad Católica Argentina, Centro de Investigaciones Ciéntificas y Técnicas para la Defensa, HYFUSEN, Argentina, **2009.**
169. Napoli, L.; Lavorante, M.J.; Franco J.; Sanguinetti, A.; Fasoli, H.Effects on nafion® 117 membrane using different strong acids in various concentrations. Journal of new materials for electrochemical systems, **2013**, 16(3),139-251.
170. Jung, G.; Su, A.; C. Tu, C.; F. Weng, F. Effect of operating parameters on the DMFC performance. Fuel Cell Science Technology, **2005**, 5, 2-81.
171. Govindarasu, R.; Somasundaram, S. Studies on Influence of Cell Temperature in Direct Methanol Fuel Cell Operation. Processes, **2020**